

NUREG/IA-0156

Vol. 1

IPSN 99/08-1

NSI RRC 2179



International Agreement Report

Data Base on the Behavior of High Burnup Fuel Rods with Zr-1%Nb Cladding and UO₂ Fuel (VVER Type) under Reactivity Accident Conditions

Review of Research Program and Analysis of Results

Prepared by
L. Yegorova
Nuclear Safety Institute of Russian Research Centre "Kurchatov Institute"
Kurchatov Square 1, Moscow 123182, Russia

Office of Nuclear Regulatory Research
U.S. Nuclear Regulatory Commission
Washington, DC 20555-0001

July 1999

Prepared for
U.S. Nuclear Regulatory Commission, Institute for Protection and Nuclear Safety (France) and
Ministry of Science and Technologies of Russian Federation

Published by
U.S. Nuclear Regulatory Commission

AVAILABILITY NOTICE

Availability of Reference Materials Cited in NRC Publications

NRC publications in the NUREG series, NRC regulations, and *Title 10, Energy, of the Code of Federal Regulations*, may be purchased from one of the following sources:

1. The Superintendent of Documents
U.S. Government Printing Office
P.O. Box 37082
Washington, DC 20402-9328
<http://www.access.gpo.gov/su_docs>
202-512-1800
2. The National Technical Information Service
Springfield, VA 22161-0002
<<http://www.ntis.gov/ordernow>>
703-487-4650

The NUREG series comprises (1) brochures (NUREG/BR-XXXX), (2) proceedings of conferences (NUREG/CP-XXXX), (3) reports resulting from international agreements (NUREG/IA-XXXX), (4) technical and administrative reports and books [(NUREG-XXXX) or (NUREG/CR-XXXX)], and (5) compilations of legal decisions and orders of the Commission and Atomic and Safety Licensing Boards and of Office Directors' decisions under Section 2.206 of NRC's regulations (NUREG-XXXX).

A single copy of each NRC draft report is available free, to the extent of supply, upon written request as follows:

Address: Office of the Chief Information Officer
Reproduction and Distribution
Services Section
U.S. Nuclear Regulatory Commission
Washington, DC 20555-0001

E-mail: <DISTRIBUTION@nrc.gov>

Facsimile: 301-415-2289

A portion of NRC regulatory and technical information is available at NRC's World Wide Web site:

<<http://www.nrc.gov>>

All NRC documents released to the public are available for inspection or copying for a fee, in paper, microfiche, or, in some cases, diskette, from the Public Document Room (PDR):

NRC Public Document Room
2120 L Street, N.W., Lower Level
Washington, DC 20555-0001
<<http://www.nrc.gov/NRC/PDR/pdr1.htm>>
1-800-397-4209 or locally 202-634-3273

Microfiche of most NRC documents made publicly available since January 1981 may be found in the Local Public Document Rooms (LPDRs) located in the vicinity of nuclear power plants. The locations of the LPDRs may be obtained from the PDR (see previous paragraph) or through:

<<http://www.nrc.gov/NRC/NUREGS/SR1350/V9/lpdr/html>>

Publicly released documents include, to name a few, NUREG-series reports; *Federal Register* notices; applicant, licensee, and vendor documents and correspondence; NRC correspondence and internal memoranda; bulletins and information notices; inspection and investigation reports; licensee event reports; and Commission papers and their attachments.

Documents available from public and special technical libraries include all open literature items, such as books, journal articles, and transactions, *Federal Register* notices, Federal and State legislation; and congressional reports. Such documents as theses, dissertations, foreign reports and translations, and non-NRC conference proceedings may be purchased from their sponsoring organization.

Copies of industry codes and standards used in a substantive manner in the NRC regulatory process are maintained at the NRC Library, Two White Flint North, 11545 Rockville Pike, Rockville, MD 20852-2738. These standards are available in the library for reference use by the public. Codes and standards are usually copyrighted and may be purchased from the originating organization or, if they are American National Standards, from—

American National Standards Institute
11 West 42nd Street
New York, NY 10036-8002
<<http://www.ansi.org>>
212-642-4900

DISCLAIMER

This report was prepared under an international cooperative agreement for the exchange of technical information. Neither the United States Government nor any agency thereof, nor any of their employees, makes any warranty, expressed or implied, or assumes any legal liability or responsibility for any third

party's use, or the results of such use, of any information, apparatus, product, or process disclosed in this report, or represents that its use by such third party would not infringe privately owned rights.

NUREG/IA-0156
Vol. 1
IPSN 99/08-1
NSI RRC 2179



International Agreement Report

**Data Base on the Behavior of High Burnup Fuel Rods
with Zr-1%Nb Cladding and UO₂ Fuel (VVER Type)
under Reactivity Accident Conditions**

Review of Research Program and Analysis of Results

Prepared by
L. Yegorova
Nuclear Safety Institute of Russian Research Centre "Kurchatov Institute"
Kurchatov Square 1, Moscow 123182, Russia

**Office of Nuclear Regulatory Research
U.S. Nuclear Regulatory Commission
Washington, DC 20555-0001**

July 1999

Prepared for
U.S. Nuclear Regulatory Commission, Institute for Protection and Nuclear Safety (France) and
Ministry of Science and Technologies of Russian Federation

Published by
U.S. Nuclear Regulatory Commission

ABSTRACT OF THE REPORT

The present report contains a data base used for analyzing the behavior of three types of VVER fuel rods (fresh fuel rods; fuel rods with fresh fuel and irradiated cladding; high burnup fuel rods) which have been tested in the Impulse Graphite Reactor (IGR) under reactivity accident conditions. The basic test parameters are as follows:

- capsule tests with stagnant water or air coolant under ambient conditions;
- pressurized fuel rods;
- fuel burnup: 0 and 48 MWd/kg U;
- pulse width - about 700 ms.

The presented data base includes the results of reactor tests of 25 fuel rods as well as results of pre- and post-test examinations of fuel rods, computer simulations of fuel rod behavior under test conditions; in addition, the report presents the results of special out-of-pile tests carried out to measure mechanical properties of Zr-1%Nb cladding.

The report consists of three volumes, each volume contains the following information:

- Volume 1: Brief description of the test program, testing and analytical techniques and summary of results;
- Volume 2: Description and validation of procedures used to obtain the data base. Summarization of test results as supported by mechanical properties of Zr-1%Nb cladding;
- Volume 3: Data base consisting of:
- parameters of VVER fuel rods before and after irradiation at the NovoVoronezh Nuclear Power Plant;
 - parameters of fresh and refabricated fuel rods before and after IGR tests;
 - results of out-of-pile mechanical tests of non-irradiated and irradiated Zr-1%Nb claddings.

ABSTRACT OF THE VOLUME 1

This volume of the report is of independent significance and contains an overview of the research program as well as results of investigations carried out to study the behavior of VVER fuel rods under reactivity accident conditions. This volume can be used as a reference book for those who would like to get an idea about the content and results of conducted investigation. In addition, the volume presents recommendations how to use it as a guidebook for the other two volumes.

TABLE OF CONTENTS

	Page
1. INTRODUCTION	1.1
2. BACKGROUND OF THE VVER-1000/RIA TEST PROGRAM	2.1
3. MAJOR PROVISIONS OF THE PROGRAM TO STUDY THE VVER HIGH BURNUP FUEL RODS BEHAVIOR UNDER RIA CONDITIONS	3.1
4. METHODOLOGICAL ASPECTS OF THE RESEARCH PROGRAM	4.1
4.1. Post-test examination of commercial fuel elements	4.2
4.2. Manufacture of refabricated fuel rods.....	4.4
4.3. Pre-test examination of refabricated fuel rods	4.5
4.4. Development of procedures to determine axial distribution of fuel mass, free gas volume and fuel isotopic composition	4.7
4.5. RIA test procedures in the IGR reactor	4.10
4.6. PIE of fuel rods tested in the IGR reactor	4.12
4.7. Determination of r,z,t distributions of energy deposition and fuel rod power in high burnup fuel....	4.15
4.8. Determination of the mechanical properties of the VVER unirradiated and irradiated claddings	4.18
4.8.1. Procedures to measure the mechanical properties versus temperature and strain rate.....	4.18
4.8.2. Procedures to measure the mechanical properties for analysis of ballooning and cladding rupture.....	4.21
4.9. Adaptation and modification of the MATPRO package, FRAP-T6 and SCANAIR codes to predict the thermal-mechanical behavior of the VVER fuel rods under IGR/RIA conditions	4.24
4.9.1. Sensitivity study of codes to material properties	4.25
4.9.2. Development of package of original VVER material properties for the MATPRO and SCANAIR codes	4.25
4.9.3. Development of calculation scheme for fuel rods and preparation of input data	4.26
4.9.4. The first stage of verification of the FRAP-T6 and SCANAIR codes by the IGR test results.....	4.26
4.9.5. Codes modification in accordance with the results of the first stage of verification procedures.....	4.28
4.9.6. Evaluating the area of application of the FRAP-T6 and SCANAIR codes for analysis of the IGR tests	4.29
4.10. Procedure to determine peak fuel enthalpy in fuel rods	4.29
5. RESULTS OF THE IGR TESTS WITH VVER FUEL RODS	5.1
5.1. High burnup fuel rods tested in water coolant	5.1
5.2. Fuel rods with irradiated cladding and fresh fuel and unirradiated fuel rods tested in water coolant.....	5.7
5.3. Fuel rods tested in the air coolant.....	5.8

6. ANALYSIS OF THE IGR TEST RESULTS BY USE OF RESULTS OF OUT-OF-PILE MECHANICAL TESTING	6.1
6.1. Formulation of the problem.....	6.1
6.2. Results of mechanical tests with simple ring samples	6.3
6.3. Results of burst tests.....	6.6
7. ANALYSIS AND GENERALIZATION OF RESEARCH RESULTS	7.1
7.1. Decomposition of the IGR/RIA test scenario and selection of the key phenomena for analysis	7.1
7.2. Analysis of PCMI stage and estimation of conditions for the departure from nucleate boiling.....	7.1
7.3. Ballooning and rupture conditions	7.5
7.3.1. Criterion of ballooning start.....	7.6
7.3.2. Criterion of cladding rupture.....	7.6
7.3.3. Maximum cladding hoop strain in the rupture zone.....	7.8
7.3.4. Analysis of possible sources of errors in predictions of cladding hoop strain due to imperfection of the data base on mechanical properties of claddings and imperfect interpretation of the data base	7.11
7.4. Criteria, thresholds and mechanisms of VVER fuel rod failure under IGR test conditions.....	7.14
7.4.1. Analysis of conditions of PCMI failure for VVER fuel rods	7.17
8. CONCLUSIONS AND RECOMMENDATIONS	8.1
9. REFERENCES	9.1

LIST OF FIGURES

	Page
Fig. 2.1. Power shapes for GIDRA (a) and IGR (b) reactors.....	2.4
Fig. 2.2. Scheme of the reactor capsule tests.....	2.4
Fig. 2.3. Main types of RIA tests with fresh fuel.	2.6
Fig. 2.4. Failure types for VVER unirradiated fuel rods.....	2.7
Fig. 3.1. Main principles for the development of the program of VVER high burnup fuel tests.....	3.1
Fig. 4.1. Main directions of methodological investigations.	4.1
Fig. 4.2. Power history for Unit 5 of NV NPP.....	4.2
Fig. 4.3. Axial burnup distribution for fuel rod #317.....	4.2
Fig. 4.4. Macro- and microstructure of the commercial fuel element #317.	4.3
Fig. 4.5. Main provisions of fuel rod refabrication.	4.4
Fig. 4.6. X-ray photography of fuel rod #H2T.....	4.5
Fig. 4.7. Results of γ -scanning (a), profilometry (b) and burnup measurements (c) for fuel rod #H2T.	4.6
Fig. 4.8. Axial fuel mass distribution and axial free gas volume distribution for fuel rod #H2T.	4.7
Fig. 4.9. Nuclear concentration of Pu^{241} isotope average on the four radial zones of high burnup fuel.	4.8
Fig. 4.10. Scheme of the procedure to determine spatial distribution of the burnup and isotopic composition in refabricated fuel rods.	4.8
Fig. 4.11. Special TRIFOB verification vs. burnup using NV NPP elements.....	4.9
Fig. 4.12. The reactor power profile measured by ionization chambers and in-core detectors.	4.10
Fig. 4.13. Results of the DINAR code verification.	4.11
Fig. 4.14. Major provision of the PIE procedure.....	4.12
Fig. 4.15. Some PIE results for unfailed fuel rod #H1T.	4.13
Fig. 4.16. Some PIE results for failed fuel rod #H7T.	4.14
Fig. 4.17. Distribution of the specific number of fissions versus time.....	4.16
Fig. 4.18. Axial distribution of the specific number of fissions.....	4.16
Fig. 4.19. Radial distribution of the specific number of fissions.	4.17
Fig. 4.20. Scheme of the ring tensile test.....	4.19
Fig. 4.21. Results of Zr-1%Nb uniform elongation measurements with simple ring samples.	4.20
Fig. 4.22. Comparison of the procedure to measure the mechanical properties of the Zr-1%Nb cladding....	4.21
Fig. 4.23. Schemes of the tests for some burst programs.	4.22
Fig. 4.24. Schemes of the burst tests in the framework of the IGR/RIA program.	4.23
Fig. 4.25. Correlation of local burst stress for unirradiated and irradiated Zr-1%Nb cladding.....	4.26
Fig. 4.26. Comparison of the measured cladding temperature and the cladding temperature predicted by the SCANAIR code for the transition from convection to nucleate boiling.	4.27
Fig. 4.27. Comparison of the measured cladding temperature and the cladding temperature calculated by the FRAP-T6 and SCANAIR codes for departure from nucleate boiling.	4.27
Fig. 4.28. Final verification results for the modified FRAP-T6 and SCANAIR codes.	4.28
Fig. 4.29. Scheme to calculate the peak fuel enthalpy.....	4.29
Fig. 5.1. Appearance of high burnup fuel rods after IGR tests in water.	5.2
Fig. 5.2. Some parameters of unfailed high burnup fuel rods tested in water coolant.	5.3
Fig. 5.3. Thermal mechanical parameters of the fuel rod #H4T calculated by FRAP-T6 and SCANAIR codes.	5.4
Fig. 5.4. Some parameters of failed high burnup fuel rods tested in water coolant.	5.6

Fig. 5.5. Some parameters of failed unirradiated high burnup fuel rod and failed fuel rod with irradiated cladding and fresh fuel tested in water coolant.	5.7
Fig. 5.6. Appearance of fuel rods of different types tested in air coolant.....	5.9
Fig. 5.7. Parameters of high burnup fuel rods tested in air coolant.	5.10
Fig. 5.8. Parameters of fuel rods with fresh fuel and irradiated and unirradiated claddings tested in air coolant.	5.12
Fig. 6.1. Comparative parameters of RIA tests with PWR and VVER high burnup fuel rods.....	6.1
Fig. 6.2. Appearance of cross-sections of the PWR and VVER cladding and corresponding microstructure after RIA tests.	6.2
Fig. 6.3. Engineering ultimate strength and yield stress vs. temperature for unirradiated and irradiated cladding at the strain rate $2 \cdot 10^{-3} \text{ s}^{-1}$	6.3
Fig. 6.4. Total elongation and uniform elongation vs. temperature for unirradiated and irradiated Zr-1%Nb cladding at the strain rate $2 \cdot 10^{-3} \text{ s}^{-1}$	6.5
Fig. 6.5. Burst pressure vs. temperature and strain rate for unirradiated and irradiated Zr-1%Nb claddings.....	6.6
Fig. 6.6. Circumferential elongation at the rupture zone vs. temperature for the unirradiated and irradiated Zr-1%Nb claddings at pressure increase rate 0.01 MPa/s.....	6.7
Fig. 7.1. FRAP-T6 predictions of VVER high burnup fuel rod behavior (#H5T) under IGR test.....	7.2
Fig. 7.2. Comparison of calculated and measured residual fuel hoop strain.	7.4
Fig. 7.3. X-ray photograph of the fuel rod #H1T after test (a), axial distributions of the fuel enthalpy (b) and measured axial distribution of the cladding hoop strain for the fuel rod #H1T after test (c).	7.5
Fig. 7.4. Summary of burst test results with Zr-1%Nb claddings.....	7.7
Fig. 7.5. Comparative burst data base for Zr-1%Nb and Zry claddings.	7.7
Fig. 7.6. Comparison burst stresses vs. temperature obtained using burst test and VVER fuel rod with irradiated cladding tested in air coolant in IGR reactor.....	7.8
Fig. 7.7. Results characterising the quality of prediction of maximum cladding hoop strain in the rupture zone.	7.9
Fig. 7.8. Comparison of the cladding hoop strains from three type of tests.	7.11
Fig. 7.9. Comparison results of burst tests and reactor tests on cladding hoop strain.	7.12
Fig. 7.10. Extrapolation of the power law beyond the test area for water-cooled fuel rod #H5T (a) and air coolant fuel rod #B10T (b).....	7.13
Fig. 7.11. Appearance of high burnup fuel rod #H7T with two ballooning and two cladding ruptures.	7.14
Fig. 7.12. Fuel enthalpy at failure vs. peak fuel enthalpy for VVER high burnup fuel rods tested in water coolant.	7.15
Fig. 7.13. Data base characterizing the outer temperature of the cladding at failure calculated with FRAP-T6 code.	7.16
Fig. 7.14. Appearance of ring samples after tests.	7.17
Fig. 7.15. Thermal mechanical parameters of the VVER high burnup fuel rod #H1T vs. pulse width, calculated using the FRAP-T6 code.....	7.19
Fig. 7.16. Thermal mechanical parameters of the VVER high burnup fuel rod #H1T vs. pulse width, calculated using the SCANAIR code.	7.20
Fig. 7.17. Margins to PCMI failure for a VVER irradiated cladding.	7.21

LIST OF TABLES

	Page
Table 2.1. Summary of the RIA tests results with LWR unirradiated fuel rods.....	2.2
Table 2.2. Comparison of RIA test results for VVER and LWR unirradiated fuel rods.....	2.8
Table 3.1. Program requirements.	3.2
Table 4.1. Balance of the energy densities for fuel rod #H1T.	4.17
Table 7.1. Description of the main stages of the thermal-mechanical behavior of high burnup fuel rod following the data presented in Fig. 7.1.....	7.3
Table 7.2. Approach, used to determine ballooning key parameters.....	7.6
Table 7.3. Possible sources of errors in predicting the maximum cladding hoop strain in rupture zone.	7.10
Table 7.4. Parameters of energy balance vs. fuel enthalpy at failure.	7.16

FOREWORD

The results presented in the published Report constitute a sum total of the final stage of the experimental and analytical research conducted in the framework of the research program to validate the behavior of VVER fuel elements under reactivity-initiated accident (RIA) conditions.

The objective of the presented stage of research was to develop the database on the behavior of high burnup fuel elements under the conditions of the accident of this type.

I would like to point out that the Russian Research Center "Kurchatov Institute" initiated this program in 1983. This was three years before the accident that shocked the whole world with a sharp reactivity rise in the RBMK type reactor in Chernobyl. That accident has demonstrated that in the case of severe fuel damage caused by a fast rise of positive reactivity, there is no time to apply procedures of the accident management, and the only way for the risk reduction is to prevent accidents of this type.

The accident in Chernobyl was the starting point for the radical revision in Russia of both the methodology of safety ensuring and the contents and scope of the scientific basis required for the employment of this methodology.

The only opportunity to realize this objective was to introduce Russia immediately into the international cooperation for studies in the field of nuclear safety, to get the access to the world knowledge base, to realize the domestic research program aimed to study specific features of Russian nuclear power, to exchange widely with partners by the scientific information obtained in the course of studies.

The work performed within the framework of the Program for the research of VVER fuel element behavior under the conditions of reactivity accidents was, as a matter of fact, the proving ground for the elaboration of basic approaches to achieve the formulated goals, to gain the experience for the management of future comprehensive research programs. This program was one of the first Russian research programs in the implementation of which our foreign colleagues took a direct part. Joint duties and responsibilities allowed to elaborate the principles of interaction between Russia and the West, to compare the employed techniques, to create a common language necessary for the mutual understanding.

The important component of this work that led, in my opinion, to the undoubtedly successful result was a constant search of a compromise between the methodical principles taking place in the Russian practice and a simultaneous development of new approaches. This allowed to obtain criteria determining the regulatory basis for safety in the field of dynamic processes associated with the reactivity variation.

A step by step movement to solve this problem led to the result obtained by the present time - to the trustworthy contribution of Russia into the world knowledge base. Only the integration of the efforts of scientists and specialists from the USA, Japan, and France in this field of research being of a great importance from the safety viewpoint allowed to achieve these results.

I would like to point out the real constitutive contribution of Dr. L.A.Yegorova into the all achievements of the presented program who was able to unite all participants of this work, representatives of different organizations and scientific schools, and to direct their efforts to the obtainment of the result published today.

Vladimir G. Asmolov
Director for R&D
RRC "Kurchatov Institute"

FOREWORD (CONTINUED)

The present report is the result of a four-year three-party cooperative effort between the Russian Research Center «Kurchatov Institute,» the French Institute for Protection and Nuclear Safety, and the United States Nuclear Regulatory Commission. This cooperative effort addressed the behavior of high-burnup fuel rods under conditions of postulated reactivity insertion accidents. The first information about reactivity insertion experiments in the Impulse Graphite Reactor (IGR) of the former Soviet Union was revealed to western countries during an International Atomic Energy Agency conference in Aix-en-Provence (France) in 1992. More details were given in later years at the NRC's Water Reactor Safety Information Meetings in Washington.

Striking differences were seen in fuel response to reactivity transients in the IGR tests compared to the fuel response in western tests. These differences have been attributed to design differences between Russian VVER fuel and western PWR fuel and to the larger pulse width of the IGR test reactor. The U.S. NRC and the French IPSN recognized the value of this test program and, in 1995, decided to join with the RRC «Kurchatov Institute» in an assessment and interpretation of the results and to sponsor the final phase of this large in-pile test program.

A coordinated work plan was developed to allow a direct comparison of conclusions from other data sources (namely, SPERT and PBF in the U.S., Cabri in France, and NSRR in Japan). This work plan included (a) data collection and assessment from the IGR tests and from post-test examination, (b) additional tests to obtain transient mechanical properties of VVER cladding, (c) analysis of results using appropriate thermo-mechanical computer codes (FRAP-T6 from the U.S. and SCANAIR from France), and (d) plant transient calculations to apply the results to the reactor case.

This important body of work has been completed by Russian scientists and engineers under the direction of Dr. Larissa A. Yegorova and the general supervision of Professor Vladimir G. Asmolov, whose skill and efficiency we wish to acknowledge.

Ralph O. MEYER
NRC (USA)

Franz K. SCHMITZ
IPSN (France)



ACKNOWLEDGMENTS

Appealing to the readers, it is necessary to note that the foundation of the work presented in the report was laid by many dozens of specialists from different institutes who had taken an active part in the investigations, therefore, I would like to acknowledge and express my appreciation to:

- IGR reactor personnel headed by V. Pakhnitz (Semipalatinsk, Republic of Kazakhstan);
- scientists of Atomic Energy Institute of National Nuclear Center of the Republic of Kazakhstan who were headed by D. Zelinski;
- scientists and production personnel of Russian Research Center "Research Institute of Atomic Reactors" (Dimitrovgrad, Russia) who were involved in this project under the direction of V. Smirnov;
- scientists and experts of Russian Research Center "Kurchatov Institute" (Moscow, Russia) who participated in the research program implemented under the supervision of V. Pavshook (1990-1991) and V. Asmolov (1990-1998).

The sponsorship of named below institutions enabled the conduct of a set of complex and versatile investigations presented in the present report:

- in 1990-1992 Ministry of Atomic Energy of the Russian Federation;
- in 1995-1998 Ministry of Science and Technologies of the Russian Federation;
- in 1995-1998 Institute for Protection and Nuclear Safety (IPSN, France);
- in 1995-1998 US Nuclear Regulatory Commission (USA).

In this context it is important to emphasize a major personal contribution to management of this project made by the following supervisors and leading specialists:

- N. Ermakov, A. Egorov (Minatom of the Russian Federation);
- E. Chukardin (Ministry of Science and Technologies of the Russian Federation);
- T. Speis, T. King (US NRC);
- M. Livolant, M. Gomolinski (IPSN, France).

The second and third volumes of the report present particular thanks to many specialists whose efforts allowed to obtain and interpret the research results. As to the present volume, I would like to express special gratitude to the following key persons who have produced a fundamental impact on the project as a whole:

- A. Vurim (IAE NNC), A. Goryachev (RIAR, Russia) because this project would have perished already at the initial stage but for their efforts and confidence in the final outcome;
- J. Papin (IPSN, France) who was the first to attract attention of the West to this research;
- J. Papin (IPSN, France), H. Scott (US NRC) who were the most attentive reviewers and critics of all intermediate versions of the report;
- E. Kaplar, K. Lioutov, A. Shestopalov, A. Konobeyev, A. Bortash (RRC KI, Russia) who bore a major burden of analytical investigations in preparation of the present report;
- G. Abyshov (RRC KI, Russia) whose skills and experience of system programmer allowed to comprehend and format about 2000 MB of information in the form of a collated data base;
- N. Jouravkova (RRC KI, Russia) who made the computer formatting of the report in a highly professional and esthetically perfect way.

Beyond the scope of the above list I would like to acknowledge the contribution of

- V. Smirmov (RIAR, Russia), because this work forced him many time to launch himself into the unknown making commitments without any guarantees of their successful fulfillment. However, it is precisely this capability that predetermined optimal solution of many topical problems presented in the present report.

I should also emphasize a special role of and should express gratitude to

- V. Pavshook (RRC KI, Russia) who directed these investigations in 1990-1991 because his intuition and professional support made this work develop despite many objective and subjective circumstances.

In addition, one should not underestimate the contribution of those specialists who provided specific counsel about VVER reactors and fuel elements. Here, of course, particular thanks should be expressed to the following persons:

- G. Lunin, V. Voznesensky (RRC KI, Russia),
- Yu. Bibilashvili, N. Sokolov, O. Nechaeva (VNIINM, Russia),
- V. Tsybulya, P. Aksionov (AO MZ, Russia).

In conclusion I cannot but highlight a principal role in this project of three personalities from three countries:

- V. Asmolov (RRC KI, Russia),
- F. Schmitz (IPSN, France),
- R. Meyer (US NRC),

because they directly supervised this project at a decisive stage and were also my principal sparring-partners during numerous analyses and discussions which enabled me to arrive to the current statement of the problem and interpretation of the results.

LIST OF ACRONYMS

AEKI	Atomic Energy Research Institute (Hungary)
ANL	Argonne National Laboratory (USA)
AO MZ	AO Mashinostroitelny Zavod (Electrostal, Russia)
BWR	Boiling-water reactor
CABRI	name of test reactor (France)
CE-Saclay	Research Centre Saclay (France)
CITATION	nuclear reactor core analysis code (USA)
DINAR	3D neutronic dynamic computer code (Russia)
EDO GP	Experimental Design Organization “Gidropress”
FGR	fission gas release
FRAP-T6	fuel rod analysis program, transient version 6 (USA)
GIDRA	name of pulse test reactor (Russia)
IAE KI	Institute of Atomic Energy “Kurchatov Institute” (former name of RRC KI)
IAE NNC	Institute of Atomic Energy of National Nuclear Centre of Kazakhstan Republic (Kazakhstan)
IGR	Impulse Graphite Reactor (Kazakhstan)
IPSN	Institute for Protection and Nuclear Safety (France)
LOCA	loss-of-coolant accident
LWR	Light-water reactor
MATPRO	Library of material properties for LWR accident analysis, version 11 (USA)
MCU	Monte Carlo code for neutron transport calculations (Russia)
MIR	loop test reactor (Russia)
NSI RRC KI	Nuclear Safety Institute of Russian Research Centre “Kurchatov Institute” (Russia)
NSRR	Nuclear Safety Research Reactor (Japan)
NV NPP	NovoVoronezh nuclear power plant
PBF	Power Burst Facility (USA)
PCMI	Pellet-cladding mechanical interaction
PIE	post-irradiation examination
PWR	Pressurized-water reactor
RIA	Reactivity-initiated accident
RIAR	State Research Centre “Research Institute of Atomic Reactors” (Russia)
RRC KI	Russian Research Centre “Kurchatov Institute” (Russia)
SCANAIR	code for describing the fuel behavior under an RIA transient (France)
SPERT	Special Power Excursion Reactor Test (USA)
TRIFOB	code for calculation of isotopic composition (Russia)
VNIINM	All-Russian Research Scientific Institute for Inorganic Materials (Russia)
VVER	Russian type of pressurized-water reactor

1. INTRODUCTION

During the period of 1990 – 1992, specialists of the Russian Research Centre “Kurchatov Institute” prepared and implemented a research program on experimental studies of fuel element behavior of VVER-type water cooled reactors with high burnup under reactivity initiated accident.

The present program was implemented in cooperation with a number of research institutions of the ex-USSR:

- Research Institute of Atomic Reactors , Dimitrovgrad – design and manufacturing of re-fabricated fuel elements and experimental capsules, conduct of pre- and post- test examination.
- AO Mashinostroitelny Zavod, Electrostal – design and manufacturing of experimental fuel elements with fresh fuel.
- “Joint Expedition, Research Institute “Luch” Scientific and Industrial Association, Semipalatinsk – preparation and conduct of reactor tests of re-fabricated fuel elements.

The Ministry of Atomic Energy of the USSR was the sponsor of the work.

The main purpose of the program was to produce the data base required to overcome the main contradiction that appeared by the beginning of 1990s in the area of safety validation of water cooled reactors under RIA conditions. The essence of the contradiction was that the practical considerations required to validate the fuel element performance during all operating cycles of the reactor; however, at that time both the Russian and the world data base contained a set of criteria which were mainly obtained as a result of tests of the fresh fuel.

In this regard, the following main problems were planned to be solved within the framework of the reactor test program of VVER-1000 type fuel elements with the burnup of about 48 MWd/kg U:

- to determine the energy thresholds of the fuel element destruction (cladding failure threshold, fragmentation threshold);
- to study specific features of the mechanism of deformation and failure of high burnup fuel elements in comparison with corresponding mechanisms in fresh fuel elements.

Unfortunately, due to features of the economic situation in Russia at the beginning of 1990s, as well as conviction of specialists (who dealt with practical validation of specific designs of nuclear power plants) that the available data base is adequate in this area, the research program was frozen at the stage of completing the post-test studies of fuel elements.

The revival of the research under the High Burnup RIA VVER program was caused by the request to perform reassessment of RIA data base and to update the safety standards taking into account the whole set of recent RIA tests with high burnup fuel at CABRI, NSRR, IGR reactors [1 – 4].

Within the years 1995 – 1998 the special cycle of researches was performed with the aim, to add to generalize and complete the data base characterizing behavior of VVER fuel rods under IGR test conditions in the framework of the agreements – NSI RRC KI – US NRC (USA), NSI RRC KI – IPSN (France) with the financial support by the Ministry of Science of RF.

This cycle of investigations allowed to expand the boundaries of the obtained data base due to the conduct of the following original test and analytical studies:

- original neutronic codes were implemented, modified and verified to determine spatial distributions of fissile isotopes and energy deposition in high burnup fuel rods, power and energy deposition in fuel rods versus time;
- FRAP-T6 (USA) and SCANAIR (France) computer codes were modified and verified to simulate scenarios of RIA tests of non-irradiated and high burnup fuel rods in the IGR reactor;
- mechanical properties of non-irradiated and irradiated Zr-1%Nb claddings were measured and included into input data in FRAP-T6 and SCANAIR codes;
- mechanical properties of Zr-1%Nb cladding at high temperature rupture were determined and used to calculate failure of test fuel rods;

- different pre- and post-test examinations were made to form the multiprofile test data base.

This volume of the report is written to give a general idea about the test program, calculation and experimental procedures, and obtained results. An emphasis is therewith made on the analysis of the obtained data base in terms of fuel rod behavior under RIA conditions.

2. BACKGROUND OF THE VVER-1000/RIA TEST PROGRAM

Schematically, the historical aspects of this problem can be summarized as follows:

1. **1974.** The development of the VVER-1000 reactor design is underway in full conformity with pertinent safety standards that stipulate non-positive total power coefficient of reactivity for all transient and accident conditions. That is why, had these provisions been observed, there would have been no necessity in performing any additional studies to prove the nuclear safety of VVER-1000 type reactors under normal, transient, and accident conditions.
2. **1980.** The putting of the first VVER-1000 type reactor into operation in accordance with the experimental research carried out demonstrated that there was a positive feedback with power via the coefficients of reactivity conditioned by the temperature and density of coolant. Nonetheless, it had been confirmed in the course of the research that the total power coefficient of reactivity was a priori negative.
3. **1982.** New standards, OPB-82, to provide for observance of general provisions on nuclear power plant safety were developed [5]. Items 2.2.2 and 2.3.7 correspondingly read as follows in the document:
 - “Generally, the fast power coefficient of reactivity may not be positive in any of operating modes of the NPP and for any state of the system for heat removal from primary circuit coolant. If the fast power coefficient of reactivity in any of the operating modes is positive, the design of this NPP shall provide for and prove the reactor safety under steady-state, transient, and accident conditions”.
 - “The maximum efficiency of reactivity control devices and the maximum possible rate of reactivity increase in cases of erroneous actions of the personnel or a single failure of any NPP device shall be restricted so that the effect of subsequent power rise does not result in:
 - ⇒ exceeding the maximum permissible pressure level in the primary circuit;
 - ⇒ intolerable deterioration of the effectiveness of heat removal or in melting of fuel elements”.

Thus, the early 1980ies were the time when the problem of reactivity initiated accidents (RIA) for VVER type reactors was considered as if it were non-existing. Very few analytical studies performed by that time had demonstrated that in the worst case the departure from nucleate boiling may occur in some fuel rods in which the highest heat power is attained. Nevertheless, certain realization of the fact that the analyses and estimations fulfilled were far from being perfect as based on a relatively imperfect data base and inadequate numerical codes did appear. That was the reason why the first step in this direction was an experimental program aimed at studying the behavior of VVER fuel under power pulse conditions. It was initiated in 1982 by the following institutes:

- the Institute of Atomic Energy (IAE), nowadays – the Russian Research Centre “Kurchatov Institute”;
- Experimental Design Organization “Gidropress”;
- All-Russian Research Scientific Institute for Inorganic Materials.

The RRC KI was put in charge of implementing the program. The program itself was developed with taking two important factors into account:

1. Some programs, similar in their objectives and aimed at studying the behavior of PWR and BWR type fuel, had been completed or were underway in the USA and Japan [6, 7].
2. VVER RIA scenarios had received practically no outlines in what concerned both set of such scenarios and expected parameters of fuel rods. The bulk of the work in this direction was carried out in the post-Chernobyl period.

That is why it was impossible to use the first of the two known methodological approaches employed when developing the program of experimental research since this approach is based on as accurate reproduction of initial and boundary conditions (typical of the commercial facility) in the experiments as possible. As noted above, such a data base was not available and therefore the second approach was used for developing the program. The approach is based on experimental validation of the behavior of the facility under investigation under the most conservative assumptions and in as broad ranges of variation in key factors as possible to solve the following basic problems:

- to obtain experimentally validated failure criteria;
- to obtain a set of empirical relationships characterizing the interrelation of the parameters of interest in such a wide range that, from the practical viewpoint, they could be considered physical correlations;
- to obtain a multi-parametrical data base for verification of computer codes intended for subsequent analysis of RIA scenarios.

Naturally, the experience and results of RIA tests with unirradiated LWR fuel rods were analyzed and taken into account when developing the VVER program. A brief summary of the results on PWR and BWR types of fuel elements, employed in preparation of VVER/RIA tests, is given in Table 2.1 [6, 7].

Table 2.1. Summary of the RIA tests results with LWR unirradiated fuel rods

Position	Comments
1. Test facilities: <ul style="list-style-type: none"> • SPERT-CDC (USA) • PBF (USA) • NSRR (Japan) 	The Special Power Excursion Reactor Tests (SPERT) conducted in the Reactor Capsule Driver Core (CDC) Facility The INEL Power Burst Facility (PBF) The Nuclear Safety Research Reactor (NSRR)
2. Types of fuel rods	LWR type with variation in cladding material, fuel material, fuel-cladding gap, outer diameter of fuel rod, fuel form, fuel enrichment, cladding heat treatment, etc.
3. Major characteristic of fuel rod design: <ul style="list-style-type: none"> • fuel stack length • internal gas pressure 	130–150 mm (SPERT-CDC, NSRR) 800 mm (PBF) generally, 0.1 MPa; special tests were accomplished with pressurized fuel rods
4. Coolant conditions: <ul style="list-style-type: none"> • capsule tests with single fuel rods • capsule tests with a shroud and small clusters • hot startup conditions with a shroud and single fuel rods or test fuel bundles 	ambient temperature, atmospheric pressure, no flow (SPERT-CDC, NSRR) ambient temperature, atmospheric pressure, no flow (SPERT-CDC, NSRR) Coolant parameters (PBF): ⇒ 538 K ⇒ 6.45 MPa ⇒ 85 cm ³ /s
5. Power shape	Power pulse from zero power with a pulse width of 4–30 ms (SPERT-CDC, PBF, NSRR)
6. Major results for SPERT-CDC tests: <ul style="list-style-type: none"> • highest enthalpy¹⁾ without cladding failure • lowest failure threshold • type of the lowest failure threshold 	203–239 cal/g fuel 240 cal/g fuel melting and then cracking of oxygen-embrittled cladding during cooldown

¹ Here and hereinafter, the radial average peak fuel enthalpy is employed for assessing the failure threshold.

Position	Comments
<ul style="list-style-type: none"> fragmentation threshold 	245–264 cal/g fuel
<ul style="list-style-type: none"> fuel dispersion threshold 	>275 cal/g fuel
7. Major results for PBF tests: <ul style="list-style-type: none"> highest enthalpy without cladding failure lowest failure threshold type of the lowest failure threshold partial fragmentation of fuel rod 	225 cal/g fuel 250 cal/g fuel cracking of oxygen-embrittled cladding during cooldown and partial fuel loss 260 cal/g fuel
8. Major results for NSRR tests: <ul style="list-style-type: none"> lowest failure threshold type of the lowest failure threshold fragmentation threshold 	210–220 cal/g fuel brittle fracture of the cladding caused by severe oxidation 285 cal/g fuel

Additionally, according to [6, 7], the results of the tests on all types of facilities demonstrated also the following:

- the failure threshold was relatively insensitive to cladding material, cladding heat treatment, fuel form, fuel material, width of fuel-cladding gap;
- a reduction of the water to fuel ratio under conditions when a special shroud was used or small clusters were under testing, gave rise to a reduction in the failure threshold by about 15 %;
- an increase in the initial gas pressure inside fuel rods to up to 0.6 MPa led to no variation in the failure threshold;
- the failure threshold for highly pressurized fuel rods (~3 MPa) was 140–150 cal/g fuel.

Thus, in conformity with the data base obtained within the research program on SPERT-CDC, PBF, NSRR facilities, it was decided that the research program on studying the behavior of VVER unirradiated fuel rod under RIA conditions should meet the following requirements:

- capsule tests under ambient coolant conditions should be envisaged;
- typical material composition and radial dimensions for VVER-1000 fuel elements (cladding of Zr-1%Nb alloy, UO₂ fuel with enrichment of 4.4 %, cladding outer diameter of about 9.11 mm);
- the fuel stack length of about 150 mm;
- the initial gas pressure inside a fuel rod from 0.1 to 2.5 MPa;
- the type of the reactor power shape is a power pulse, starting from zero power.

However, after accounting for both the total uncertainty in parameters of RIA scenarios at VVER type NPPs and the experimental potential of research reactors in the former USSR, the range of varied parameters was increased by two more items:

- the pulse width of the reactor power of 4–1000 ms;
- the initial coolant pressure of up to 16 MPa.

In addition, within the framework of the main program, a special research subprogram was developed as well to provide for measurements of thermal mechanical parameters of test fuel rods.

In agreement with the decision to amplify the range of reactor power pulse width, two research impulse reactors were chosen to perform the tests (see Chapter 2 of Volume 2 of the present report):

- the GIDRA reactor [8];
- the IGR reactor.

In the required range of energy deposition, the characteristic pulse width of the GIDRA reactor is 4–8 ms. The respective quantity for the IGR reactor is 600–1000 ms. To provide for intermediate pulse width values (100–500 ms), a special procedure was evolved some time later, which envisaged addition of a certain amount of boric acid in the coolant and thereby assured a drop in energy deposition in the fuel rods, with the requisite pulse width retained. The set of power shapes, illustrating the test conditions for IGR and GIDRA reactors, is depicted in Fig. 2.1.

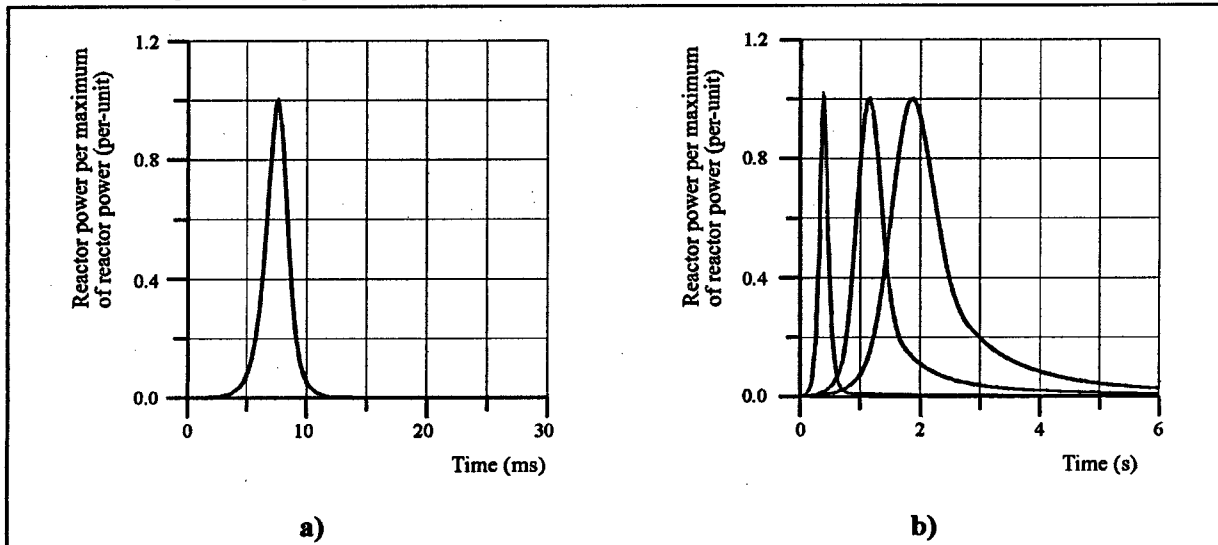


Fig. 2.1. Power shapes for GIDRA (a) and IGR (b) reactors.

The schemes of capsule tests were practically the same for both reactors and corresponded to the approach shown in Fig. 2.2.

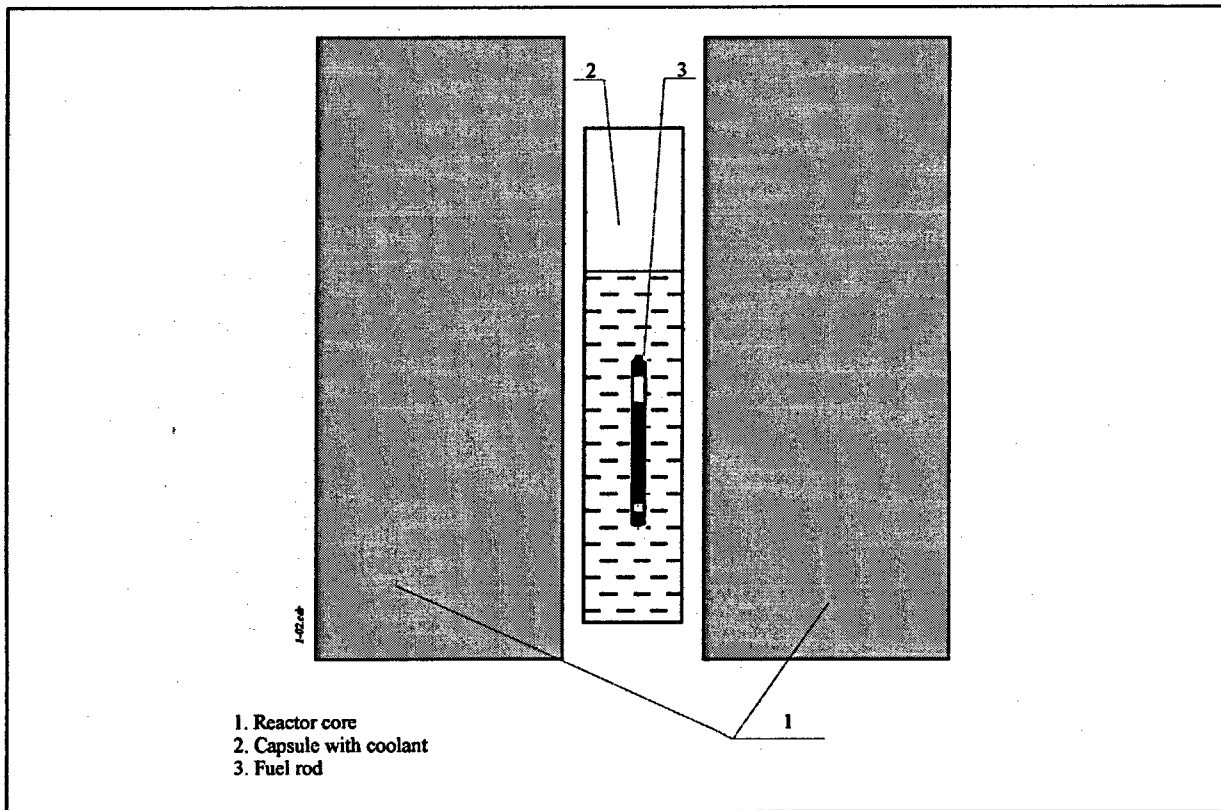


Fig. 2.2. Scheme of the reactor capsule tests.

Both schemes involved a capsule width presetting for test fuel rods in the central channel of the reactors, with further provision for the given energy deposition in the fuel rods via extracting control rods out of the reactor. Actually, this resulted in that the given positive reactivity shaped the front edge of the power pulse. The rear edge of the power pulse was provided in the IGR reactor owing to a negative temperature coefficient of reactivity of the reactor core, and as for the GIDRA reactor, it was provided through a negative void coefficient of reactivity.

In general, the program of RIA tests of VVER fuel rods was subdivided into two major stages:

- tests of unirradiated fuel rods;
- tests of irradiated fuel rods.

Evidently, the program was developed so that the first stage including the tests on unirradiated fuel rods was to be performed with an allowance for as many key factors capable of having an impact upon failure threshold and failure mechanism as possible. The second stage of the program addressed testing of high burnup fuel rods under such conditions that would make possible to determine the lowest failure threshold in the course of tests on unirradiated fuel rods. Such an approach allowed clarification of the difference in behavior of high burnup fuel rods as compared to that of unirradiated ones under the most unfavorable test conditions, and formation of a basis for the further stage of the research.

That is why a distinct revealing of key factors that determine the failure threshold and failure mechanisms for unirradiated fuel rods was a very important program phase. A generalization of the complex of the studies performed on unirradiated fuel rods allowed the following preliminary conclusions:

- the failure threshold of unirradiated fuel rods depends only weakly on fuel enrichment, fuel form, fuel-cladding gap, and a number of other design parameters;
- variation in the initial internal gas pressure in a range of 0.1–0.7 MPa does not give rise to variation in the failure mechanism or failure threshold.

Other test parameters that were subjected to variation within the program are as follows:

- the reactor power pulse width;
- the initial pressure drop on the cladding (tests of highly pressurized fuel rods and test with high pressure of coolant);
- the energy deposition in fuel rods.

The data base characterizing these types of tests on unirradiated VVER fuel rods is presented in Fig. 2.3.

The results of these tests evidenced that three different failure mechanisms and three different failure thresholds were observed for the following three fuel rod types (see Fig. 2.4):

- highly pressurized fuel rods;
- standard fuel rods (fuel rods without a pressure drop on the cladding);
- fuel rods tested at a high pressure of the coolant.

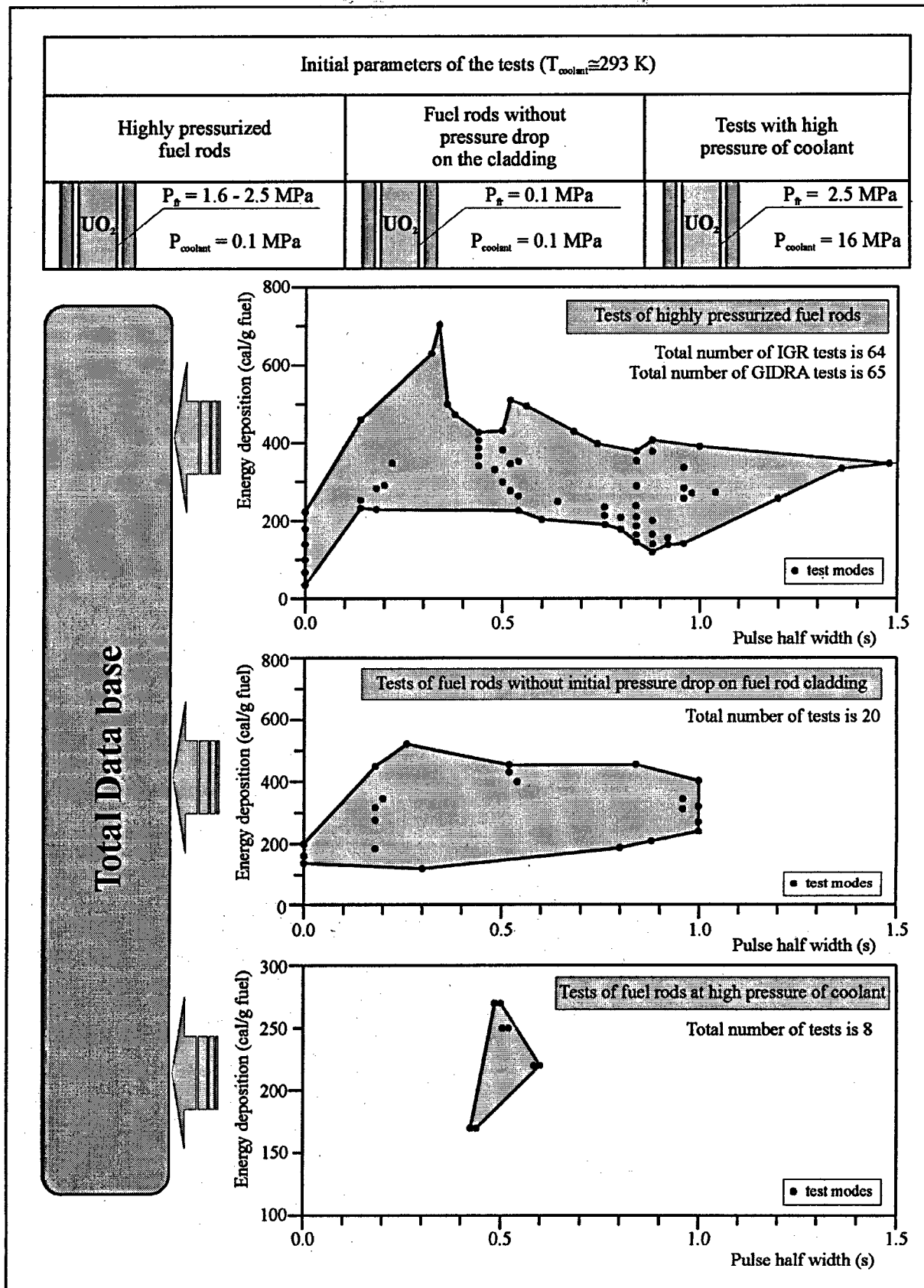


Fig. 2.3. Main types of RIA tests with fresh fuel.

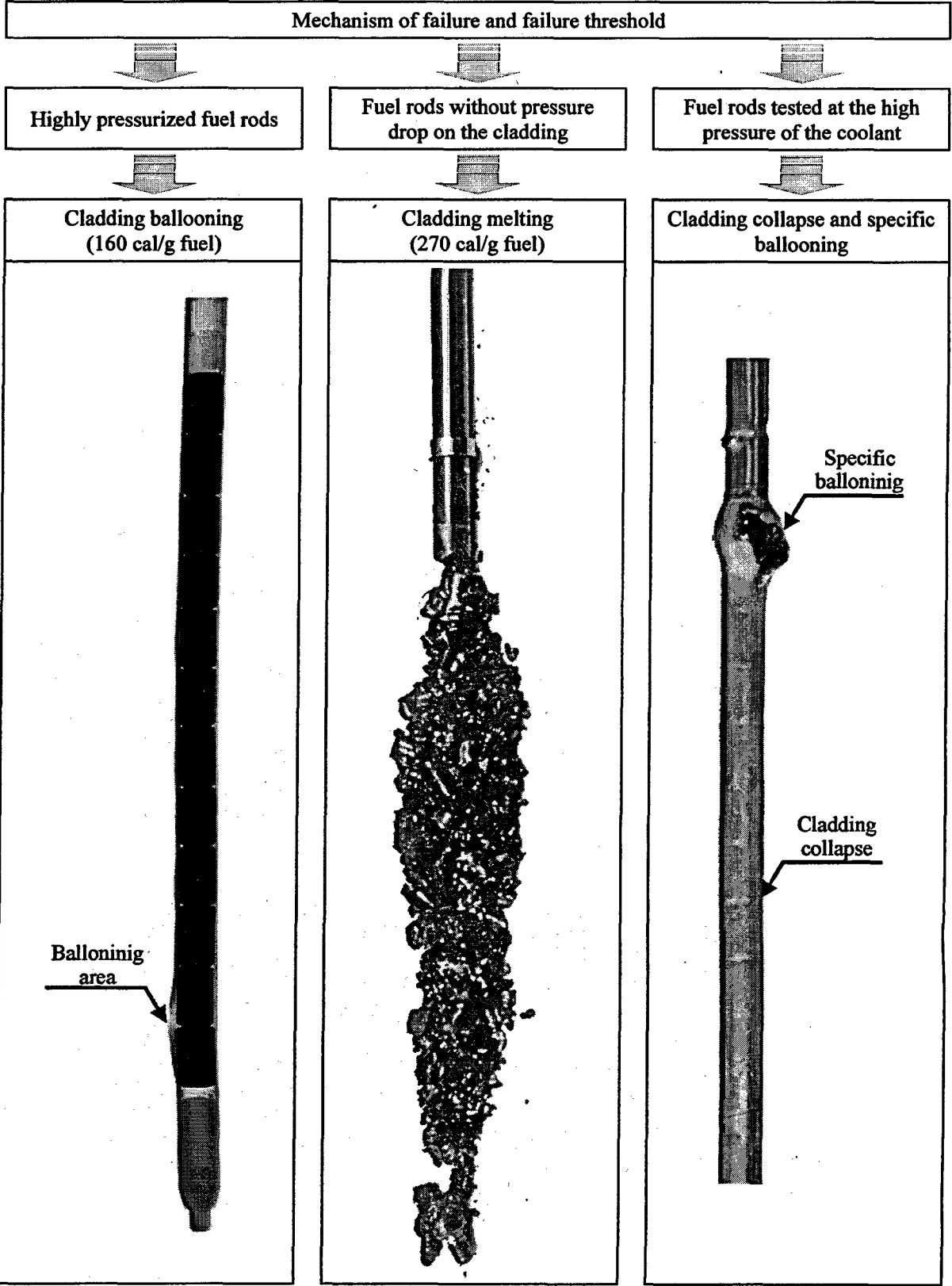


Fig. 2.4. Failure types for VVER unirradiated fuel rods.

A comparison of the obtained results with those derived from testing other types of LWR fuel rods is given in Table 2.2.

Table 2.2. Comparison of RIA test results for VVER and LWR unirradiated fuel rods.

Type of the test	VVER fuel rods		LWR fuel rods		Comments
	Test facilities	Failure threshold and mechanism	Test facilities	Failure threshold and mechanism	
1. Capsule tests of the standard single fuel rods under ambient conditions	IGR	Fragmentation due to fuel and cladding melting and cracking of the oxygen embrittled cladding at 270 cal/g UO ₂	SPERT-CDC NSRR	Fragmentation due to fuel and cladding melting and cracking of the oxygen embrittled cladding at: 270 cal/g UO ₂ (SPERT-CDC); 285 cal/g UO ₂ (NSRR)	Standard fuel rods were tested in the GIDRA also, but the failure threshold was not achieved
2. Capsule tests of the highly pressurized fuel rods under ambient conditions	GIDRA IGR	Ballooning and cladding rupture (high temperature cladding burst) at 160 cal/g UO ₂	SPERT-CDC NSRR	Ballooning and cladding rupture (high temperature cladding burst) at 140–150 cal/g UO ₂	Initial gas pressure in VVER fuel rods was lower and VVER fuel rods had the large size of upper gas plenum
3. Capsule tests under high coolant pressure (16 MPa)	IGR	Collapse of cladding and specific ballooning due to fuel melting at 250 cal/g UO ₂	NSRR	Collapse of cladding and cracking in axial directions at 230 cal/g UO ₂	Initial gas pressure in NSRR fuel rods was 0.1 MPa, the corresponding value for IGR fuel rods was 2.5 MPa

Thus, the comparison data presented in Table 2.2 allow the conclusion that the behavior of VVER and LWR unirradiated fuel rods under similar RIA conditions has very much in common. However, it should be noted that for the standard type of fuel rods (initial internal pressure of 0.1 MPa) in VVER fuel rods, no lowest threshold of failure due to cracking of the oxygen-embrittled cladding during cooldown (210–250 cal/g UO₂) was detected as distinct from LWR fuel rods. An additional analysis should be carried out to reveal this difference in behavior. In addition, the tests on the two types of VVER fuel rods (standard and highly pressurized ones) showed that the pulse width exerts practically no impact upon the failure mechanism or failure threshold of unirradiated fuel rods.

After the first stage of the program of tests on unirradiated VVER fuel rods was completed, the development of the second stage dedicated to the behavior of high irradiated VVER fuel rods under RIA conditions was started. The report as a whole and this Volume in particular deal with presentation of the results of this program stage and analysis of the results obtained.

3. MAJOR PROVISIONS OF THE PROGRAM TO STUDY THE VVER HIGH BURNUP FUEL RODS BEHAVIOR UNDER RIA CONDITIONS

So, in the late 1980ies the basic data characterizing the behavior of VVER unirradiated fuel rods were obtained and the development of the program addressing the testing of high burnup fuel was initiated. A specific complexity of the task consisted in that the then available data base with parameters of high burnup fuel rods was extremely scarce. Moreover, practically all the data had been obtained under conditions of base irradiation simulated in research reactors. As for the experiments with high burnup fuel under RIA conditions, a limited number of papers contained a small amount of information regarding the tests performed on the BWR type of fuel rods in the SPERT reactor and those on the PWR type of fuel rods in the PBF reactor [6]. When doing so, the preliminary irradiation of those fuel rods was carried out in research reactors as well.

Despite all this, it was decided to develop a program meeting the principles presented in Fig. 3.1.

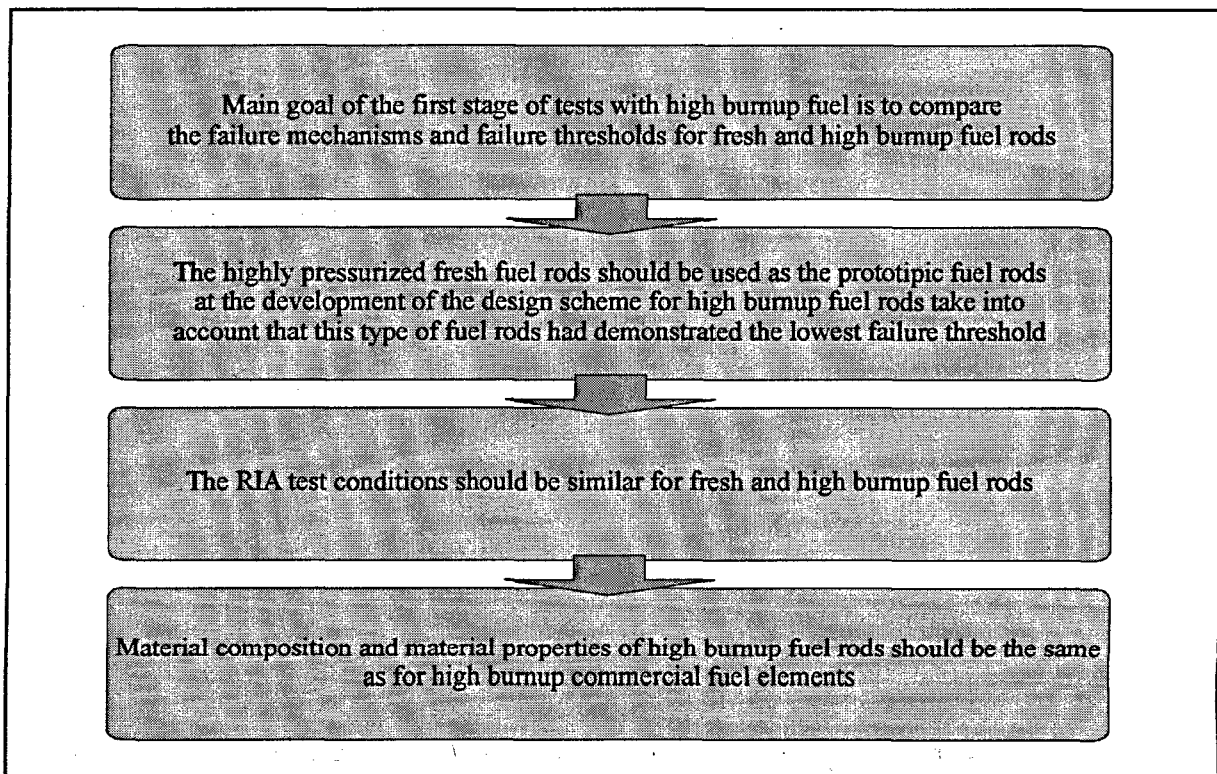


Fig. 3.1. Main principles for the development of the program of VVER high burnup fuel tests.

In accordance with these principles, the technical requirements given in Table 3.1 were evolved. Commercial fuel elements of the VVER-1000 type with a burnup of about 48 MWd/kg U irradiated in the 5th unit of NV NPP were picked up for preparation of 13 high burnup fuel rods through refabrication. In addition, the irradiated claddings of these commercial fuel elements were used for manufacture of 10 fuel rods with fresh fuel and an irradiated cladding. And, finally, 20 unirradiated fuel rods more were fabricated to be tested within the framework of one and the same research program.

Table 3.1. Program requirements.

Program requirements	Motivation
<p>1. Type of test fuel rods:</p> <ul style="list-style-type: none"> • irradiated highly pressurized fuel rods (type C); • highly pressurized fuel rods with irradiated cladding and fresh fuel (type D) • unirradiated highly pressurized fuel rods (type E) 	<p>To obtain a comparative data base characterizing the behavior of unirradiated and irradiated fuel rods in the framework of one cycle of the tests (C and E types of fuel rods)</p> <p>To reveal specific features of the irradiated-cladding behavior in comparison with that of an unirradiated cladding (D and E types of fuel rods)</p>
<p>2. The burnup of fuel for irradiated fuel rods was of about 48 MWd/kg U)</p>	<p>This value of the burnup corresponded to the burnup of the maximum heat loading fuel assembly of the VVER-1000 type at the end of 3-year fuel cycle</p>
<p>3. Type of the reactor for the high burnup RIA tests:</p> <ul style="list-style-type: none"> • IGR reactor 	<p>Calculations had demonstrated that for high burnup fuel it is impossible to achieve an energy deposition higher than 80-100 cal/g fuel in the GIDRA reactor</p>
<p>4. Method to manufacture high burnup fuel rods:</p> <ul style="list-style-type: none"> • refabrication from VVER commercial fuel elements 	<p>To guarantee reproduction of the material composition, material properties and radial geometrical sizes</p>
<p>5. Type of the tests:</p> <ul style="list-style-type: none"> • capsule tests under standard initial conditions (293 K, 0.1 MPa) 	<p>Similarity to earlier performed tests</p>

In compliance with the requirements given in Table 3.1, it was decided to provide the following test conditions in the course of testing on these fuel rods:

- those of capsule tests of fuel rods in the IGR reactor;
- the reactor power shape is a power pulse with a pulse width of about 600–900 ms;
- fuel rods should be tested with two types of coolant: water and air;
- initial parameters of the coolant are as follows:
 - ⇒ atmospheric pressure;
 - ⇒ ambient temperature;
 - ⇒ no flow rate.

Unfortunately, in view of the specific requirements imposed upon the safety of the tests, no thermal mechanical parameters of the fuel rods and the coolant were measured in the course of the experiments. This circumstance, in combination with the absence of the diagnostics of fuel rod condition (failed / non-failed) at the IGR reactor both in the course of and after RIA tests, resulted in, actually, a “blind” performance of the tests. Some steps described in Volume 2 of the report were undertaken to reduce the negative consequences of these factors. However, one should bear this in mind while analyzing the results of the tests when sometimes it is not quite clear for which purpose precisely this or that test mode was implemented.

To suit the technical requirements above and account for the restrictions described, the following tasks had been developed for testing those types of fuel rods:

- testing of 8 high burnup fuel rods in water coolant under conditions of a stepwise increase in energy deposition from test to test, starting from the value at which the peak fuel enthalpy is slightly lower than 85 cal/g fuel (at such an enthalpy, a high burnup fuel rod was damaged in a SPERT test [6]);
- testing of high burnup fuel rods in air coolant under conditions of a stepwise energy deposition increase;
- testing of 5 fuel rods with an irradiated cladding and fresh fuel in both water and air coolant;
- placing fresh-fuel rods into each capsule with high burnup fuel rods in order to get a data base characterizing the behavior of the two different fuel rod types under the same reactor test conditions.

It should be explained additionally that the objective of testing fuel rods in air coolant was two-fold. On the one hand, they could contribute to elucidation of some effects of fuel rod tests in water coolant since the boundary conditions of air cooled tests are far simpler as compared to water cooled ones and lend themselves easier to numerical analysis. That is, those tests were intended for obtaining a verification data base of a sort. On the other hand, taking into account that in the course of IGR tests pressurized fuel rods were examined, for which the ballooning was the expected deformation mechanism, it decided reasonable to use the obtained data base later, in analysis of the behavior of high burnup fuel rods under LOCA conditions. From this viewpoint, the amplification of the data above with the results on the test version with gas coolant was a justified step. A further analysis of the results obtained (it is presented partially in Chapter 7 of this Volume) confirmed the rationality of such an approach.

The final objective of the entire test cycle was to identify failure thresholds and failure mechanisms for high burnup fuel rods, with as clear revealing of specific physical phenomena characterizing the behavior of this fuel rod type under RIA conditions as possible. However, an attempt of practical implementation of the task faced immediately a number of problems that can be generalized as follows:

- the parameters of high burnup fuel rods prior to RIA tests had been practically unknown since the studies of VVER commercial fuel elements after base irradiation had not been started;
- there was a lack in test procedures for measuring parameters of high burnup fuel rods;
- the procedure for manufacture of refabricated fuel rods was unavailable either;
- there was no method to determine energy deposition versus time in high burnup fuel rods under RIA conditions;
- there were no computer codes for adequate description of the thermal mechanical behavior of high burnup fuel rods or at least calculation of the (r, z, t) distribution of fuel enthalpy;
- a data base with mechanical properties of high burnup fuel rods was unavailable.

Therefore, the spectrum of the tasks that had to be solved within the framework of the program under consideration was amplified significantly through adding a series of additional studies.

The next Chapter contains a description of the structure of the whole complex of the research efforts aimed at solving the entire scope of methodological problems.

4. METHODOLOGICAL ASPECTS OF THE RESEARCH PROGRAM

Practical implementation of this research program provided for development of many original calculation and experimental procedures; these were developed to obtain a multi-parameter system of results necessary for execution of the following program basic tasks:

- determine failure mechanisms;
- determine failure thresholds;
- develop data base for comprehensive analysis of the RIA phenomena.

For the List of the main directions of methodological investigations, see Fig. 4.1.

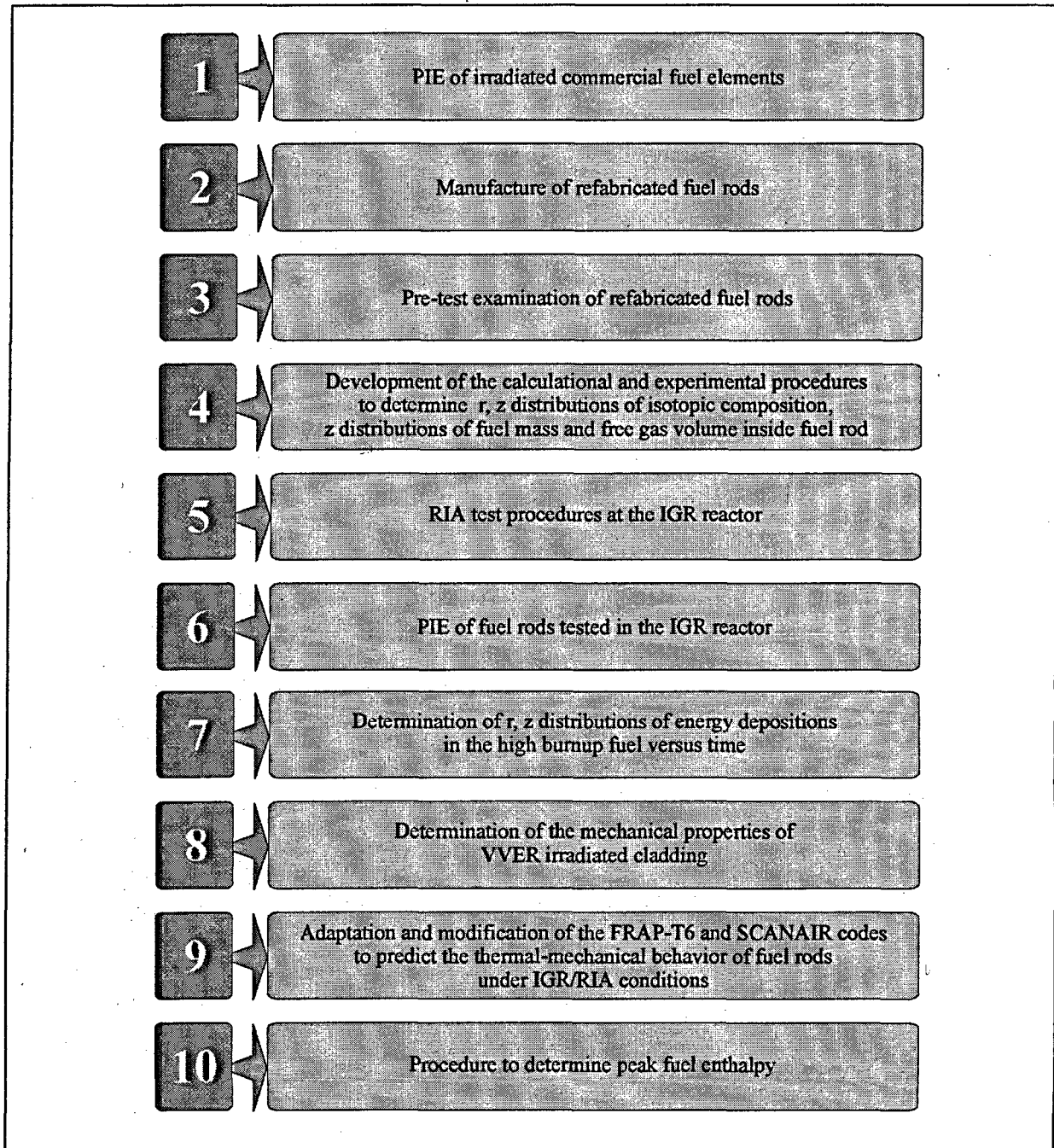


Fig. 4.1. Main directions of methodological investigations.

The purpose of this Chapter is to briefly characterize each direction of methodological investigation, paying special attention to high burnup fuel because careful justification of all the procedures is contained in Volume 2 of the present report.

4.1. Post-test examination of commercial fuel elements

Two commercial fuel elements ## 22 and 317, removed from assembly #1114 of the 5th unit of the NV NPP, were subjected of this investigation (see Appendix B of Volume 3 of the report). Fig. 4.2 shows power history of this unit.

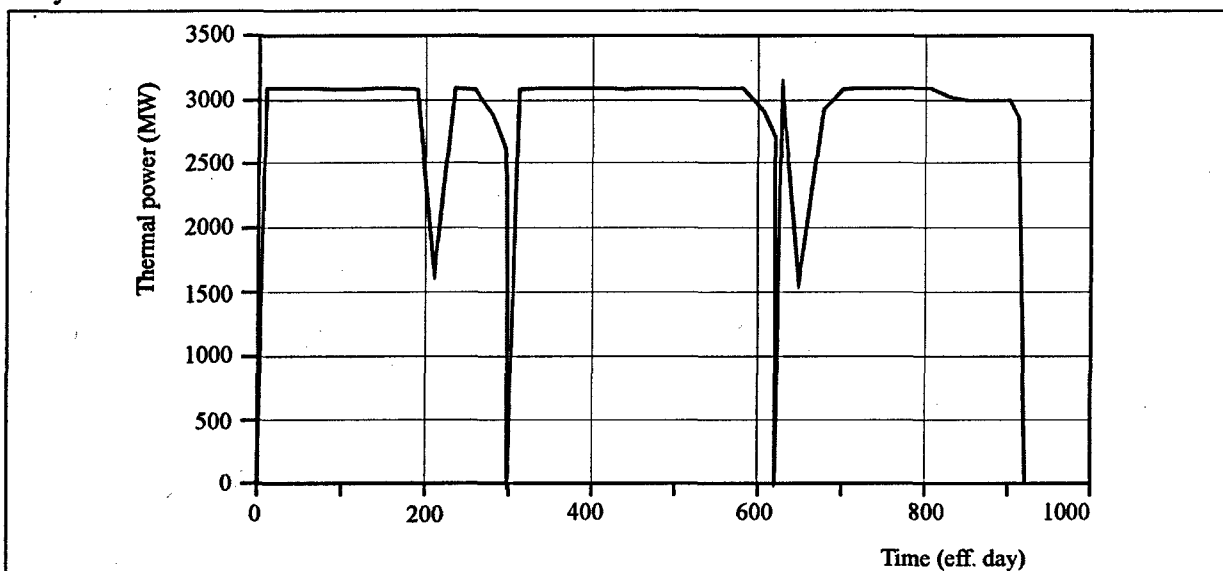


Fig. 4.2. Power history for Unit 5 of NV NPP.

One of the most important phase of the PIE was measurement of fuel elements burnup. Results of spectrometer measurements of z distribution of Cs^{137} , Cs^{134} and Ru^{106} isotopes were used as the basis for obtaining z distribution of burnup for fuel element #317 shown in Fig. 4.3. Special radiochemical measurements were performed on the fuel samples to determine absolute burnup values.

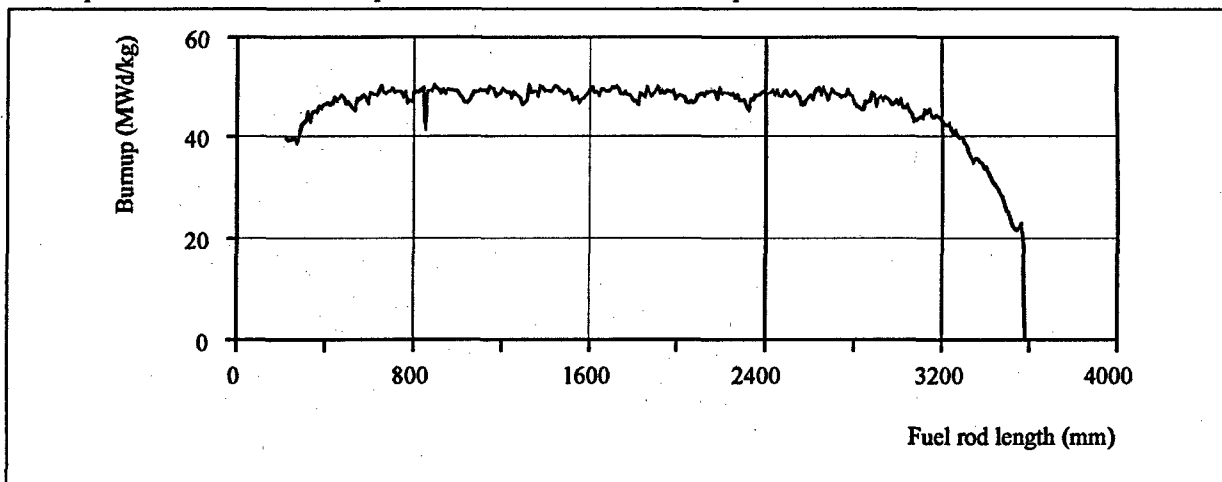


Fig. 4.3. Axial burnup distribution for fuel rod #317.

As can be seen from the data presented in Fig. 4.3, the burnup distribution versus fuel element length is rather uniform within the range from 400 to 2800 mm. Therefore, this part of the fuel element was subsequently used to manufacture refabricated fuel rods. In addition to burnup measurements the following parameters of fuel elements were measured using special procedures:

- density of fuel, grain size, average pellet outer diameter;
- cladding thickness, ZrO_2 thickness, coefficient of the hydride orientation in the cladding, hydrogen content in the cladding;
- gas gap width, gas pressure inside fuel element, gas volume, and gas composition.

To evaluate the actual condition of these fuel elements after the base irradiation, use may be made of some data obtained as a result of the PIE and shown in Fig. 4.4.

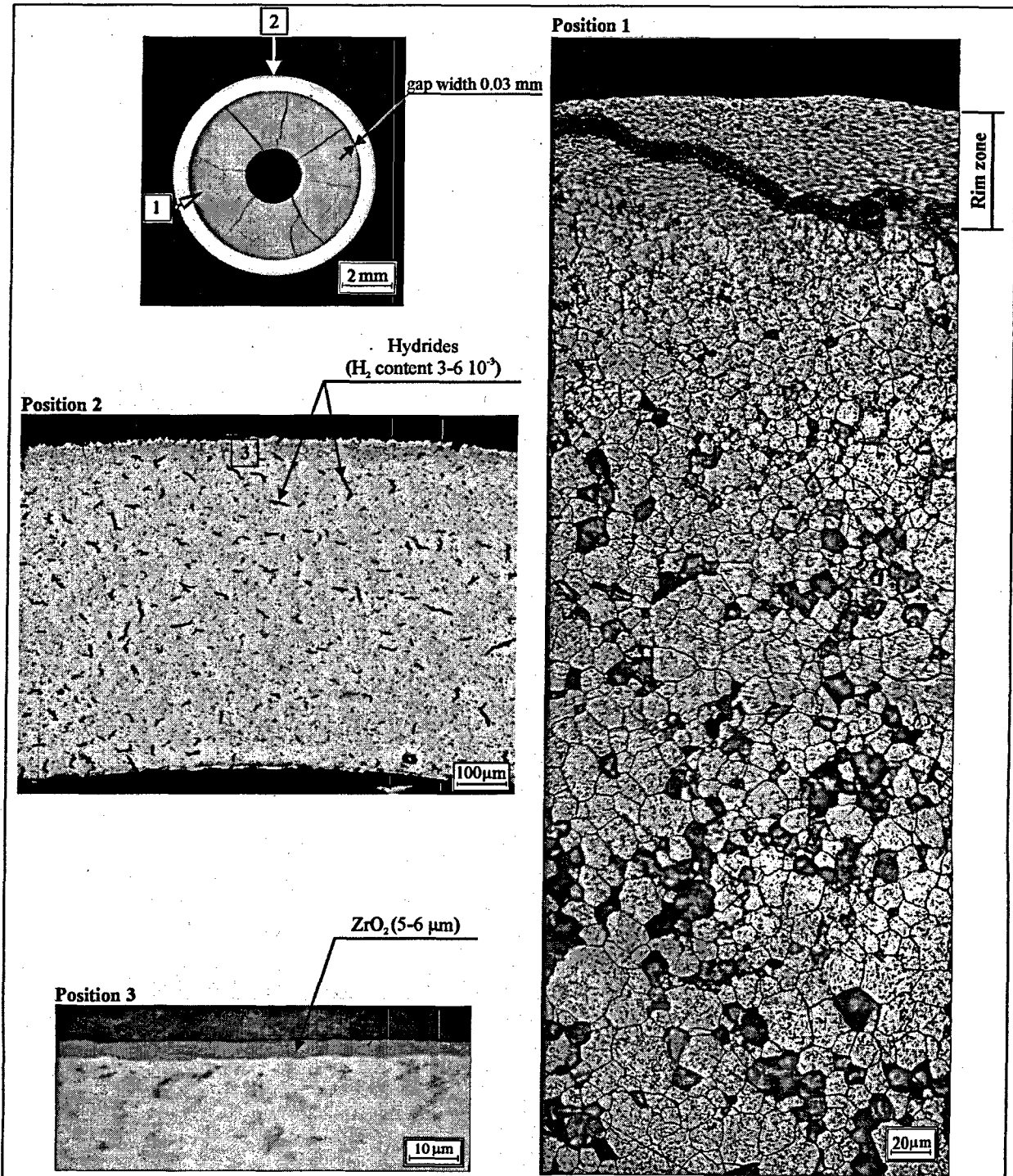


Fig. 4.4. Macro- and microstructure of the commercial fuel element #317.

4.2. Manufacture of refabricated fuel rods

To manufacture high burnup fuel rods the original procedures and equipment have been specifically developed in RIAR. The basic provisions of refabricated high burnup fuel rods manufacturing procedure are shown in Fig. 4.5.

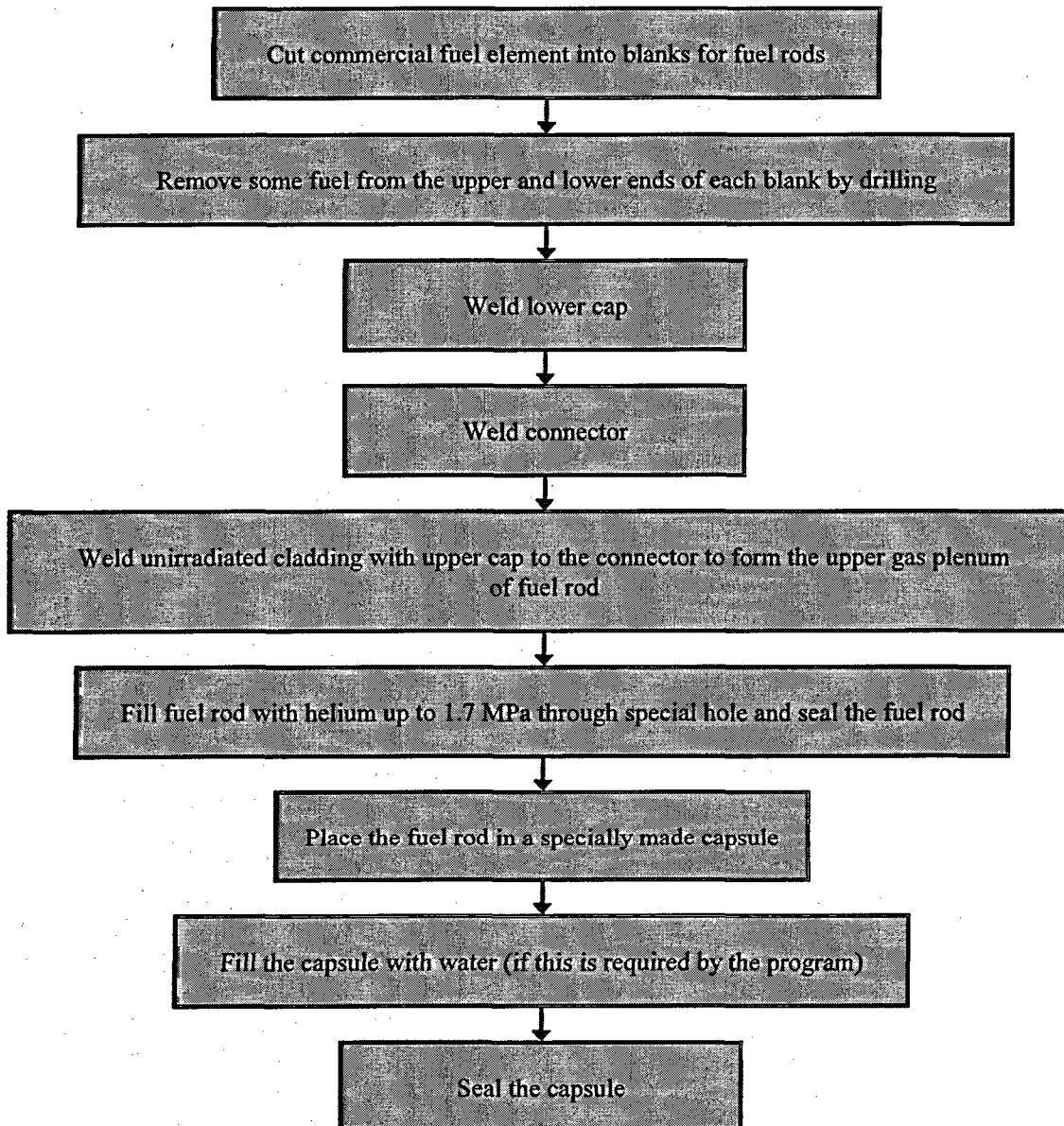


Fig. 4.5. Main provisions of fuel rod refabrication.

In addition to these fuel rods, two other types of fuel rods (fuel rods with irradiated cladding and fresh fuel, unirradiated fuel rods) were also manufactured and placed into capsules. In doing so, normally, two fuel rods were placed in each capsule. One of them was irradiated fuel rod and the other was unirradiated fuel rod. This was done to demonstrate the difference in behavior of these types of fuel rods at one and the same reactor power. In total 23 capsules with fuel rods were manufactured and sent to the IGR reactor for testing.

4.3. Pre-test examination of refabricated fuel rods

Main objective of this phase of investigation was to obtain the data base to characterize the following parameters for each manufactured fuel rod (see Appendixes G, H, I of Volume 3 of the report):

- axial coordinates of some elements of fuel rods;
- axial distribution of fission products;
- axial distribution of cladding outer diameter.

Three basic methods were used to measure these parameters:

- computer analysis of radiography results;
- axial γ -scanning of each fuel rod;
- profilometry of fuel rod.

Besides, as it was previously mentioned, to obtain axial distribution of the burnup in each fuel rod special procedure was used to process the γ -scanning results. For the typical results of this cycle of investigation, see Fig. 4.6 and Fig. 4.7.

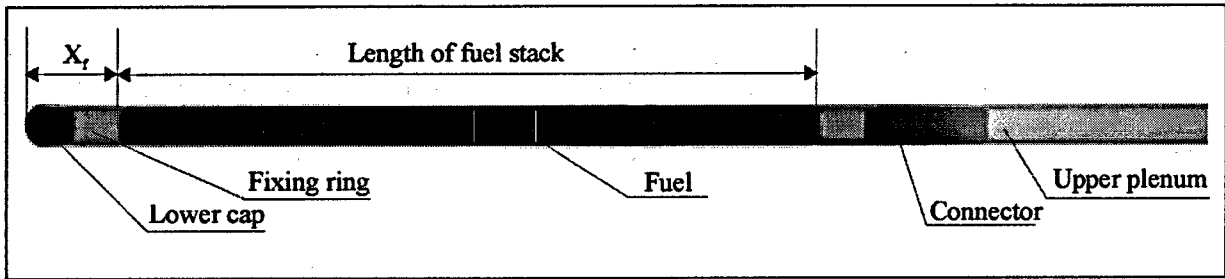


Fig. 4.6. X-ray photograph of fuel rod #H2T.

Reviewing the typicality of these investigations, we must specifically note that due to faults in the refabricated fuel rods manufacturing process some axial geometrical sizes of the fuel rods were inconsistent. This is mainly true of the fuel stack position inside the fuel rod. However, apparently, determination of z-distribution of energy deposition and fuel enthalpy requires establishment of unambiguous link between the fuel stack axial coordinates, and axial coordinates of the capsule, and the IGR reactor. Therefore, this task was resolved individually for each fuel rod by computer processing of radiography data. In doing so, we first of all measured value X_f (see Fig. 4.6) and the fuel stack length. Profilometry of fuel rods was a very important step in pre-test examination because its results formed a data base for analyzing fuel rods deformation and destruction processes during tests under RIA conditions. In addition to what has already been said about the γ -scanning, its results will be further reviewed in the next Section of the report.

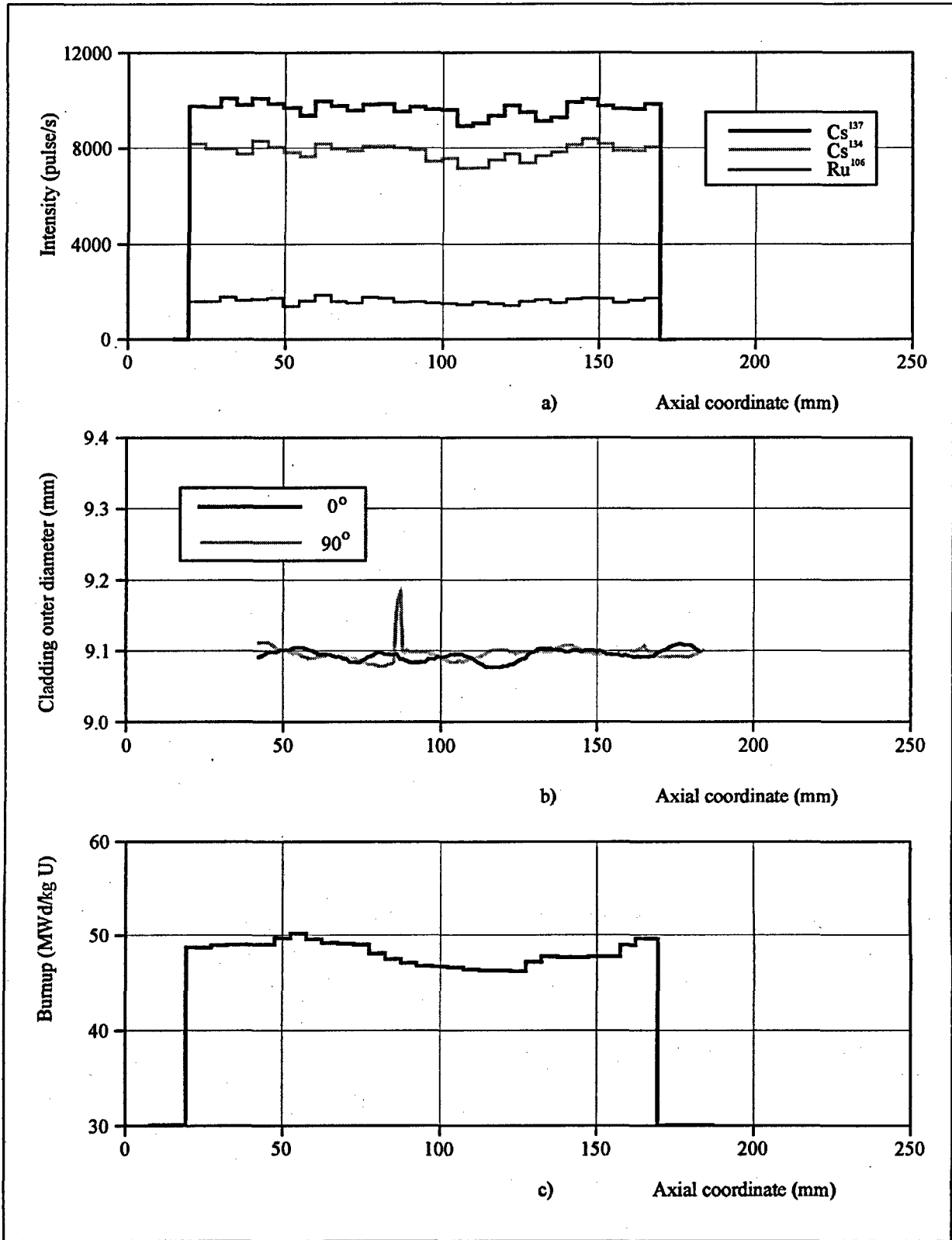


Fig. 4.7. Results of γ -scanning (a), profilometry (b) and burnup measurements (c) for fuel rod #H2T.

4.4. Development of procedures to determine axial distribution of fuel mass, free gas volume and fuel isotopic composition

As to the input data base characterizing parameters of refabricated fuel rods, fuel mass versus fuel length is one of the most important characteristics, which is vital for determining energy deposition and fuel enthalpy in the fuel rod. Normally, when unirradiated fuel rods are tested, this problem is resolved fairly easily since the fuel manufacturer is providing all necessary information. However, special procedure is required when fuel rods are manufactured by refabrication. In this case, the procedure was based on quantitative analysis of spectrometry results, and was verified by performing special tests (see section 3.2.2 of Volume 2 of the report). At the same time, special calculation procedure was developed to determine free gas volume versus fuel rod length, because in calculation of the peak fuel enthalpy and other thermal-mechanical parameters this data file was used to select individual geometrical layout for each fuel rod (see section 3.2.6 of Volume 2 of the report). Results of the test procedures used on one of the high burnup fuel rods are shown in Fig. 4.8.

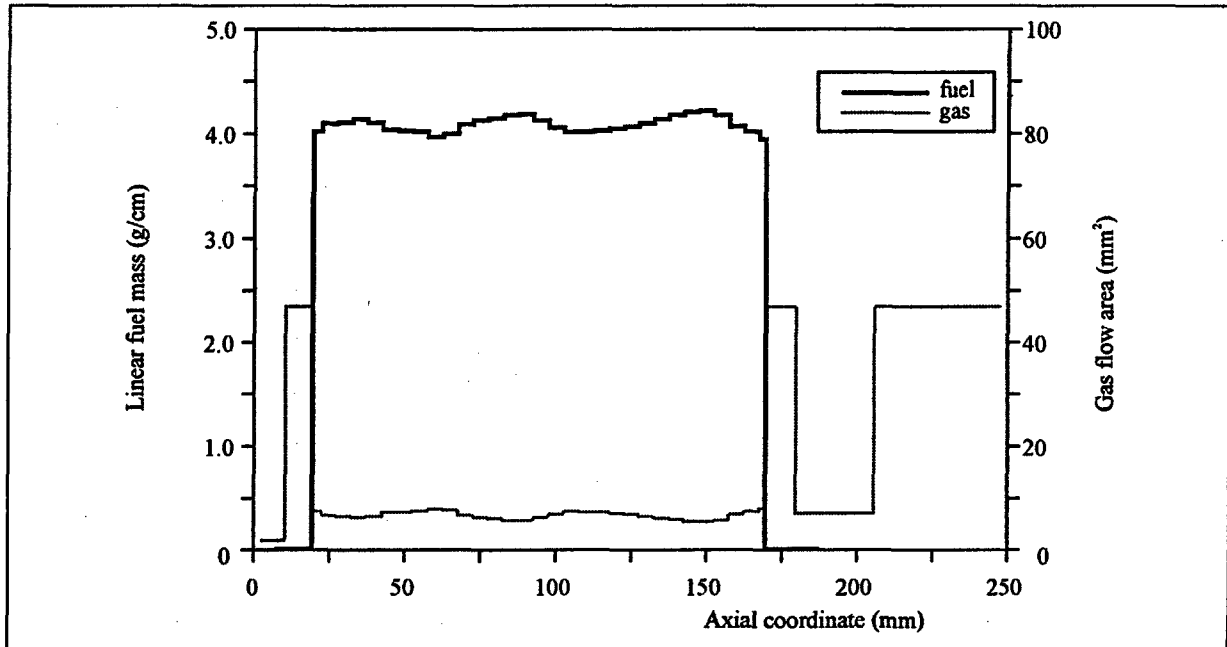


Fig. 4.8. Axial fuel mass distribution and axial free gas volume distribution for fuel rod #H2T.

However, development of procedure for determining r and z distribution of isotopic composition in high burnup fuel for each of the tested fuel rods was the most important problem during preparation of the input data base for the IGR tests. In essence, the problem is there due the fact that energy deposition in fresh fuel practically happens due to fission of isotope U^{235} , which is known to be uniformly spread in the fuel mass. The process of base irradiation of the VVER fuel in the NPP causes gradual accumulation of fissionable nuclides, such as Pu^{239} , Pu^{241} , and a number of other nuclides in addition to U^{235} . Any failure to account for fission of these isotopes would lead to 70 % underestimation of energy deposition during the tests of high burnup fuel rods in the IGR reactor. That is why special requirements were placed on development of procedures for determining isotopic composition of high burnup fuel before the IGR tests. In doing so, when developing the procedure, we had to resolve one more important problem. In essence, the problem was to check radial distribution of Pu isotopes; this was required due to the fact that during base irradiation Pu isotopes are concentrated very irregularly throughout the fuel rod radius. Thus, nuclear concentrations of Pu isotopes in the narrow layer exterior, called the rim zone, exceed concentrations of these isotopes in the center of the pellet more than 2.5 times (see Fig. 4.9). Please note, that neither experimental data pertaining to these effects in fuel rods VVER type, nor verified computer codes required for these purposes were available before this set of procedures was developed (see section 3.2.3 of Volume 2 of the report). Therefore, this procedure was elaborated in compliance with the scheme shown in Fig. 4.10.

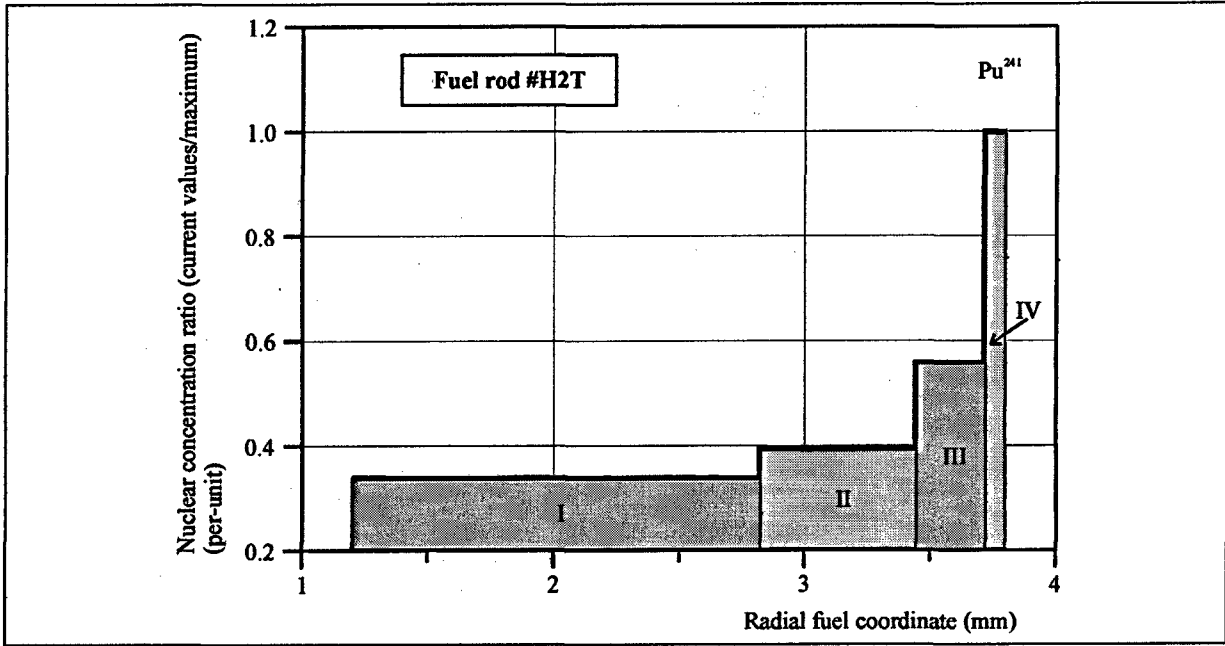


Fig. 4.9. Nuclear concentration of Pu²⁴¹ isotope average on the four radial zones of high burnup fuel.

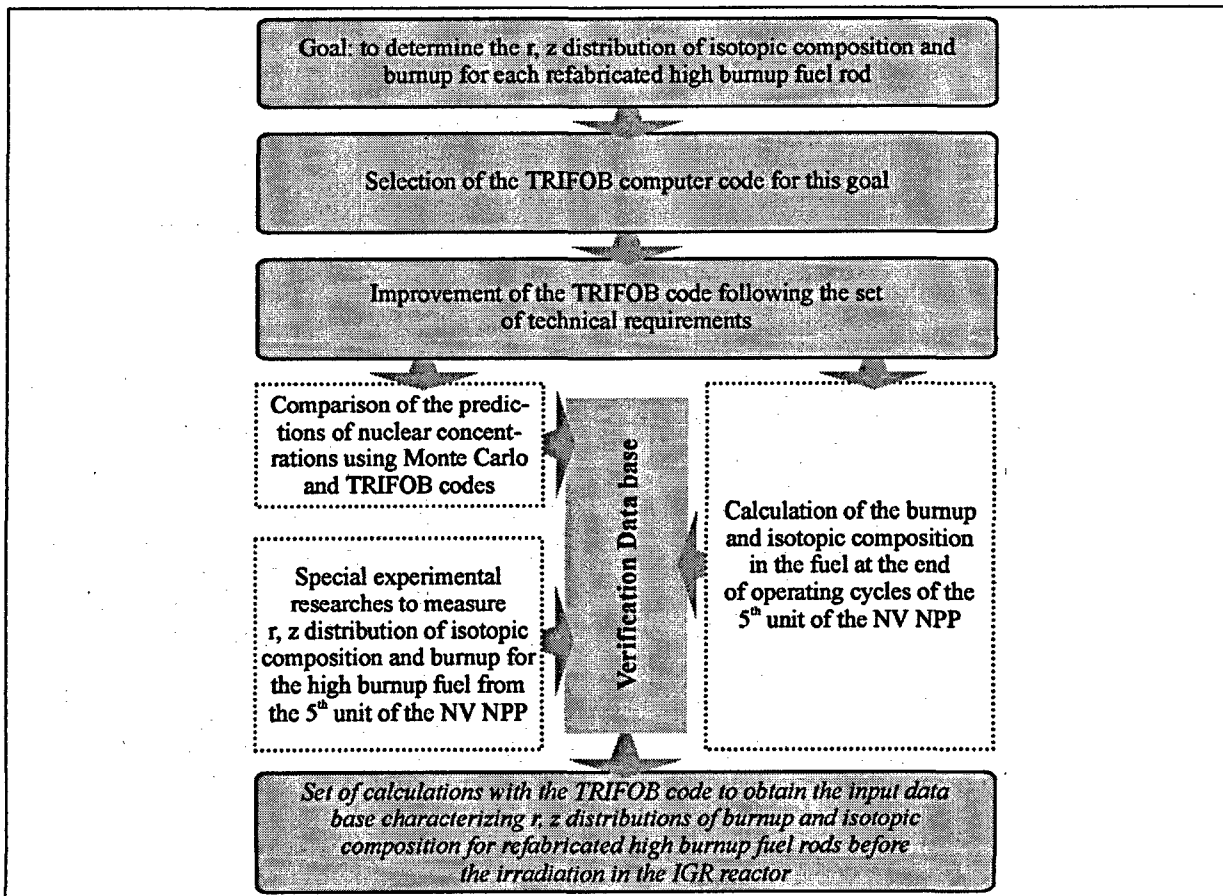


Fig. 4.10. Scheme of the procedure to determine spatial distribution of the burnup and isotopic composition in refabricated fuel rods.

As shown in the scheme, the TRIFOB computer code was selected to compute the required fuel parameters. For the detailed explanation of this choice, see Section 3.2.3 of Volume 2 of the present report. However, some results of the verification procedures to support the use of this code are shown in Fig. 4.11.

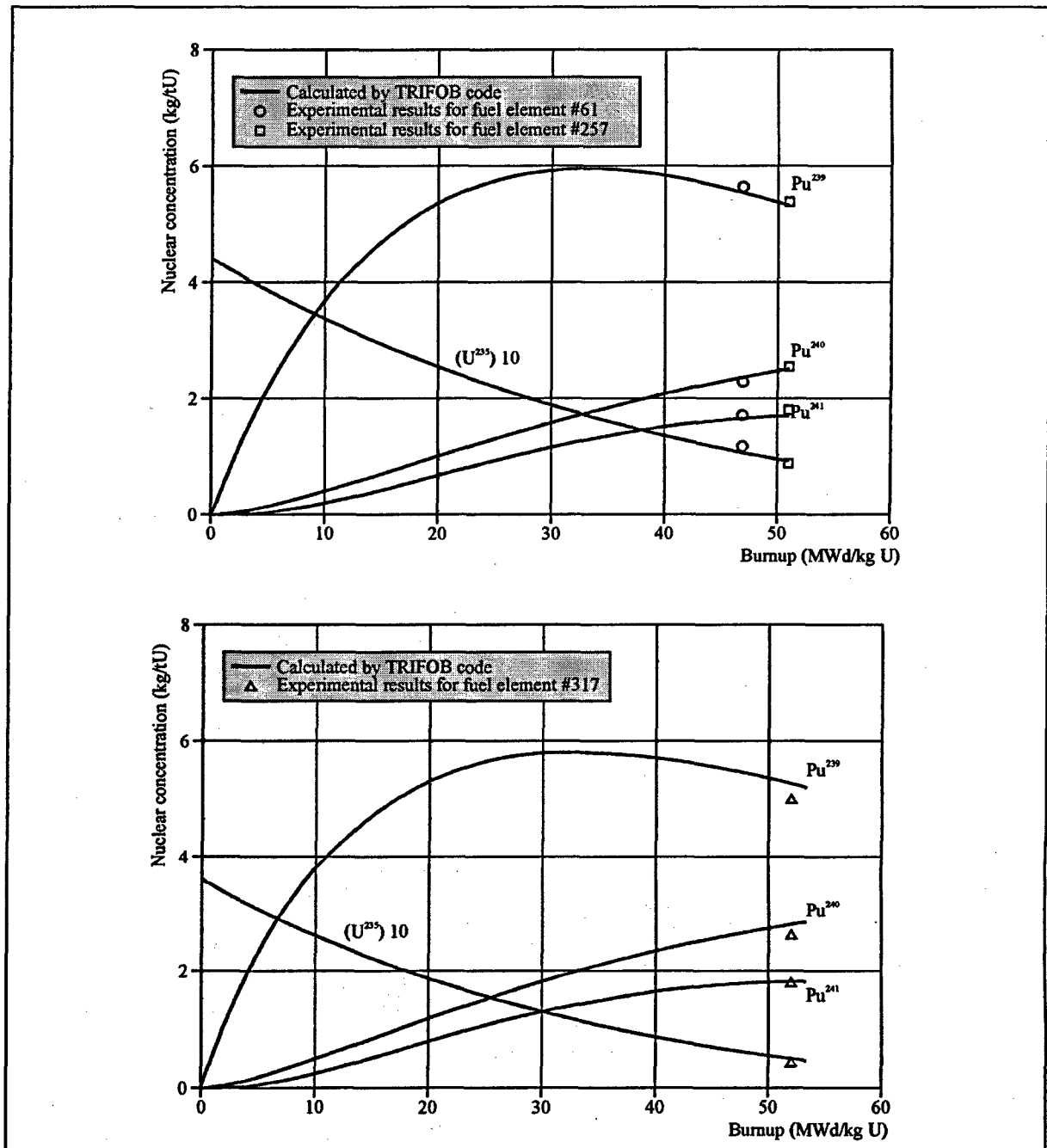


Fig. 4.11. Special TRIFOB verification vs. burnup using NV NPP elements.

After completion of a special investigation cycle aimed at modification of the task code, isotopic distributions was calculated for each fuel rod, taking into account the base irradiation parameters of fuel elements #22 and #317, and the axial coordinates of refabricated fuel rods. As a result, height effects of the reactor core were taken into account in these calculations.

4.5. RIA test procedures in the IGR reactor

As far as the test procedures used on the IGR reactor is concerned, two basic items were specifically looked at:

1. Power shape
2. Absolute number of fissions in special detectors during pulse of power.

Analysis of item 2 will be given in Section 4.7. The present Section will characterize only item 1.

So, apparently, power profile of a fuel rod versus time was to be found eventually for each fuel rod. However, no direct measurements of this parameter are possible. As a result, in all similar cases given task is defined as determination of the factor of proportionality of two power profiles:

- reactor power profile;
- fuel rod power profile.

It is implied that both power profiles are set in relative coordinates (current power per maximum power during the pulse).

To evaluate the scope of the problem, a special test cycle was performed on the IGR reactor. To this purpose, the power shape was measured with the use of several ionization chambers located along the reactor outer perimeter; in addition to that, power shape was registered by several in-core neutron detectors mounted on the circumference around the fuel rod under test. Measurement results obtained in one of the tests are given in Fig. 4.12. These results precisely demonstrate that there are no azimuthal or other spatial effects, which may influence the power profile in the IGR reactor. Therefore, further direct power measurements versus time obtained by reactor ionization chambers were used as the input data base. Yet, one additional problem associated with restoration of power profile versus time required special procedure. This problem was caused by the fact that ionization chamber has a measurement uncertainty near zero. Therefore, taking into account the fact that during pulse the IGR power changes more than 8 orders of magnitude, it was concluded that reactor power cannot be measured in the portion of the pulse where delayed neutron fission occurs and where absolute power value is small.

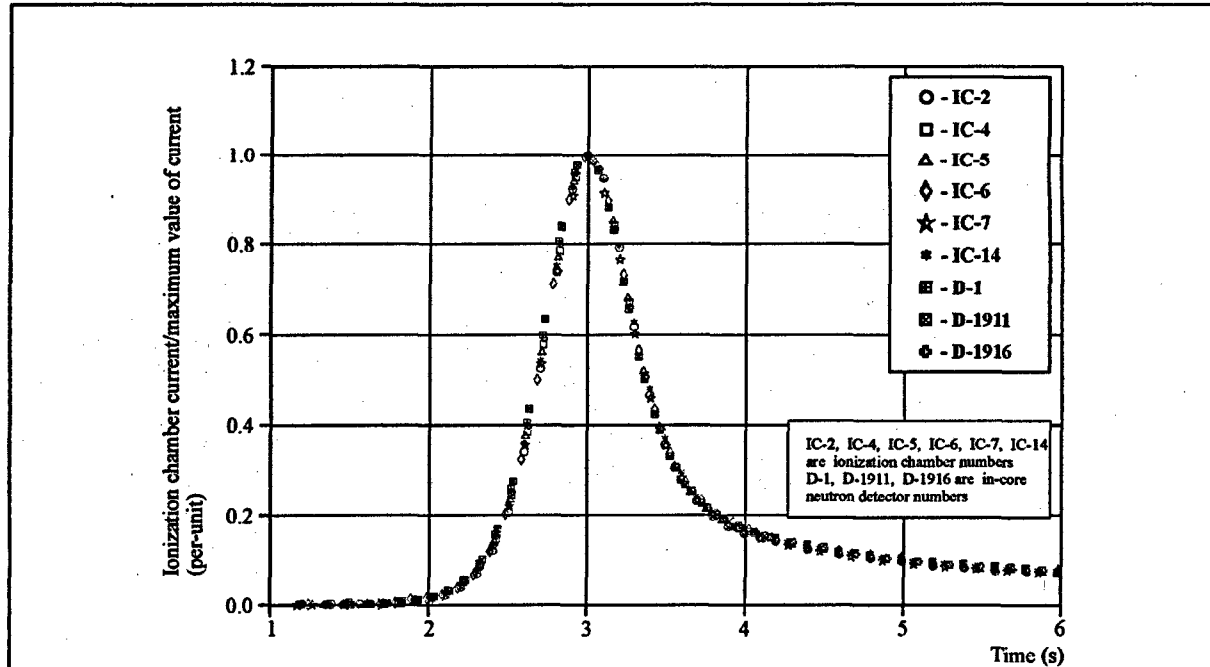


Fig. 4.12. The reactor power profile measured by ionization chambers and in-core detectors.

However, if this problem is left unresolved, then error in determining fuel rod absolute power versus time may be impermissibly high. This is caused by the fact that the fuel rod absolute power was determined by differentiating energy deposition measured in time interval $(0, \infty)$ with respect to measured reactor power profile. As a result, error of power profile prediction at low power values could cause power prediction errors in all other time intervals. This problem was resolved as follows:

- prediction of the IGR reactor power profile near zero power was carried out with the use of 3D dynamic computer code DINAR (see section 4.6 of Volume 2 of the report);
- special modifications of the DINAR code were developed to adapt the code to the IGR tests conditions;
- original tests were developed and performed on the IGR reactor to verify results obtained with the help of the DINAR code.

For evaluation of the quality of the developed procedure Fig. 4.13 shows comparison between calculated and measured power profiles. Special tests were performed with the use of sensitive ionization chambers to obtain experimental data characterizing power profile near zero (see Section 4.6 of the Volume 2 of the report).

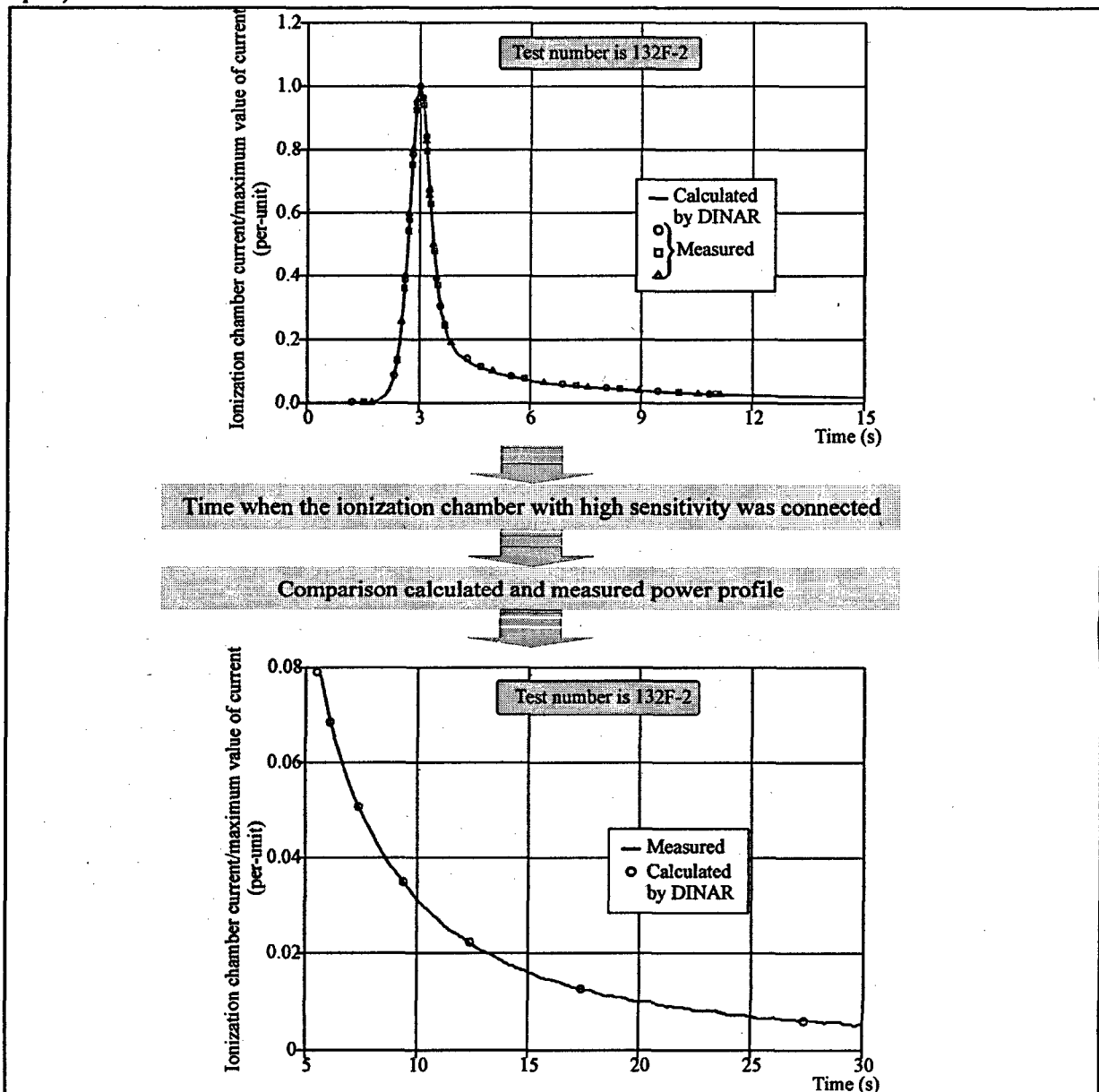


Fig. 4.13. Results of the DINAR code verification.

4.6. PIE of fuel rods tested in the IGR reactor

The main objective of the fuel rods post-test examinations after the IGR tests was to obtain data base to characterize thermal, mechanical, chemical and other processes, which occur during fuel rod tests; this data base is required to find the fuel rods damage and failure mechanisms, calculate fuel rod failure thresholds, develop systematized data for computer codes verification and improvement, and, in the final analysis, improve our knowledge of physical phenomena taking place in the fuel rods under these conditions. To attain this objective, special approach shown schematically in Fig. 4.14 was developed.

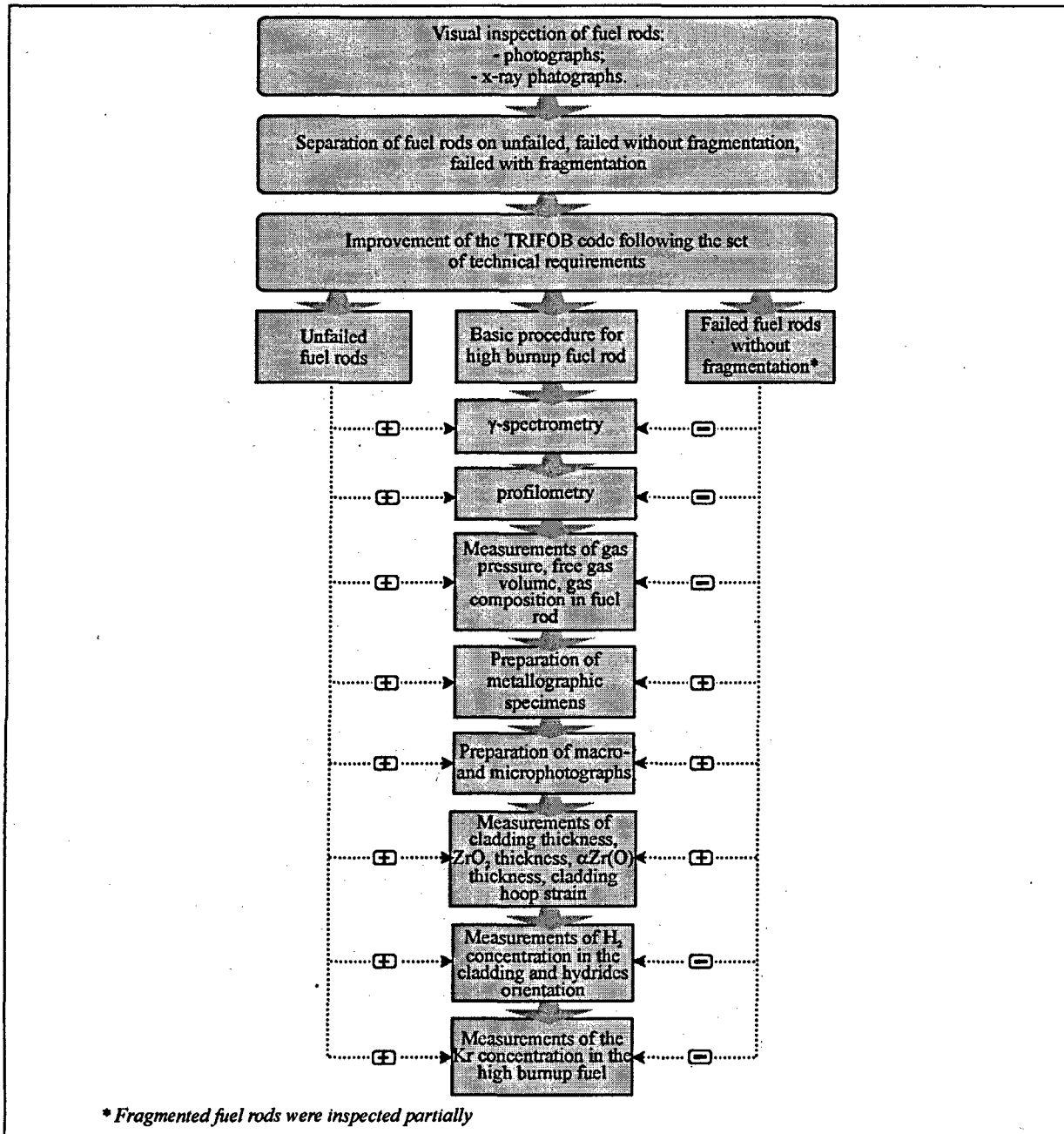


Fig. 4.14. Major provision of the PIE procedure.

To practically implement this approach, the following set of special procedures was developed and certified in RIAR:

- measurement of radial geometrical sizes (cladding thickness, ZrO_2 thickness, $\alpha Zr(O)$ thickness);
- measurement of cladding residual hoop strain;
- measurement of hydrogen concentration and hydride orientation in the cladding;
- measurement of internal gas composition in fuel rod, internal gas pressure in fuel rod, free gas volume in fuel rod and Kr concentration in fuel.

Typical results of the use of this approach are shown in Fig. 4.15 and Fig. 4.16 for two cases under consideration:

- unfailed fuel rod;
- failed fuel rod.

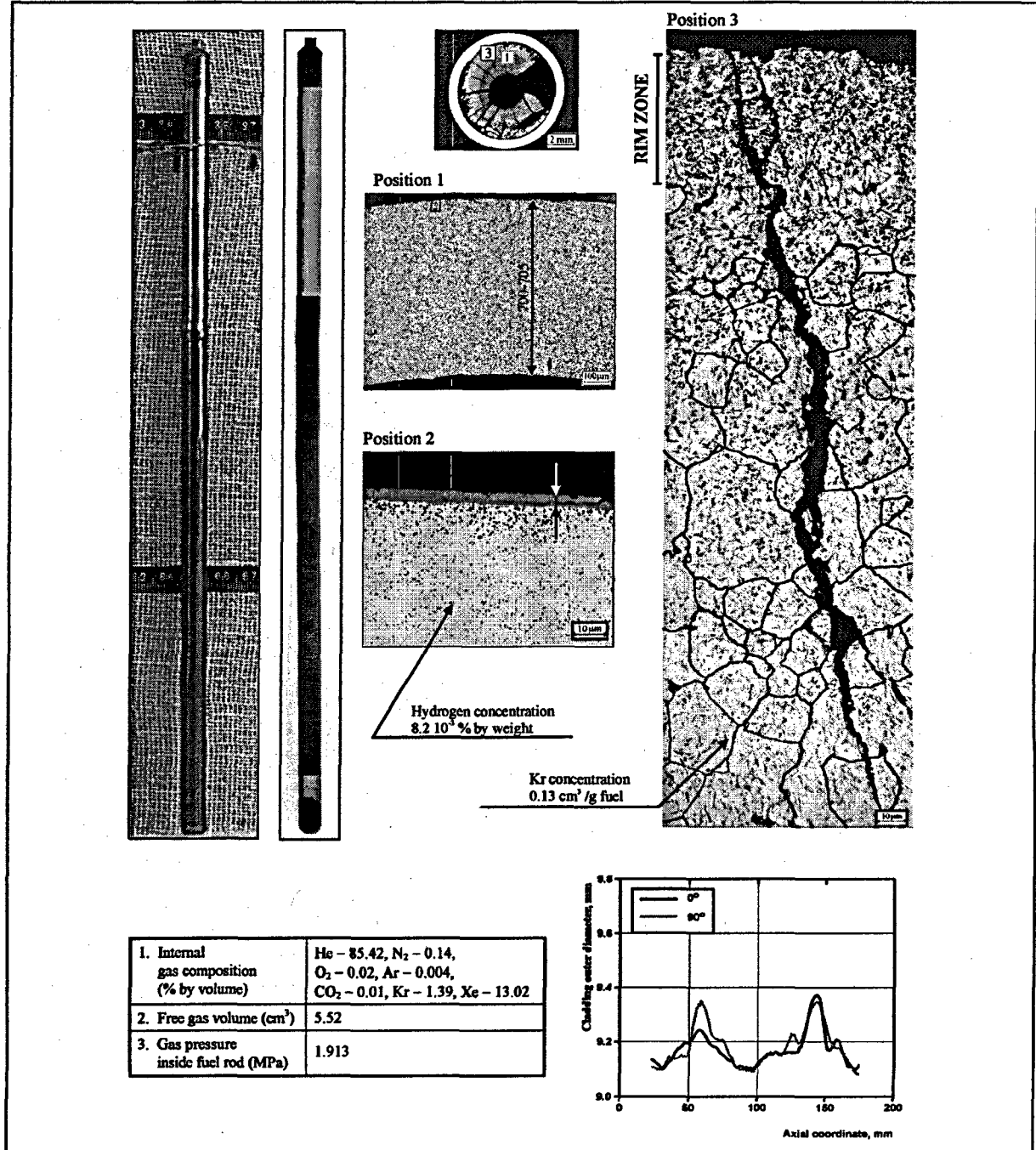


Fig. 4.15. Some PIE results for unfailed fuel rod #H1T.

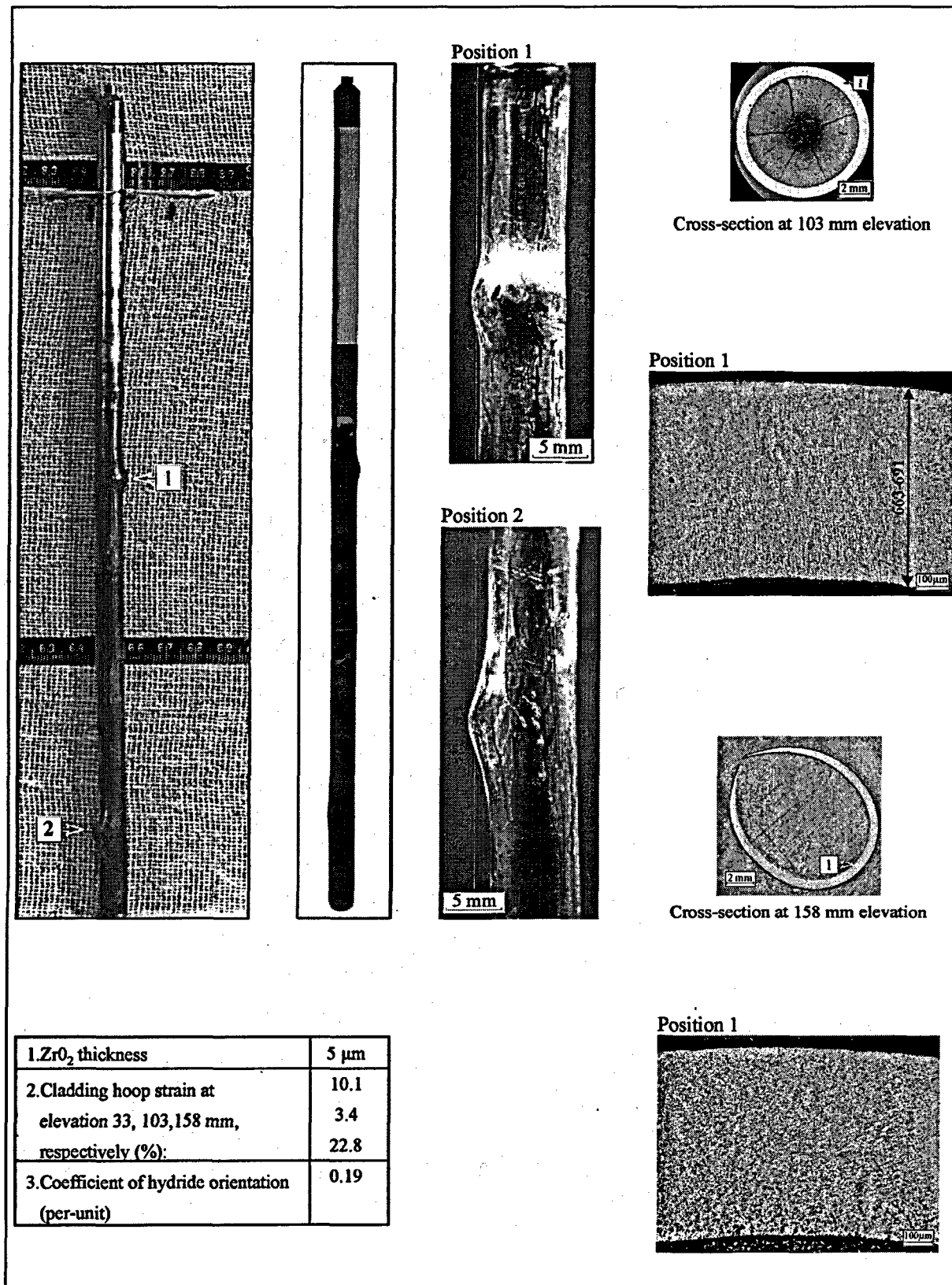


Fig. 4.16. Some PIE results for failed fuel rod #H7T.

4.7. Determination of r , z , t distributions of energy deposition and fuel rod power in high burnup fuel

Determination of energy deposition in high burnup fuel during the reactor power pulse is a rather specific and challenging problem, which can be divided into two relatively independent problems:

1. Determination of cumulative number of fissions which occurred in fuel on each of the fissile isotopes (U^{235} , U^{238} , Pu^{239} , Pu^{241} etc.), and determination of r , z , and t distribution of these fissions.
2. Determination of thermal effect in each act of fission on each isotope with due regard not only to fission fragments energy, but also to β - and γ -radiation contribution.

Both these problems were reviewed in their sequential interrelation within the framework of this program.

Analysis of the first problem showed that classical approach based on spectrometry measurements of the number of fissions in fuel cannot be applied in this case because of high background radiation due to presence of a great number of long-lived isotopes in high burnup fuel. Apparently, in this case, radiochemical method of isotope separation from fuel samples is preferable. However, as a result, two new problems arise:

- high cost associated with radiochemical analysis of fuel samples, and, therefore, practical impossibility of carrying out this investigation on the required number of samples;
- considerable nonuniformity of distribution of total fissions over the fuel rod radius and height, due to which measurements in one fuel sample are not representative for other sections of the fuel rod.

That is why, special calculation-and-experimental procedure was developed to solve the first problem (see Chapter 4 of Volume 2 of the report). Schematically, the main steps of this procedure may be presented as follows:

1. Three-dimensional dynamic simulation of the IGR reactor was performed using the DINAR code for each of these tests. Results of these calculations were used to specify the boundary data for certain isolated geometrical region V containing two fuel rods under test (irradiated and unirradiated) surrounded by the coolant.
2. The stationary criticality problem for each IGR reactor test was solved using the Monte Carlo MCU computer code (see section 4.7 of Volume 2 of the report) within the framework of the following approach:
 - the IGR reactor simulation was approximate;
 - V region containing fuel rods was simulated in maximum detail with the use of the boundary data obtained as a result of calculation as per Item 1.

At the end of this step, a set of data characterizing the r and z distribution of fission density for each of the fissile nuclides was obtained.

3. To obtain absolute values of spatial distributions of the number of fissions for each high burnup fuel rod, use was made of experimentally obtained factor characterizing the relationships between calculated and actually measured number of fissions.

All steps of this procedure were subject to thorough verification including specially prepared experiments on the IGR reactor and the MIR reactor located in RIAR. Typical results obtained at this phase of investigation are shown in Fig. 4.17 – Fig. 4.19.

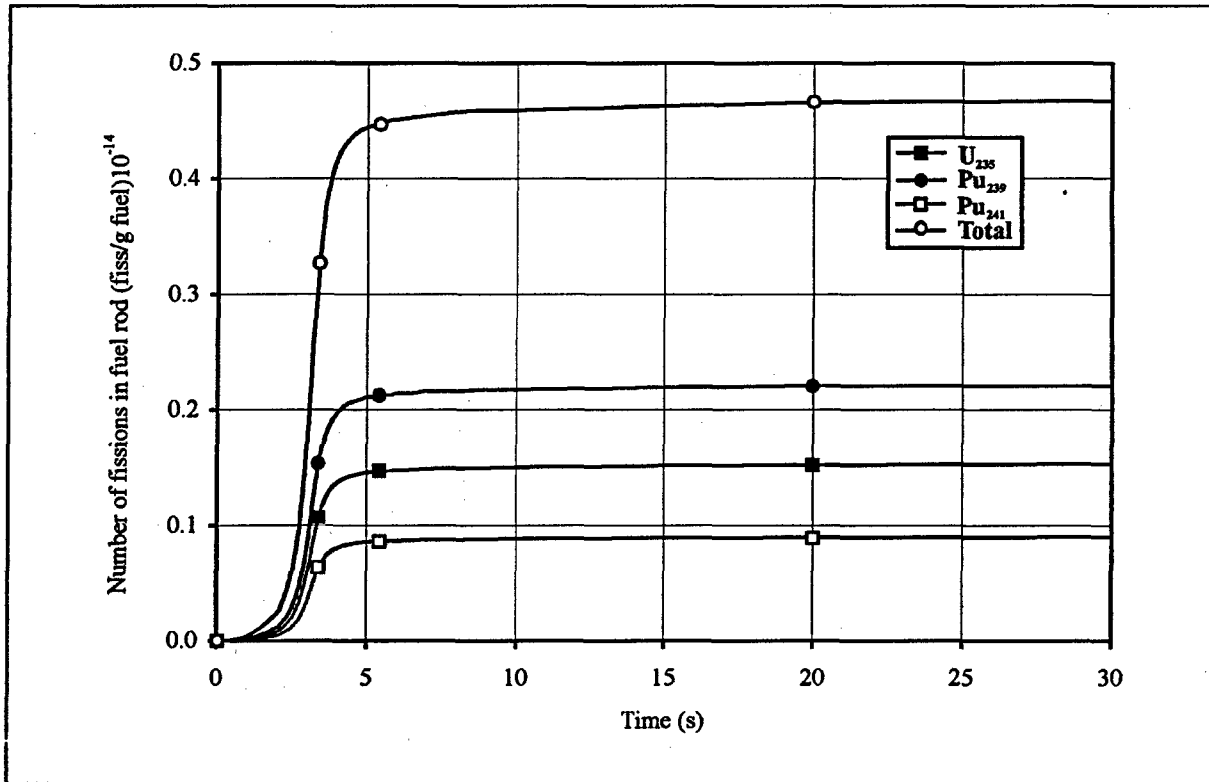


Fig. 4.17. Distribution of the specific number of fissions versus time.

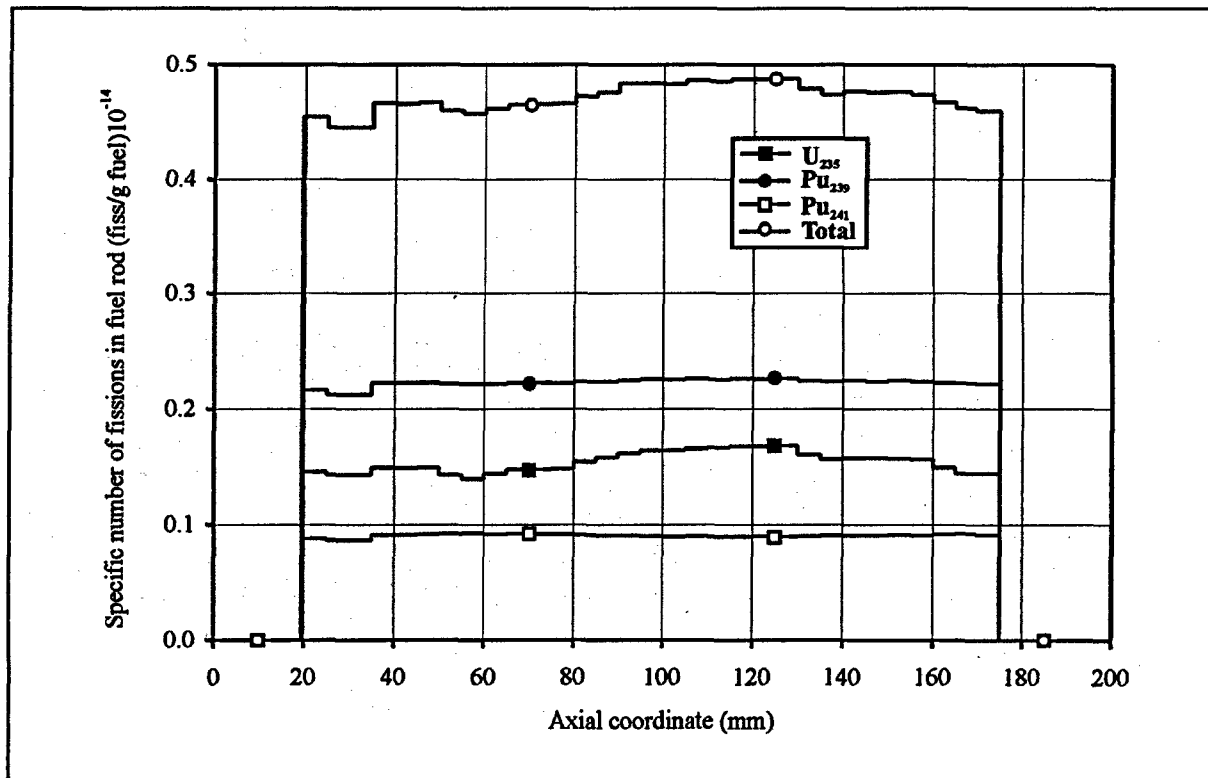


Fig. 4.18. Axial distribution of the specific number of fissions.

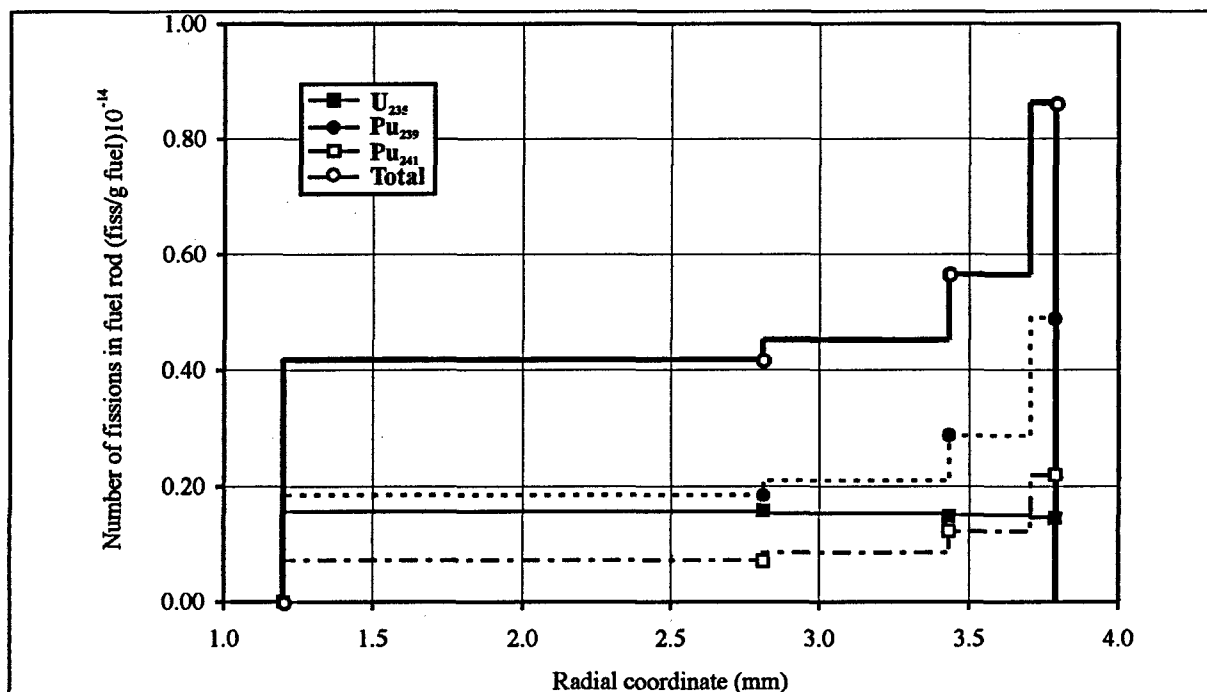


Fig. 4.19. Radial distribution of the specific number of fissions.

Next problem, which required development of special procedure, was determination of the r , z , and t distribution of energy deposition (see Chapter 4 of Volume 2 of the report).

Generally, specific energy liberated in the fuel rod elementary volume by time t can be found from the following equation:

$$E_z(t) = E_f(t) + E_{pr}(t) + E_\beta(t),$$

where $E_z(t)$ = the integral energy deposition in the elementary volume of fuel rod at time t (J/cm^3);

$E_f(t)$ = the energy deposition due to fission fragments of all fissile isotopes (J/cm^3);

$E_{pr}(t)$ = the energy deposition in the fuel due to prompt neutron and gamma radiation (J/cm^3);

$E_\beta(t)$ = the energy deposition in the fuel due to delayed beta and gamma radiation (J/cm^3).

Thus, to solve this equation, it was necessary to define all presented components versus time. Due to the fact that at the previous investigation step, fission densities for each fissile isotope were defined versus time, the main problem with the energy deposition due to fission fragments was to select the constants characterizing kinetic energy of the fragments. To define two other components, IGR reactor calculations were performed for each test conditions with the use of the ANISN and SINATION neutronic codes (see section 4.8 of Volume 2 of the report). Qualitative evaluation of parameters of the above equation for one of the high burnup fuel rods is shown in Table 4.1.

Table 4.1. Balance of the energy densities for fuel rod #H1T.

Time (s)	E_z (cal/g)	E_f (cal/g)	E_{pr} (cal/g)	E_β (cal/g)
580 \approx ∞	253	235.2	10.6	7.18

Note, that despite the fact that all key steps in the procedure to determine the number of fissions and energy deposition were properly verified, the developed procedure is a rather complex one. Therefore, evaluation of uncertainty in determination of energy deposition with this procedure was included in the list of mandatory

investigation steps. Special method was applied to perform uncertainty analysis for all the procedure steps. In doing so, individual contribution to random and systematic errors was considered, and, in addition, sensitivity analysis was performed for a number of parameters. Results of this investigation showed that total error in determination of energy deposition in high burnup fuel rods may reach $\approx 12\%$ at 0.95 confidence level.

The last step in this investigation cycle was determination of r , z and t distribution of fuel rod power. This was obtained by using simple procedures based on the data array characterizing energy deposition, and the data array characterizing reactor power profile. Note, that the final reactor power profile for each test was obtained by joining the following two data arrays:

1. Profile measured with the use of reactor ionization chamber up to 3–5 % of power at the pulse trailing edge.
2. Power profile calculated with the DINAR code from 3–5 % power up to $t=\infty$.

4.8. Determination of the mechanical properties of the VVER unirradiated and irradiated claddings

As soon as the tests of high burnup fuel rods in the IGR reactor were completed, and preliminary evaluation of their results was performed, it was evident, that data base obtained as a result of these tests is inadequate for the multi-parameter analysis of the behavior of tested fuel rods. In addition to presenting the test results and discussing probable cause-effect interrelationships on which these results were dependent, two more data bases should be obtained to provide for argumentative analysis of the test results. These two data bases are as follows:

- data base with mechanical properties of Zr-1%Nb cladding;
- data base characterizing thermal-mechanical behavior of high burnup fuel rods.

Suitable investigations were performed to obtain these data bases. Methods and procedures used to solve these problems are presented in the report Section, which follows.

To obtain data base of mechanical properties of Zr-1%Nb cladding, investigation in the following two areas was undertaken:

- measuring the set of basic short term mechanical properties versus temperature and strain rate;
- measuring specific mechanical parameters, characterizing ballooning and rupture of the cladding.

4.8.1. Procedures to measure the mechanical properties versus temperature and strain rate

Analysis performed demonstrated that, normally, to measure mechanical properties of cladding, use is made of three major methods:

1. Testing of cladding samples for longitudinal tension. A section of cladding tube or a Zr-1%Nb bar is used as test specimen.
2. Testing of cladding samples for transverse tension. A plate sample is made out of the cladding ring sample by straightening it flat.
3. Testing of ring cladding samples for tension.

Evaluation of these three methods in reference to specific conditions demonstrated the following:

- the first method is not representative for this problem because real cladding is mechanically loaded mainly in transverse direction. Taking into account pronounced anisotropy of mechanical properties of Zr-1%Nb alloy we can clearly see that results obtained at longitudinal tensile test are not adequate for the required data base;

- disadvantage of the second method is due to the fact that manufacturing of a plate sample from an annular blank requires its considerable deformation which, in its turn, changes mechanical properties of the material under test;
- as a result, the third method was selected as preferable for solving this problem. However, this approach is not perfect from the methodological point of view because, initially, the simple ring sample is subjected not only to tensile but also to bending stress (see Fig. 4.20). Therefore, test procedure for this sample should be developed so as to precisely register only those deformation response, which are caused by tension.

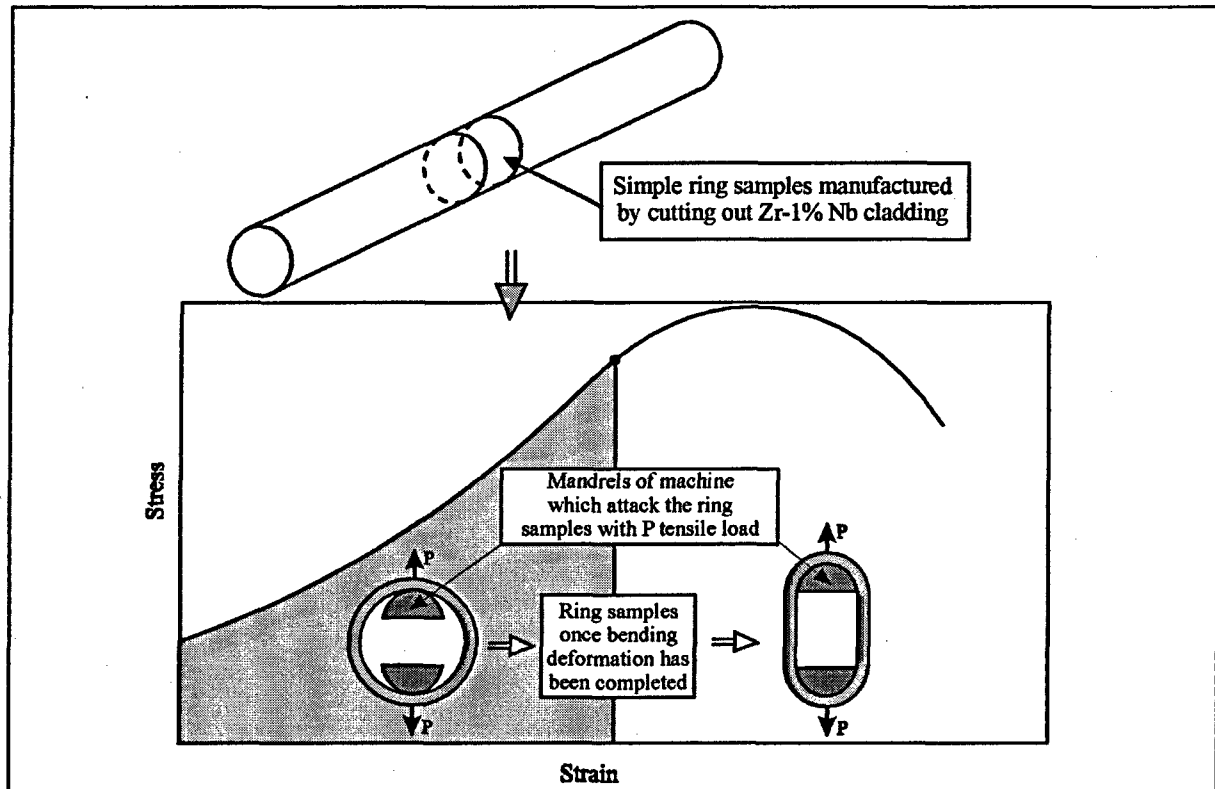


Fig. 4.20. Scheme of the ring tensile test.

In Russia this problem was normally resolved by isolating certain gauge length from the perimeter and subjecting it to tensile test. Procedure for calculating the gauge length was developed some time ago, and all previously published results were obtained by using this procedure. However, analysis of results obtained shows that despite the use of unified procedure, results, published by different sources are somewhat contradictory, and the spread of uniform elongation results is totally unacceptable. To illustrate the scope of the problem, the uniform elongation measurement results obtained in the RIAR are shown in Fig. 4.21. It should be specifically noted that uniform elongation is a key parameter in computer simulation of cladding ballooning.

Results shown in Fig. 4.21 allowed Russian experts to come to a conclusion that simple ring samples fail to resolve the whole complex of problems pertaining to measuring mechanical properties of Zr-1%Nb cladding. Analysis of foreign experience (USA, France) in solving similar problems with Zry cladding shows that the following methods were used to prevent bending from affecting the ring samples test results:

- using mandrels with maximum diameter;
- shape of machined ring samples provided for concentrating deformation in the precisely selected portion of the sample.

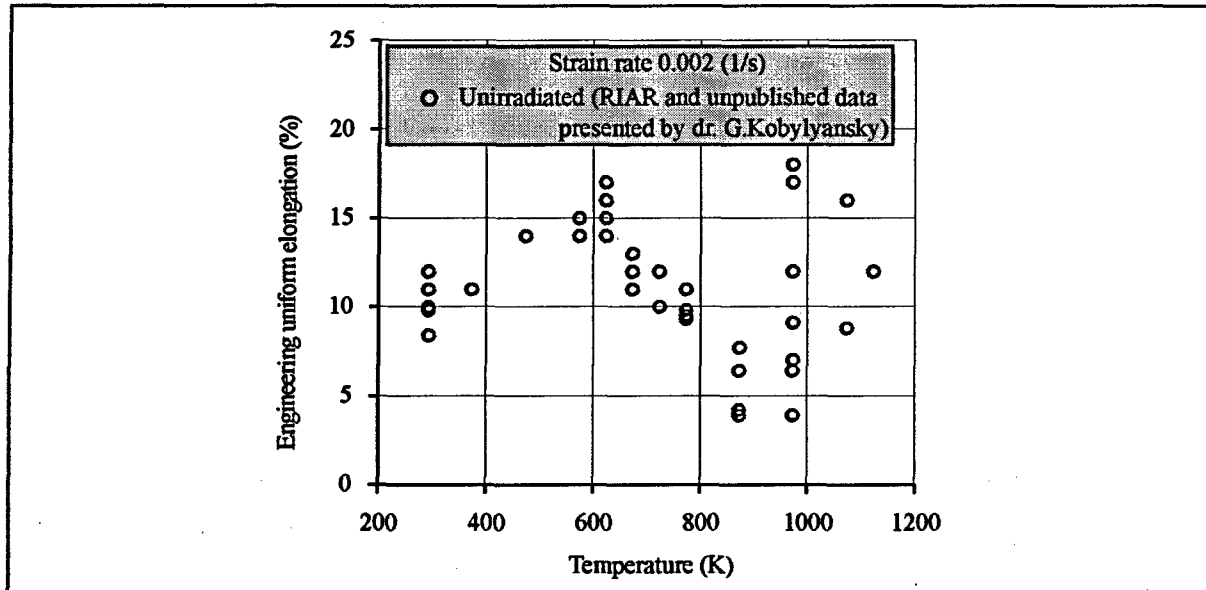


Fig. 4.21. Results of Zr-1%Nb uniform elongation measurements with simple ring samples.

Considering all above mentioned aspects of the problem, decision was taken to perform comparative measurement of mechanical properties of the samples manufactured of one and the same Zr-1%Nb cladding tube in compliance with three original procedures used in the following research organizations:

- RIAR (Russia);
- ANL (USA);
- CE-Saclay, (CEA-IPSN, France).

Analysis of results of this research demonstrated the following (see Fig. 4.22):

- there is good agreement between the results of all three ultimate strength procedures;
- there is considerable discrepancy between the results of yield stress, total and uniform elongation.

In addition to that, analysis showed that in all three procedures the main systematic error was caused by the fact that the ring samples were bent during the tests. In Russian procedure bending happens in the initial section of the stress-strain curve, and practically finishes completely by the moment of transition into the plastic region, which causes reduction of uniform elongation. In the French approach the use of larger mandrels decreases the bending during initial loading and the use of a machined gauge sections tends to concentrate the plastic strain in the well-defined gauge section. However, for the non-optimized geometry used in this study, both plastic flow in the flange region and later – stage bending must be accounted in the conversion of load-displacement data to material stress-strain data. In the American approach the bending during initial loading was minimized by the use of special transverse insert (a dog-bone type) and machined type of the gauge section was applied in an attempt to concentrate plastic flow in gauge length. But for the non-optimized geometry used in this study, the plastic flow in the flange area was large compared to the plastic flow in the gauge area. Also the friction caused by contact between the special insert and the gauge resulted in a lowering of the load in the gauge section. Both of these factors must be accounted for to convert the load-displacement data to material stress-strain results with reasonable uncertainty. Thus, these researches have demonstrated, that all three procedures should be modified to account for such effects as the deformation and work hardening due to bending, the plastic flow in the flange region of specimen and friction between specimen and insert.

That is why the special investigation program aimed at enhancing Russian procedure was initiated. Within the framework of this program tests were performed on cylindrical, plate and ring samples. Special measurements were performed at intermediate points of the stress-strain curve, including annealing of samples at

these points. As a result of these special investigations we managed to develop a simple and efficient method of separating plastic strain due to bending from elastic strain due to tension. Besides, the original investigation cycle was aimed at determining the gauge length. As a result of these investigations, a modified procedure was developed to measure mechanical properties on the simple ring samples.

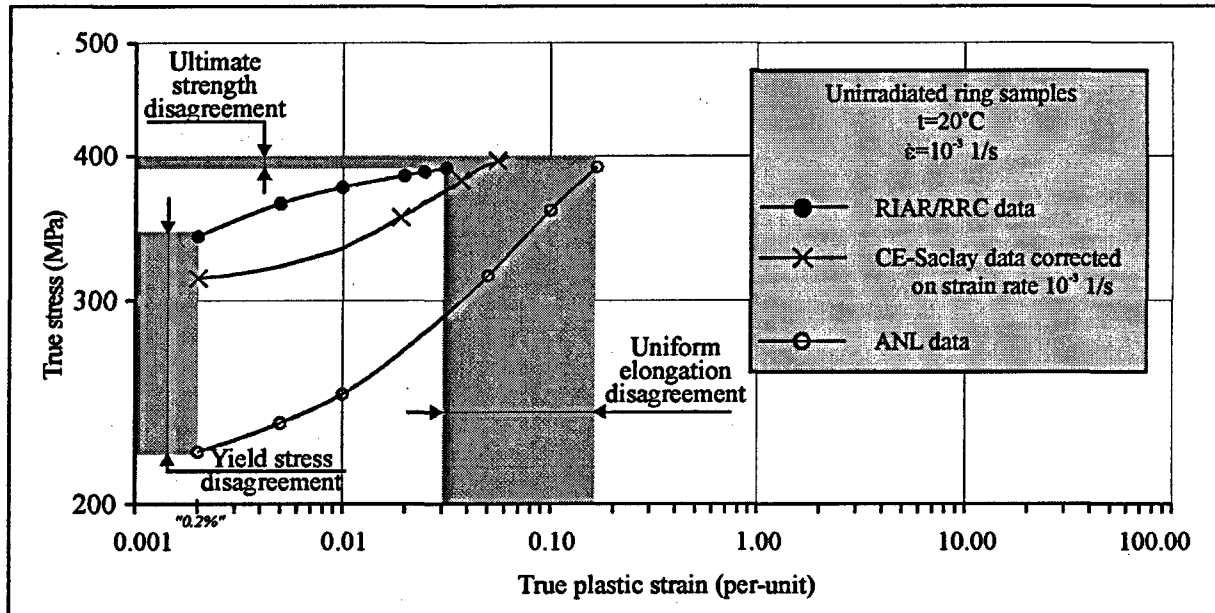


Fig. 4.22. Comparison of the procedure to measure the mechanical properties of the Zr-1%Nb cladding.

Development of methodological approach to the content of the data base of mechanical properties of Zr-1%Nb cladding was an important practical aspect of work on the data base obtaining procedure, because it is known that, generally, the cladding mechanical properties are dependent on cladding material composition, heat treatment, temperature, strain rate, irradiation, O₂ and H₂ content, etc. However, in this case, the main purpose of development of the data base of cladding mechanical properties was to analyze the results of the VVER RIA tests in the IGR reactor. That is why, to solve this problem, the following methodological approach was implemented:

1. Measurement of mechanical properties was performed on two types of cladding:
 - unirradiated Zr-1%Nb cladding of the VVER-1000 type;
 - irradiated Zr-1%Nb cladding, taken out from commercial fuel elements of the 5th unit of the NV NPP, irradiated till burnup of approximately 48-50 MW d/kg U.
2. Mechanical properties measurements were performed versus temperature and strain rate in the range of these parameters selected with due regard to parameters of the fuel rods tested under the RIA conditions in the IGR reactor.

4.8.2. Procedures to measure the mechanical properties for analysis of ballooning and cladding rupture

Tests of unirradiated and high burnup fuel rods under the RIA conditions in the IGR reactor demonstrated that the main cladding failure mechanism for highly pressurized fuel rods is rupture of the cladding due to ballooning. That is why, it was important to conduct supporting tests to obtain the data base characterizing mechanical behavior of cladding under these conditions. Burst tests are a classical type of such experiments. The burst tests schemes may vary depending on specific test objectives, but generally, these are characterized by the following features:

1. Pressurized fuel rod simulator is produced. Either fuel rod cladding filled with gas or cladding filled with pellets and gas are used as simulators.
2. The temperature scenario in the cladding is simulated either by heating the cladding externally with a heater, or by using a heater installed along the fuel rod simulator center axis.
3. Pressure inside the cladding is set using independent system in compliance with the selected law, or by heating gas inside the cladding.

Examples of practical implementation of such schemes are shown in Fig. 4.23.

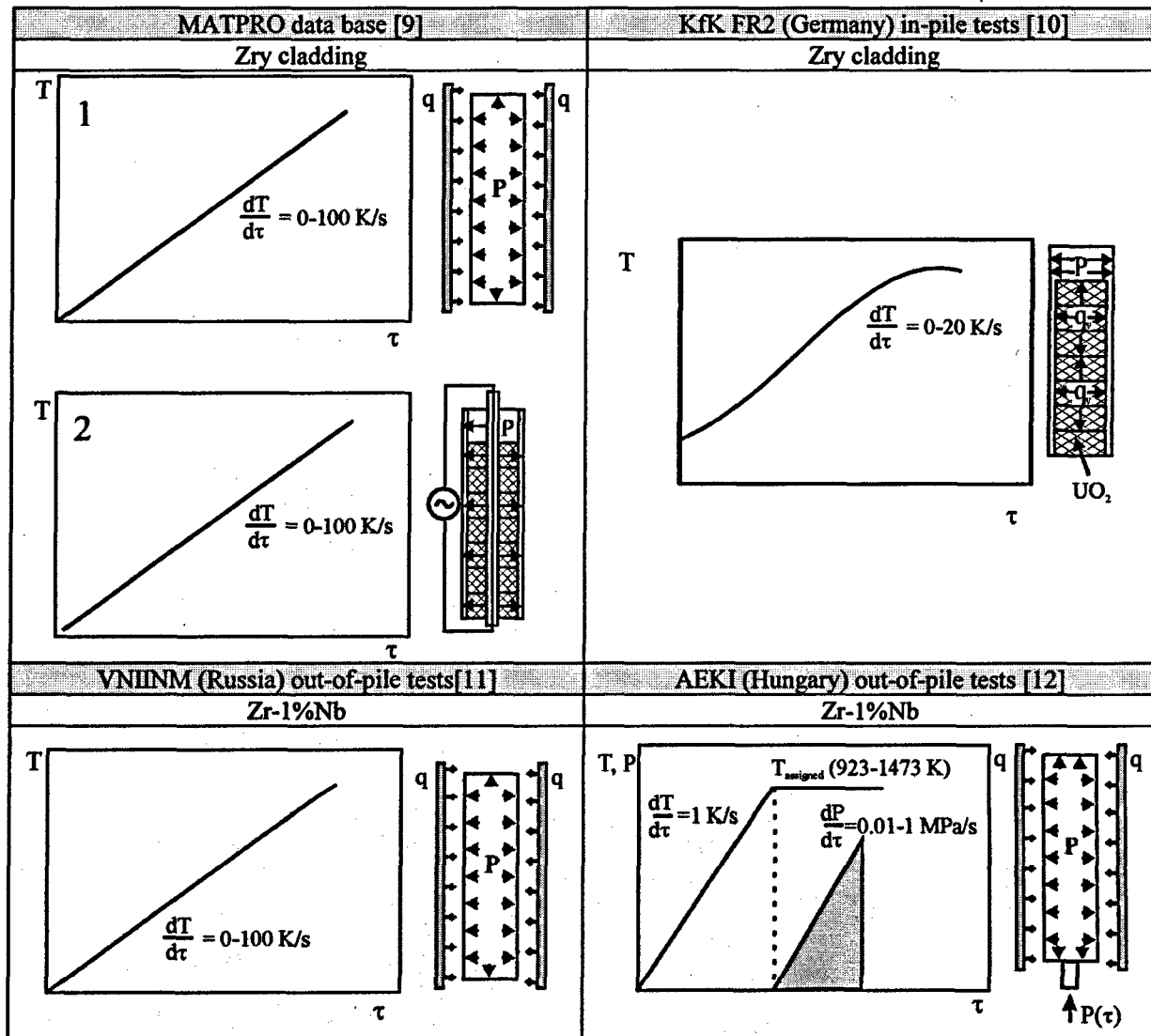


Fig. 4.23. Schemes of the tests for some burst programs.

Analysis of these burst programs showed that practically all of them were oriented to studying the processes of ballooning and rupture under the LOCA conditions. These conditions are characterized by the fact that the main variable parameter is the heat up rate, with the pressure inside simulator initially set at the level of several megapascals. These test conditions cause a situation when the cladding mechanical behavior is dependent not only on a set of short term mechanical properties (ultimate strength, yield stress, total elongation, uniform elongation), but also, on long term mechanical properties (creep), which may affect the results.

Therefore, in developing the burst test program for studying fuel rods behavior under RIA conditions, main emphasis was made on (see Section 6.3 of Volume 2 of the report):

- excluding any influence of creep on the test results;
- ensuring possibility for studying mechanical properties versus strain rate, which is an important factor for the RIA conditions;
- determining burst parameters for irradiated commercial Zr-1%Nb cladding.

Therefore, for this type of tests the test scheme shown in Fig. 4.24 was developed. Test samples were as follows: 150-mm sections of irradiated Zr-1%Nb tubes and irradiated commercial cladding.

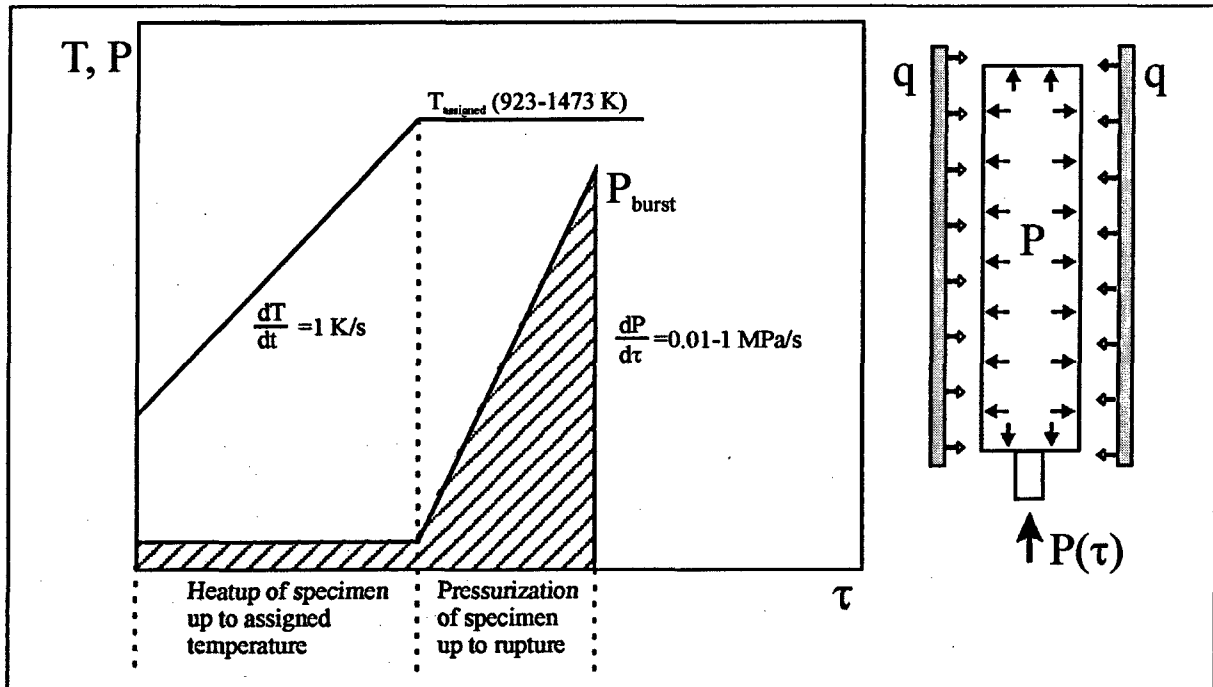


Fig. 4.24. Schemes of the burst tests in the framework of the IGR/RIA program.

An important feature of these burst tests was the fact that in addition to such parameters as burst pressure versus burst temperature, use was made of the third important parameter, pressure increase rate, reflecting the cladding strain rate dynamics. Besides, the burst test procedure also provided for determining the complex of experimental parameters required for computer simulation of the fuel rod cladding under the IGR conditions with the use of the FRAP-T6/BALON2 computer codes. To this end, the following measurements were performed:

- determination of the middle line profile for each cross section of the cladding;
- measurement of the cladding thickness;
- measurement of the ballooning axial radius;
- measurement of the circumferential radius of curvature;
- measurement of the peak circumferential elongation.

To solve this problem a set of special procedures was developed, and a series of special post-test examinations was performed so that the required set of parameters was measured for each burst test.

4.9. Adaptation and modification of the MATPRO package, FRAP-T6 and SCANAIR codes to predict the thermal-mechanical behavior of the VVER fuel rods under IGR/RIA conditions

Apparently, the full-scale analysis of high burnup fuel rod behavior under the IGR/RIA conditions was not possible without additional data base characterizing the physical phenomena, which may affect deformation and failure of the fuel rods. As was noted in Section 4.8, one of these additional data bases were the results obtained by measuring mechanical properties of Zr-1%Nb claddings. The second additional data base for analysis of thermal-mechanical behavior of fuel rods at all the stages of the IGR/RIA scenario was obtained with the use of the following computer codes (discussed in detail in Chapter 5 of Volume 2 of the report):

- FRAP-T6 code (USA);
- SCANAIR code (France).

FRAP-T6 is basically designed for simulating behavior of the LWR fuel rods under the LOCA conditions. The code contains a set of strongly coupled mathematical models reflecting the basic physical processes in the fuel rod under these conditions, including models describing fuel rod mechanical behavior both, due to contact tension at the PCMI (Pellet Cladding Mechanical Interaction) stage, and at the cladding rupture stage due to ballooning. In this last case, use is made of special code BALON2 joined with the FRAP-T6 code. To prepare the input data on material properties, the FRAP-T6 code will use the MATPRO package.

Preliminary analysis of possibilities for adaptation of the FRAP-T6 code and the MATPRO package for evaluating behavior of the VVER high burnup fuel rod under the IGR conditions showed that:

- data base, characterizing material properties of the VVER cladding and fuel is not available in the MATPRO package;
- the MATPRO packages has not been upgraded for a long time, therefore, material properties of the commercial high burnup fuel and commercial irradiated cladding are practically not represented there;
- specific phenomena of the high burnup fuel, such as the rim-zone, are not simulated by the FRAP-T6 code;
- the FRAP-T6 code description contains no results of the RIA conditions code verification.

The SCANAIR computer code (version 2.2) was developed specifically for simulating the PCMI stage under the RIA conditions. Therefore, the code considers the phenomena specific to the high burnup fuel rod at high-rate loading, but lacks cladding rupture models; also, it is not designed for evaluating large cladding plastic strains characteristic of many IGR tests. Besides, like in the FRAP-T6 code, it contains material properties of the PWR fuel elements only.

That is why, the program aimed at adapting the FRAP-T6 and SCANAIR codes for analyzing the VVER high burnup fuel rod behavior under the RIA conditions, included the following successive steps:

1. Study of sensitivity of the FRAP-T6 and SCANAIR codes to uncertainties of material properties input data.
2. Development of package of the VVER materials original properties for the MATPRO and SCANAIR codes.
3. Development of computational scheme for the IGR tests and relevant input data.
4. Preparation of experimental data base for verification of the FRAP-T6 и SCANAIR codes by the IGR test results.
5. Verification of the VVER version of the FRAP-T6 and SCANAIR codes.
6. Modification of the code models by the results of the verification procedures.
7. Evaluation of each code application for the analysis of the IGR tests and making a series of variational calculations for 25 fuel rods tested under the RIA conditions.

Basic features of the program implementation stages are discussed in Subsections of the present Section of the report.

4.9.1. Sensitivity study of codes to material properties

Preliminary study of the published data base with material properties showed that it is not adequate. The main problem was the fact that it practically contained no data characterizing material properties of high burnup fuel and irradiated cladding.

Analysis of sensitivity of the codes was performed to understand possible consequences of the use of incorrect material properties (see section 5.2 of Volume 2 of the report). Sensitivity analysis procedure was rather primitive, however, it helped to evaluate the code response dependence on the preselected disturbance in each of the material properties under consideration and, on this basis, formulate the following set of requirements to the data base for the original VVER material properties:

- if specific heat of the VVER fuel differs from the corresponding data base for the PWR fuel, then this data must be entered into the MATPRO package and the SCANAIR input data;
- fuel conductivity for the high burnup fuel must be entered into the MATPRO package and the SCANAIR input data;
- original VVER mechanical properties for unirradiated and irradiated Zr-1%Nb cladding must be entered into the MATPRO package and the SCANAIR input data;
- it is advisable to enter other original VVER material properties into the MATPRO package and the SCANAIR input data, however, if this is not done, then calculation results will not be significantly different from those obtained with standard data.

4.9.2. Development of package of original VVER material properties for the MATPRO and SCANAIR codes

The following was included in the package of original VVER material properties (see section 5.6 of Volume 2 of the report):

- thermal-physical properties for air coolant, Zr-1%Nb cladding, VVER fuel;
- mechanical properties for Zr-1%Nb cladding;
- mechanical properties for VVER fuel.

It should be emphasized that experimental results obtained within the framework of this program were used as the data base Zr-1%Nb cladding mechanical properties. All the data for the FRAP-T6 code was prepared in compliance with the MATPRO standards. For example, results of the ring samples tensile test were processed in such a way that they could be used in the form of the following base equation:

$$\sigma = K \varepsilon^n \left(\frac{\dot{\varepsilon}}{\dot{\varepsilon}_0} \right)^m,$$

- where σ = true effective stress (MPa);
 K = strength coefficient (MPa);
 ε = true effective strain (per-unit);
 n = strain hardening exponent (per-unit);
 $\dot{\varepsilon}$ = current strain rate (1/s);
 $\dot{\varepsilon}_0$ = basic strain rate (1/s);
 m = strain rate sensitivity exponent (per-unit).

The whole set of functionals required for use of this equation in calculation of unirradiated and irradiated Zr-1%Nb cladding stress – strain state, was developed and included in the MATPRO package. Besides, in

compliance with the MATPRO approach, experimental data from the burst tests was processed to obtain correlation for the local burst stress versus temperature. Local burst stress is used in the FRAP-T6/BALON2 code as a criterion for the cladding failure under ballooning conditions. For the graphic presentation of this correlation, see Fig. 4.25.

The standard of input data base for the SCANAIR code provides for simpler requirements to preparation of the material property data, therefore, computer tables for the required range of measured material properties versus temperature were developed and included in the input data package.

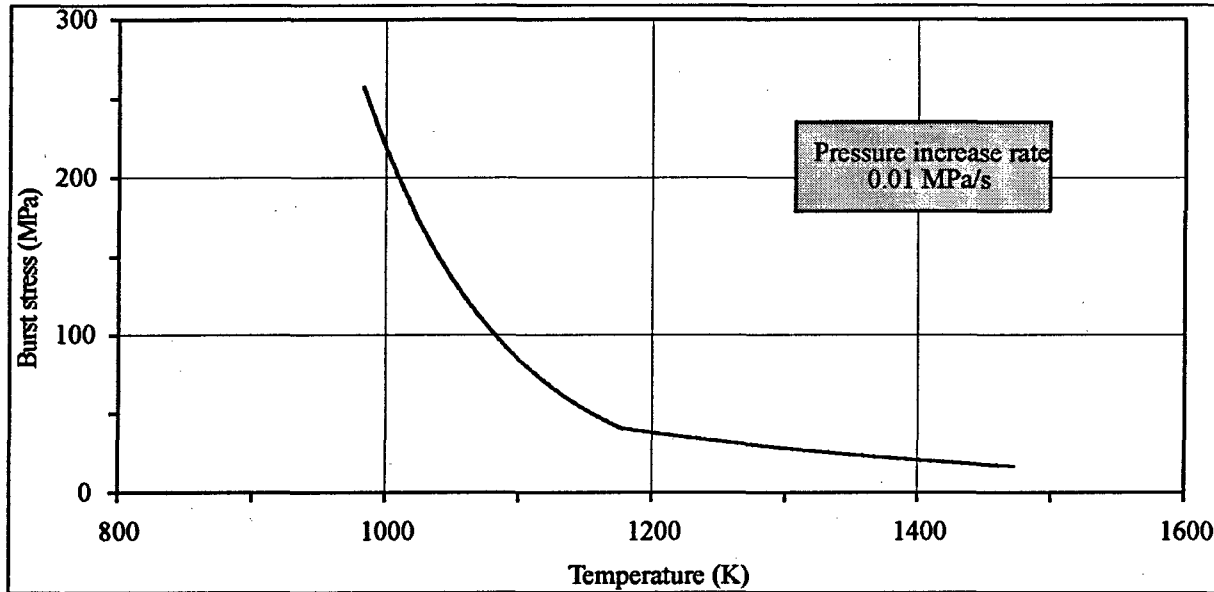


Fig. 4.25. Correlation of local burst stress for unirradiated and irradiated Zr-1%Nb cladding.

4.9.3. Development of calculation scheme for fuel rods and preparation of input data

Optimized calculation scheme of the VVER fuel rods was developed as a general-purpose scheme for the FRAP-T6 and SCANAIR codes. The scheme included:

- 10 axial nodes;
- 31 radial nodes.

Geometrical scheme of fuel rods consisted of fuel stack with central hole, fuel-cladding gap, cladding, upper and lower gas plenum and coolant. Calculation of each fuel rod was performed in accordance with its individual geometrical sizes and material composition. The corresponding input data was taken from Volume 3 of the present report, where Appendixes C, D, I contain the corresponding data base for each of 25 fuel rods.

4.9.4. The first stage of verification of the FRAP-T6 and SCANAIR codes by the IGR test results

No doubt, the main objective of the FRAP-T6 and SCANAIR series of calculations was to determine the peak fuel enthalpy in each of the fuel rods under test. Therefore, the main objective of code verification at this stage was to verify calculation of the cladding temperature – because this parameter indicates the correctness of calculation of thermal balance between heat flux from the fuel rod center to cladding and heat flux from cladding to coolant. Unfortunately, fuel rods equipped with temperature sensors were not used during the tests of high burnup fuel rods. As a result, to verify the FRAP-T6 and SCANAIR codes, several tests previously performed with the fuel rods equipped with the instruments were selected (see sections 5.4, 5.5 of Volume 2 of the report).

Verification was divided into two stages:

1. Verification for conditions of transition from convective heat transfer to nucleate boiling.
2. Verification for conditions when the departure of nucleate boiling (DNB) occurred on the cladding surface.

The FRAP-T6 code verification by the results of experiments corresponding to item 1 showed good agreement between the actual and predicted cladding temperature. A different situation was with the SCANAIR code. Data shown in Fig. 4.26 demonstrate that the SCANAIR code generally overestimates the cladding temperature for these test conditions.

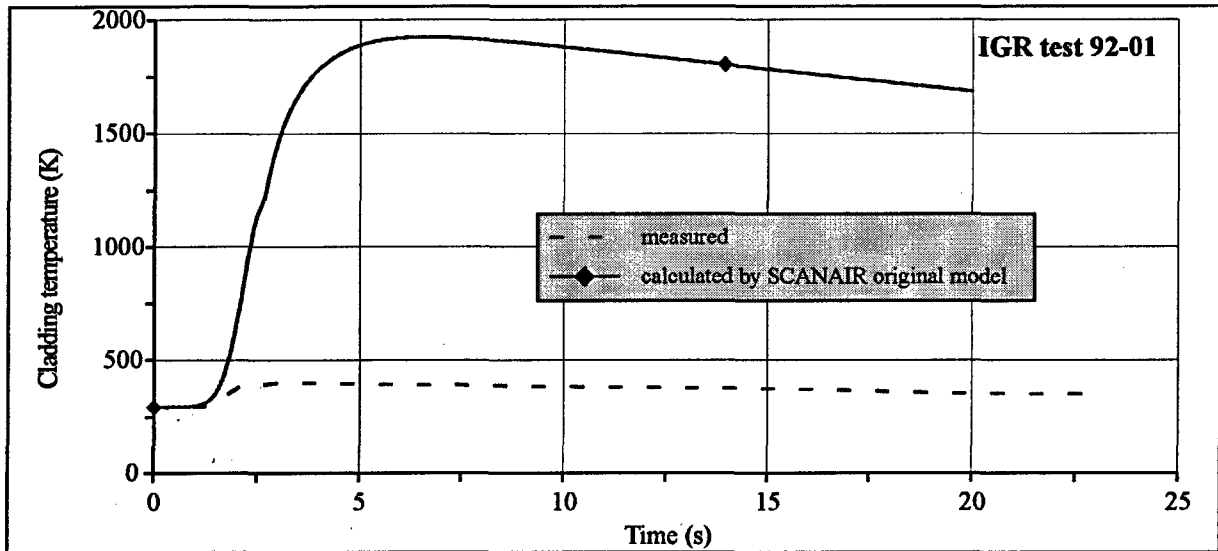


Fig. 4.26. Comparison of the measured cladding temperature and the cladding temperature predicted by the SCANAIR code for the transition from convection to nucleate boiling.

Verification results for DNB conditions are shown in Fig. 4.27.

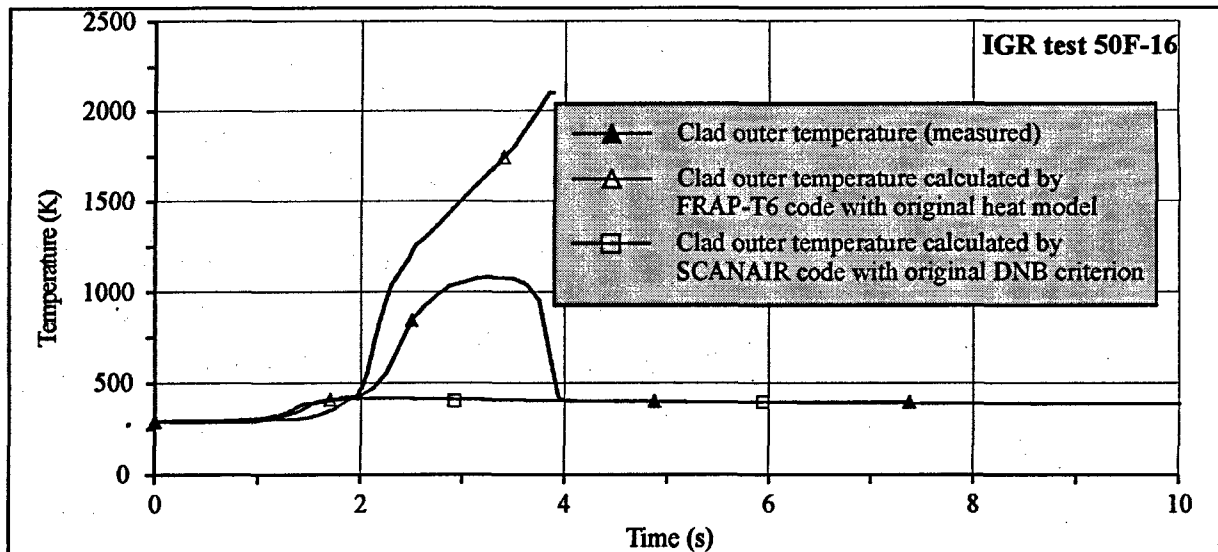


Fig. 4.27. Comparison of the measured cladding temperature and the cladding temperature calculated by the FRAP-T6 and SCANAIR codes for departure from nucleate boiling.

Analysis of obtained results clearly demonstrates that the FRAP-T6 code overestimates the cladding temperature, while the SCANAIR code underestimates the temperature due to the fact that the condition for the DNB start is not provided.

4.9.5. Codes modification in accordance with the results of the first stage of verification procedures

Special stage was run to modify the models of heat exchange on the cladding outer surface, and also, to modify the calculation scheme of the heat flux from cladding to coolant at the changeover of the heat exchange mode. In doing so, the most complex task was the rewetting model. No existing heat exchange correlation can provide plausible prediction of the cladding temperature at this heat exchange stage. Therefore, special model based on the assumed appearance of the wetting wave was developed and included in both codes. As a result of these efforts, data shown in Fig. 4.28 was received and found acceptable, so that modified FRAP-T6 and SCANAIR codes can be used for calculation of the IGR tests.

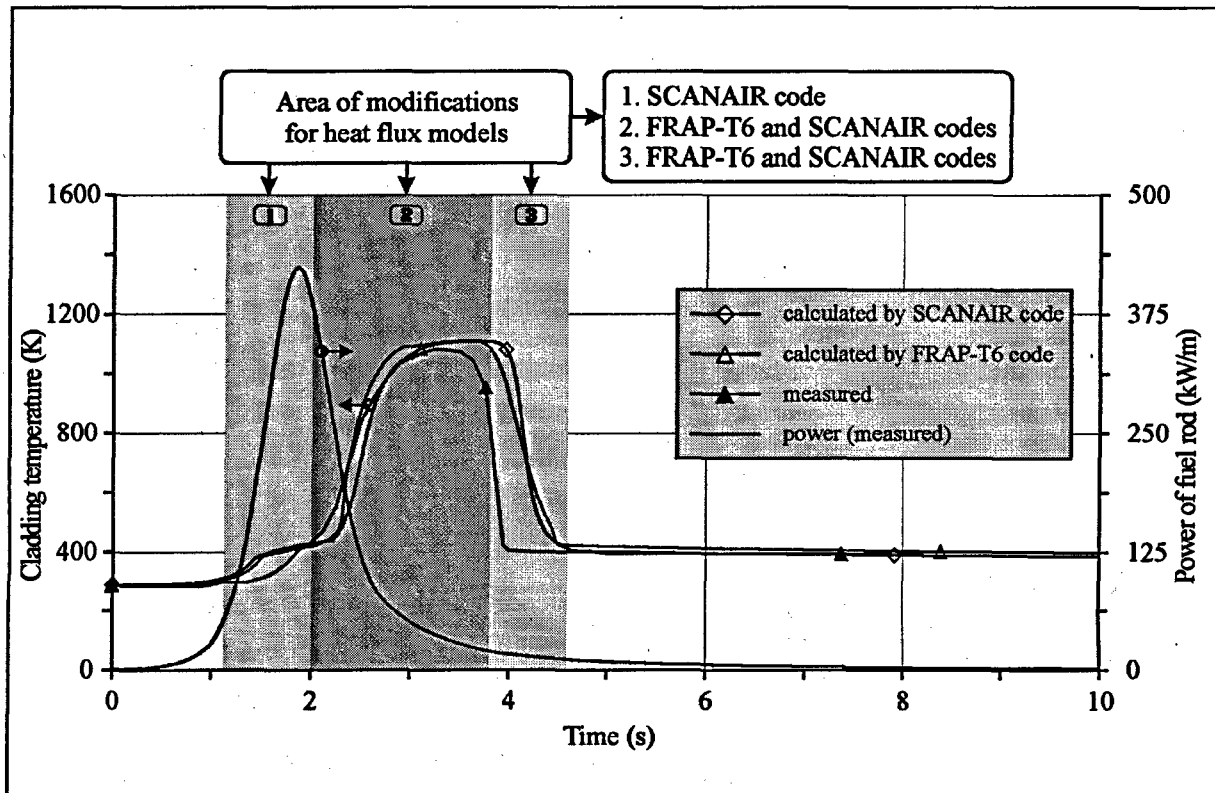


Fig. 4.28. Final verification results for the modified FRAP-T6 and SCANAIR codes.

Note that the process of modification of the codes, like the process of their verification was not limited to the examples presented in present Section. This special work cycle is discussed in detail in Volume 2 of the present report for each physical process studied within the framework of this program.

4.9.6. Evaluating the area of application of the FRAP-T6 and SCANAIR codes for analysis of the IGR tests

The FRAP-T6 code does not contain models describing fuel rods behavior in conditions of material melting and fragmentation. Therefore, for the whole group of melting and fragmentation fuel rods calculation was done up to the moment the melting temperature is reached in the fuel center. As for the SCANAIR code, it was mentioned earlier that the SCANAIR code lacks cladding failure models and does not provide for correct calculation of high values of cladding plastic deformation caused by internal gas pressure at high temperatures. Still, special optimization calculations were carried out to expand the area of application of the SCANAIR code for analysis of the IGR tests without significant loss of calculation accuracy. The following parameters were used as the calculation termination criteria:

- pellet-cladding gap reopening;
- cladding stress achieves the yield stress.

4.10. Procedure to determine peak fuel enthalpy in fuel rods

To calculate fuel enthalpy, FRAP-T6 and SCANAIR codes were used (see section 5.8 of Volume 2 of the report). However, basic calculations of the peak fuel enthalpy were performed with the FRAP-T6 code. This happened due to the fact that the SCANAIR code application for analysis of the IGR tests was limited. For the detailed calculation scheme of the peak fuel enthalpy, see Fig. 4.29.

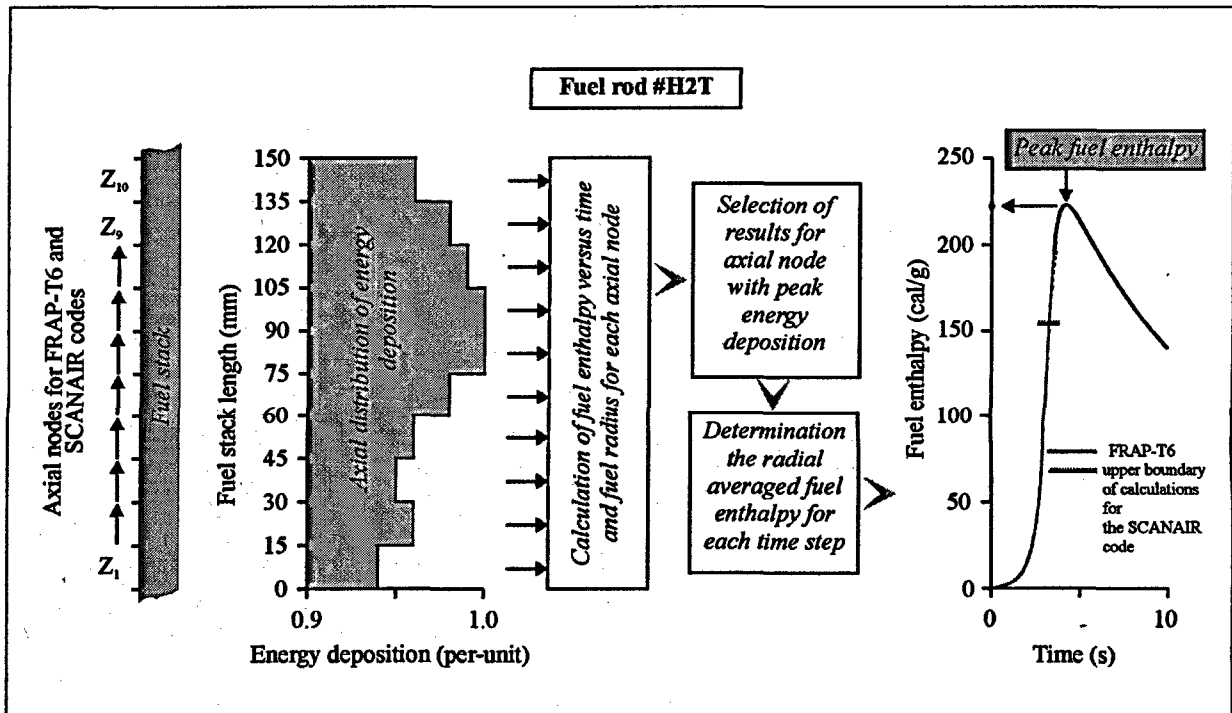


Fig. 4.29. Scheme to calculate the peak fuel enthalpy.

5. RESULTS OF THE IGR TESTS WITH VVER FUEL RODS

It is appropriate to begin this Chapter by emphasizing the fact that, from a philosophical point of view, results of any experiment are boundless. In other words, it may take infinite time to develop a comprehensive data base characterizing a variety of processes and events defining the test object behavior. That is why, defining the structure of requirements to the object and the content of the test results is always a complex and responsible task. Test result requirements are being specified in the framework of the target function formulated in the research program. In this case, this function included the following components:

- parameters characterizing change of shape, deformation and damage of cladding of each fuel rod;
- parameters characterizing physical and chemical processes in the fuel rods cladding (oxidation, hydriding);
- parameters characterizing fission products release;
- parameters characterizing neutron physical processes in the fuel during tests;
- parameters characterizing thermal and mechanical processes in fuel rods during tests;
- parameters defining the failure threshold of the fuel rods during tests.

The data base of results obtained in accordance with these requirements is specified in Volume 3 of the report (Appendices F, G, H, I). The purpose of this Chapter is to present a summary of these results, characterize specific features of various fuel rods behavior under the IGR test conditions, and sum up the data on mechanisms and failure thresholds.

These results will be discussed in reference to three groups of fuel rods:

- high burnup fuel rods tested in water coolant;
- fuel rods with irradiated cladding and fresh fuel and unirradiated fuel rods tested in water coolant;
- fuel rods of different types tested in air coolant.

5.1. High burnup fuel rods tested in water coolant

Eight high burnup fuel rods were tested in the IGR reactor at different energy depositions in conditions of power pulses. Appearance of these fuel rods after tests is shown in Fig. 5.1.

The obtained results demonstrated the following:

- four unfailed fuel rods tested at peak fuel enthalpy of 61–151 cal/g fuel;
- four failed fuel rods tested at peak fuel enthalpy of 176–252 cal/g fuel;
- in all the cases, the failure mechanisms were ballooning and rupture of the cladding;
- specific feature was observed in three high burnup fuel rods (##H7T, H2T and H3T) tested above the failure threshold, i.e. there were two cladding ruptures in each of the fuel rods;
- there was no fragmentation of fuel rod #H3T followed by melting of portions of fuel and its flowing into the coolant despite considerable cladding oxidation and its local melting.

To discuss the obtained results in more detail the tested group of fuel rods was split into two subgroups, and additional information was provided to characterize specifics of the physical processes in unfailed and failed fuel rods. Additional parameters describing behavior of unfailed fuel rods are shown in Fig. 5.2.

These results indicate that no additional cladding oxidation takes place during the tests. ZrO_2 thickness is preserved at the initial level of 5 μm . Hydrogen concentration in cladding varies from 30 – 40 to 80 ppm. Concentration of Kr and Xe in the fuel rod gas increases in a practically linear way depending on the peak fuel enthalpy.

However, the most important test results of this group of fuel rods are the results characterizing residual hoop strain of the cladding. To evaluate this parameter, we should discuss thermal mechanical test scenario for one of the fuel rods shown in Fig. 5.3.

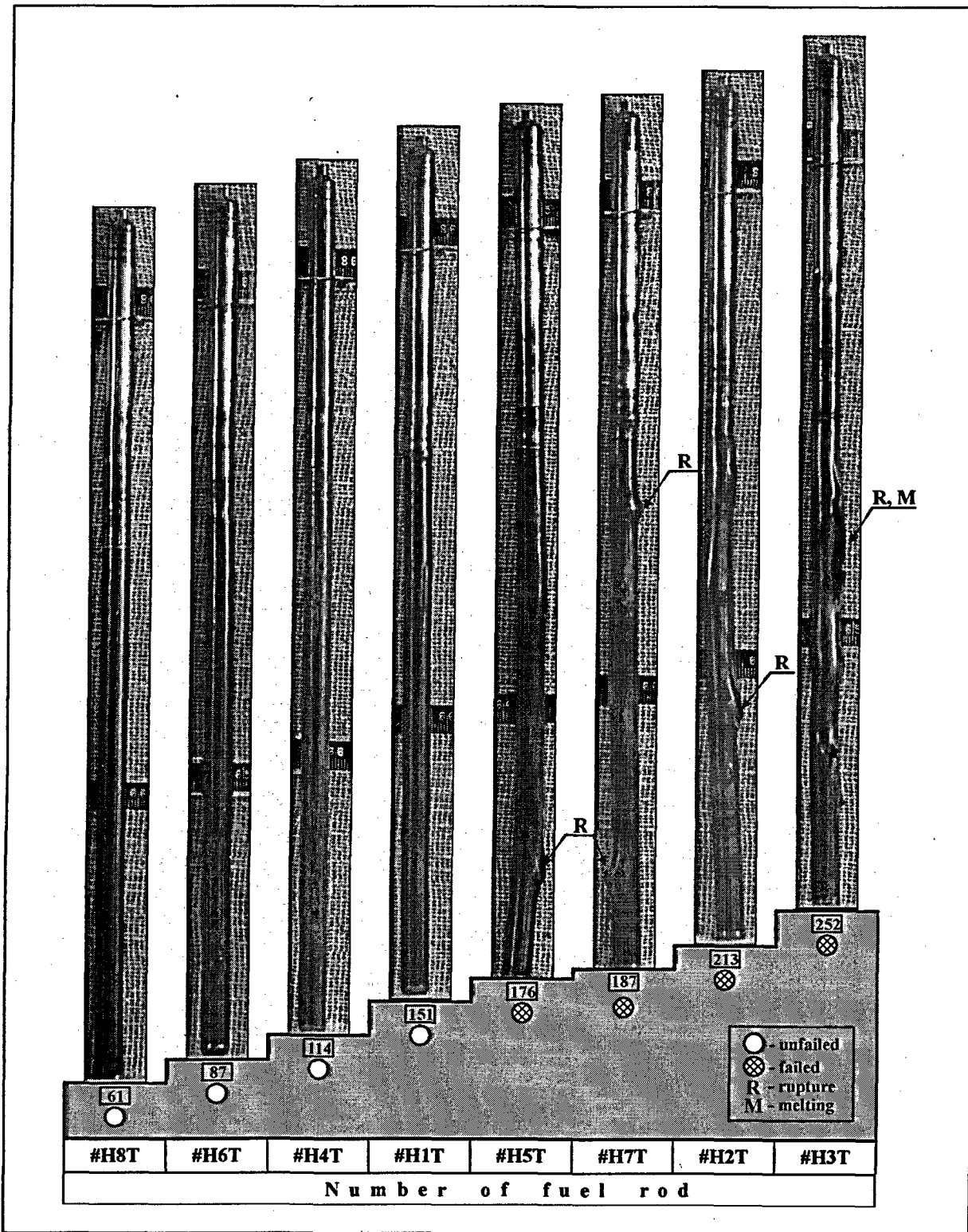


Fig. 5.1. Appearance of high burnup fuel rods after IGR tests in water.

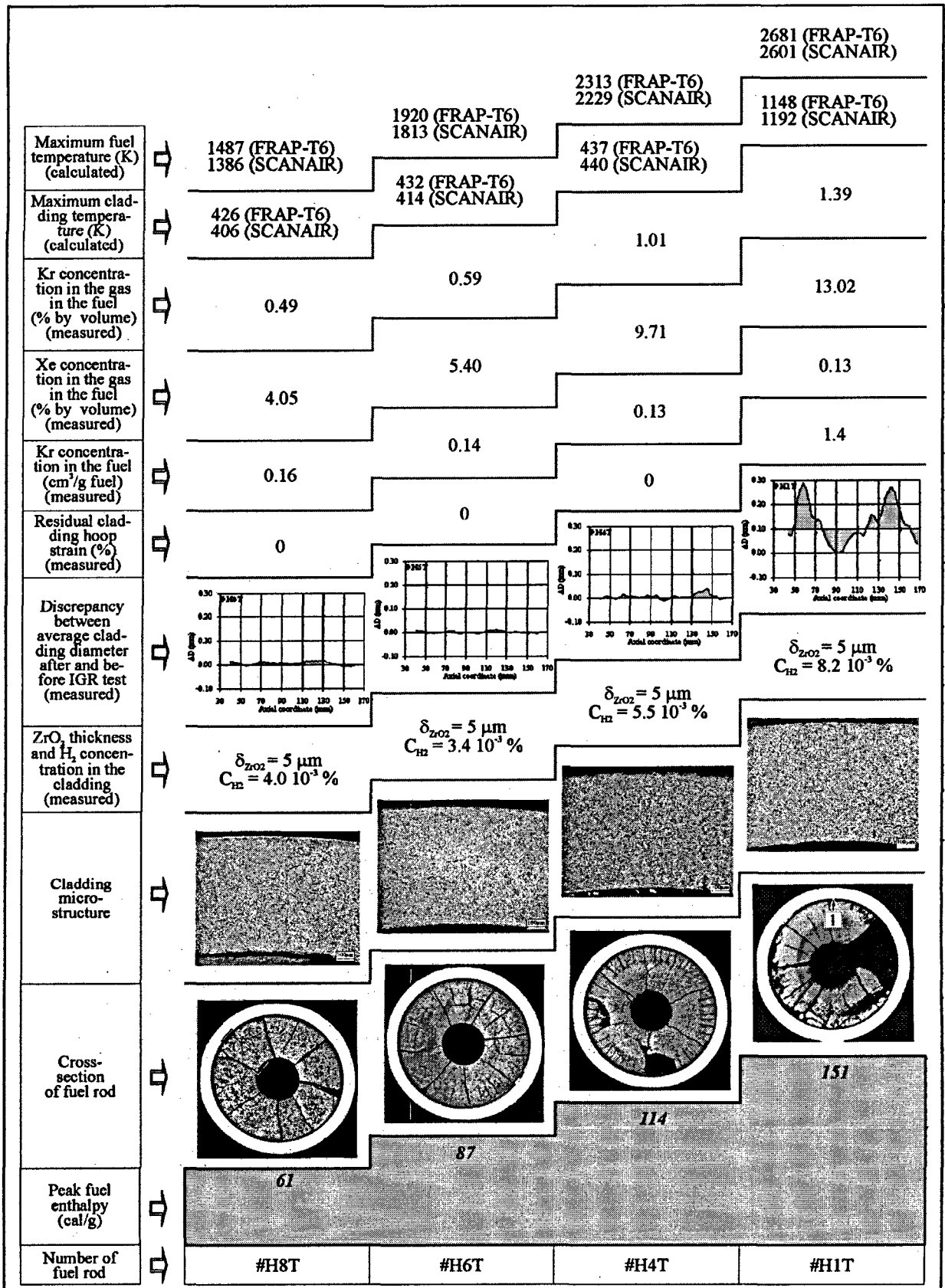


Fig. 5.2. Some parameters of unfailed high burnup fuel rods tested in water coolant.

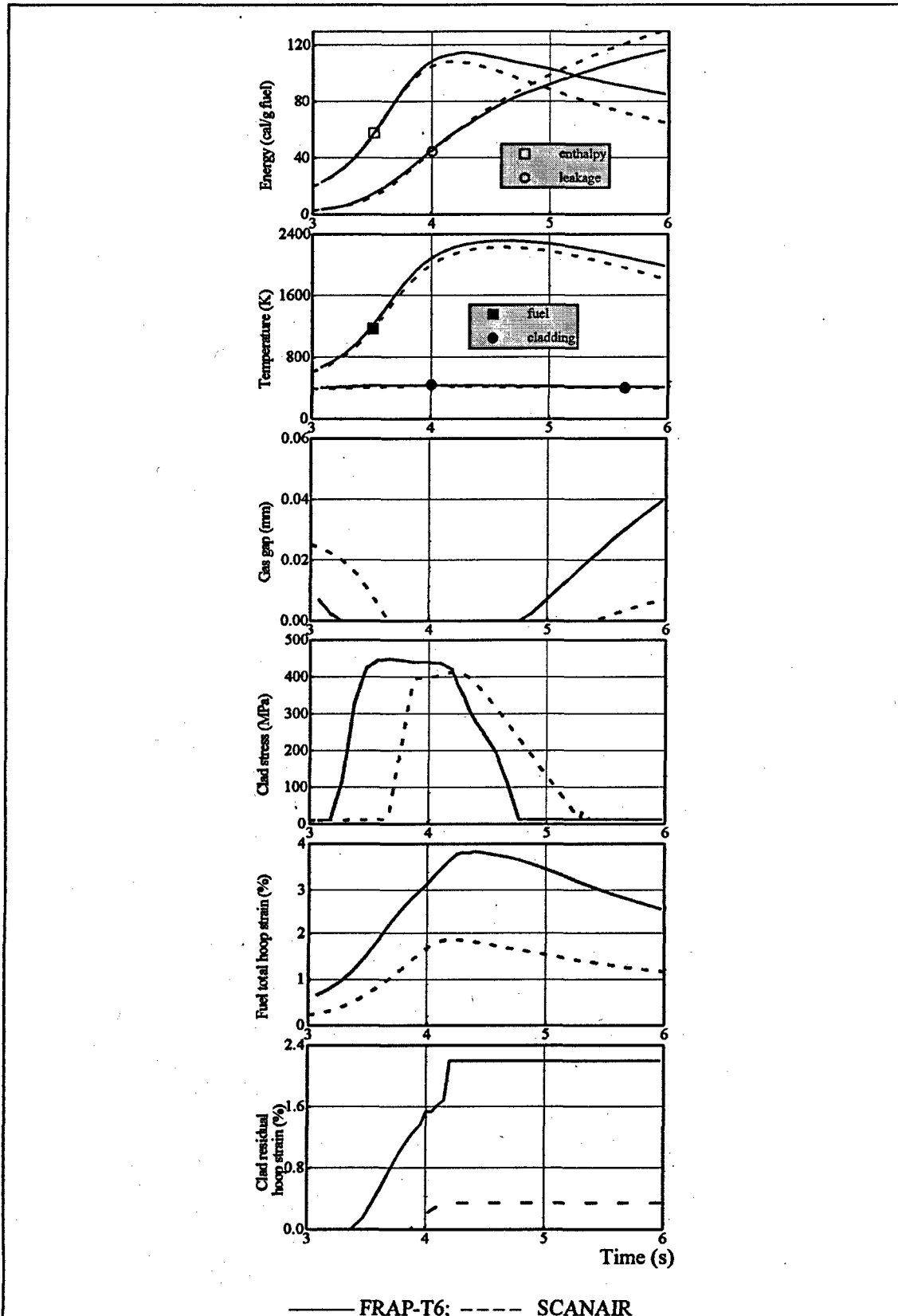


Fig. 5.3. Thermal mechanical parameters of the fuel rod #H4T calculated by FRAP-T6 and SCANAIR codes.

If we ignore the discrepancy between the FRAP-T6 and SCANAIR code predictions analyzed in detail in Volume 2 of the present report, it is clear that one of the main mechanisms, which may lead to cladding failure, take place already at low peak fuel enthalpy. This mechanism may occur due to the fact that when the gas gap closes fuel temperature is already high, therefore, fuel strain increases significantly. In case of high burnup fuel this effect is aggravated by the fact that fuel strain is a sum total of thermal expansion and fuel swelling. Meanwhile, cladding temperature still remains low, which causes considerable cladding stresses due to a phenomenon known as PCMI. In the worst scenario these stresses may cause cladding deformation and subsequent failure. These aspects of the problem will be discussed in more detail in Chapter 6. As far as the results shown in Fig. 5.2 is concerned, the following conclusions can be made on the basis of comparison of the external diameter of cladding of unfailed fuel rods before and after the tests:

1. Up to peak fuel enthalpy of 114 cal/g fuel, the PCMI stress practically fails to cause residual plastic strain in cladding which testifies to the effect that the cladding stress does not exceed yield stress.
2. When peak fuel enthalpy reaches 151 cal/g fuel, residual clad hoop strain versus fuel stack length appears.

Consideration must be given to the fact that cladding temperature in this case reaches 1100 K and more. Therefore, residual hoop strain is not only a function of the PCMI stresses, but also, a function of stresses caused by internal gas pressure under gap reopening conditions. As a result, this condition of the fuel rod cladding can be considered as the pre-threshold condition before it is ruptured by ballooning. However, final conclusion on this issue will be made on the basis of analysis given in Chapter 7 of this Volume.

To sum up the above, we can make the following conclusions:

- despite high stress under the PCMI conditions, not only does irradiated VVER cladding remain intact, but also it remains free from any considerable residual hoop strain;
- the phase immediately preceding the failure of VVER cladding is characterized by the following parameters:
 - ⇒ gas gap reopens;
 - ⇒ cladding temperature reaches 1100 K and more;
 - ⇒ residual hoop strain of cladding reaches 4-5 %.

Then, the following four failed fuel rods shown in Fig. 5.4 should be discussed. Detailed parameters of these fuel rods are summed up in Fig. 5.5.

The following effects were observed when peak fuel enthalpy grew from 176 to 252 cal/g fuel:

- fuel central hole closure is observed in tests above 171 cal/g peak fuel enthalpy;
- fuel melting is first observed, when the peak fuel enthalpy exceeds 252 cal/g fuel;
- cladding rupture due to ballooning was observed in this group of fuel rods;
- in agreement with the FRAP-T6 code predictions, maximum temperature of fuel rod claddings reached 1226–1366 K which caused oxidation of a number of fuel rods;
- maximum thickness of ZrO_2 in fuel rods tested below fuel melting temperature was 18 μm ;
- measured value of ZrO_2 in the cladding of fuel rod #H3T in zone of contact with the molten fuel reached 103 μm ;
- maximum cladding hoop strain out of rupture zone reached 8.6 %;
- cladding thickness reduced by 20–30 μm outside the ballooning zone.

Comparing results obtained in each of the two groups of fuel rods, we can make a conclusion that the failure threshold of high burnup fuel rods is within the range between 151 cal/g fuel and 176 cal/g fuel. For practical purposes, arithmetical mean of these values is proposed as the failure threshold, i.e. failure threshold of high burnup fuel rods tested in the IGR reactor under RIA conditions is 160 cal/g fuel.

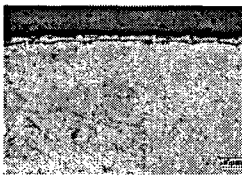
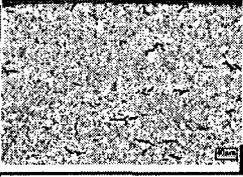
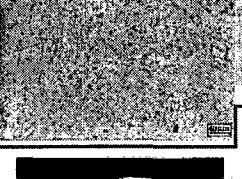
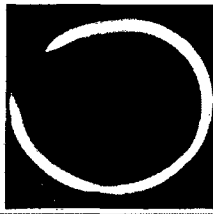
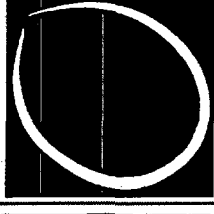
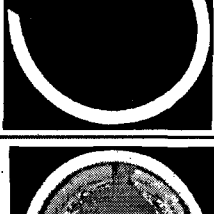
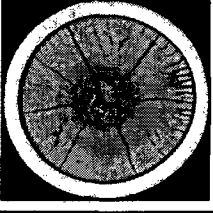
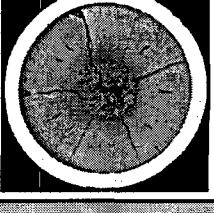
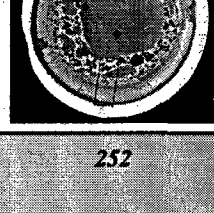
	169 (FRAP-T6)	171 (FRAP-T6)	195 (FRAP-T6)	212 (FRAP-T6)
Fuel enthalpy at failure (cal/g fuel) (calculated)	169 (FRAP-T6)	171 (FRAP-T6)	195 (FRAP-T6)	3113 K (FRAP-T6)
Peak fuel temperature (calculated)	2818 K (FRAP-T6)	2783 K (FRAP-T6)	3057 K (FRAP-T6)	1366 K (FRAP-T6)
Peak cladding temperature (calculated)	1226 K (FRAP-T6)	1231 K (FRAP-T6)	1280 K (FRAP-T6)	2.33 MPa (FRAP-T6)
Internal gas pressure at failure (calculated)	2.32 MPa (FRAP-T6)	2.32 MPa (FRAP-T6)	2.39 MPa (FRAP-T6)	1237 K (FRAP-T6)
Outer cladding temperature at failure (calculated)	1223 K (FRAP-T6)	1229 K (FRAP-T6)	1236 K (FRAP-T6)	667-691 μ m
Cladding thickness out of the rupture zone (measured)	663-677 μ m	663-691 μ m	667-691 μ m	<i>It was impossible to identify the ballooning parameters through melting effects</i>
Cladding hoop strain in the rupture zone (measured)	6.5%	10.1% } two 22.8% } ruptures	12.6% } two 11.4% } ruptures	
Cladding hoop strain out of the rupture zone (measured)	3.1%	3.4%	7.9%	$\delta_{ZrO_2} = 10-105 \mu$ m
ZrO ₂ thickness (measured)	$\delta_{ZrO_2} = 8-17 \mu$ m	$\delta_{ZrO_2} = 5 \mu$ m	$\delta_{ZrO_2} = 8-18 \mu$ m	
Cladding micro-structure				
Cross-section of fuel rod in rupture zone				
Cross-section of fuel rod out of rupture zone				
Peak fuel enthalpy (cal/g fuel)	176	187	213	252
Number of fuel rod	#H5T	#H7T	#H2T	#H3T

Fig. 5.4. Some parameters of failed high burnup fuel rods tested in water coolant.

5.2. Fuel rods with irradiated cladding and fresh fuel and unirradiated fuel rods tested in water coolant

Data base of the test results of these groups of fuel rods, shown in Volume 3 of the report, contains data pertaining to five fuel rods with irradiated cladding and one unirradiated fuel rod. Since four out of five fuel rods with irradiated cladding were tested at rather low peak fuel enthalpies, and did not reach the failure threshold, and obviously the PCMI stresses in this case were much less in these fuel rods than in the high burnup ones due to a big gas gap, there is no point in presenting the test results of these four fuel rods in much detail. That is why, Fig. 5.5 shows the test results of following two fuel rods:

- failed unirradiated fuel rod #H6C;
- failed fuel rod #H15T with irradiated cladding and fresh fuel.

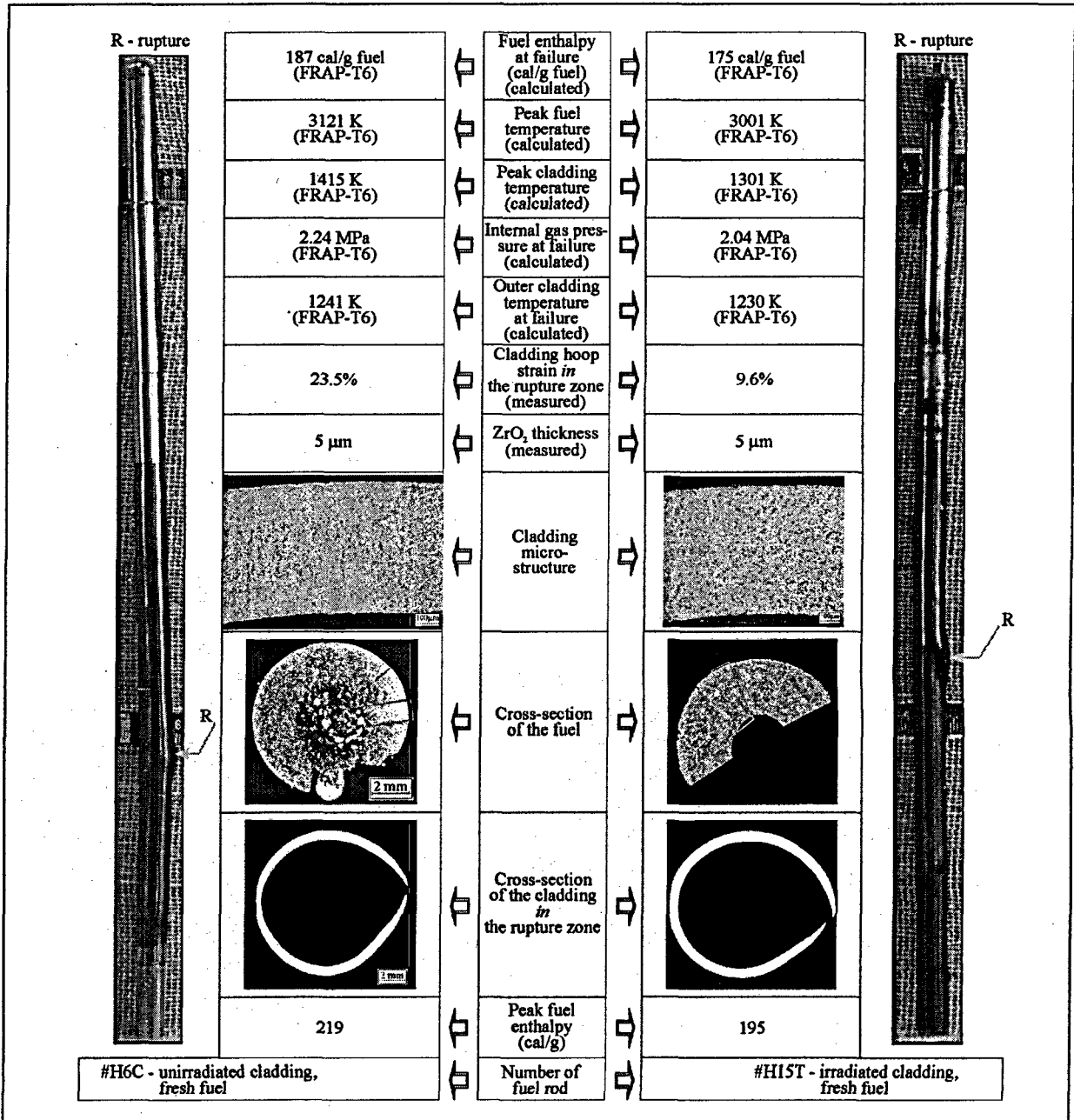


Fig. 5.5. Some parameters of failed unirradiated high burnup fuel rod and failed fuel rod with irradiated cladding and fresh fuel tested in water coolant.

As it is seen from Fig. 5.5 both fuel rods are damaged due to cladding ballooning and rupture. Fuel enthalpy at failure was 175–187 cal/g fuel. Peak fuel enthalpy in fuel rod #H6C was higher and so central hole in the fuel pellet disappeared, and there are symptoms of micromelting of fuel in the center. On the other hand, energy deposition, and obviously, peak fuel enthalpy for fuel rod #H15T are overestimated, because fuel condition in this rod shows that its maximum temperature was noticeably lower than that in fuel rod #H6C. However, we cannot fully exclude uncertainty in evaluation of corresponding parameters by the FRAP-T6 code. Nevertheless, presented results demonstrate that failure thresholds of these fuel rods approximately correspond to the data obtained earlier for unirradiated fuel rods (160–180 cal/g fuel). A separate problem is the cause of abnormally high cladding hoop strain in the rupture zone for fuel rod #H6C (23.5 %). Analysis of this result and other results pertaining to fuel rods deformation as a function of key factors will be given in the following Chapter of the report.

5.3. Fuel rods tested in the air coolant

The present Section will discuss the test results of a very specific group of fuel rods, i.e. fuel rods tested in the air coolant. This coolant is not a standard one for the RIA conditions, and it was used for the following considerations:

- study physical phenomena inside the fuel rod under ordinary boundary conditions on the wall, and use this data base for verification of computation codes;
- understand regularity of fuel rods deformation in the uniform temperature field conditions;
- use obtained data for comparison with out-of-pile data base containing the input data for calculation of ballooning and rupture processes in pressurized claddings.

Like in the case of water coolant, three types of fuel rods were tested in the air coolant:

- high burnup fuel rods;
- fuel rods with irradiated cladding and fresh fuel;
- unirradiated fuel rods.

In general, we have to admit that not all fuel rods were tested in the required range of peak fuel enthalpies. Since the whole of test cycle was performed practically at the same time, evaluation of ratio between energy deposition in the IGR reactor and energy deposition in this type of fuel rods was rather coarse, and its use caused a situation when peak fuel enthalpies in most fuel rods were considerably higher than it was envisaged in the program. Therefore, fuel rods were tested above failure threshold, and some fuel rods were fragmented. Nevertheless, the group of fuel rods shown in Fig. 4.9 allows us to summarize some important test results (full data base on tested fuel rods is given in Volume 3 of the report.)

All seven fuel rods shown in Fig. 4.9 have one failure mechanism independent of the type of fuel rod and the peak fuel enthalpy. Also, phenomenon of two ruptures in one and the same fuel rod was not observed.

More detailed information, characterizing parameters of three high burnup fuel rods, is given in Fig. 5.7.

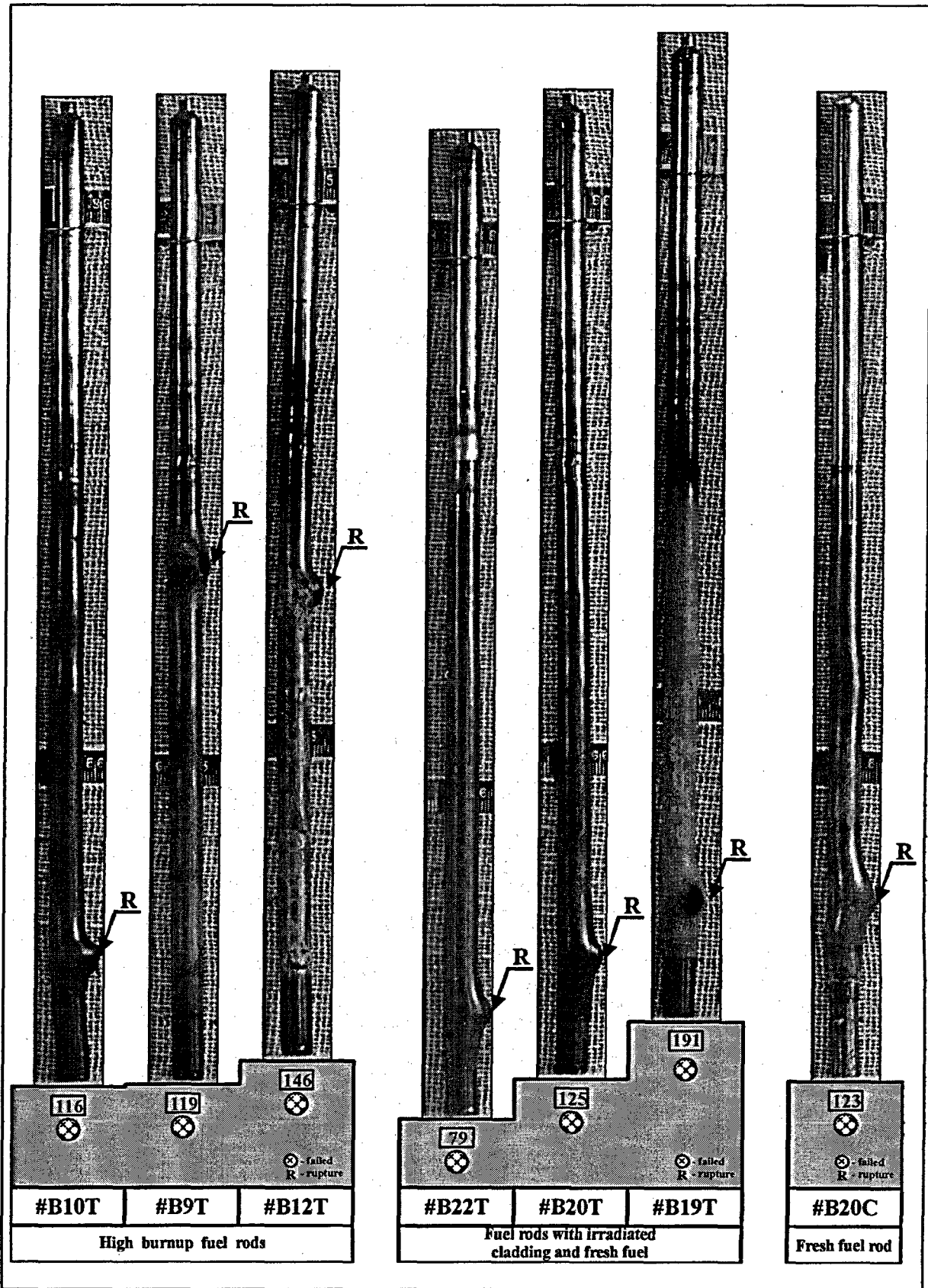


Fig. 5.6. Appearance of fuel rods of different types tested in air coolant.

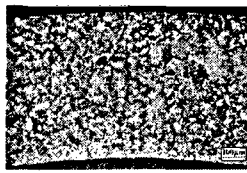
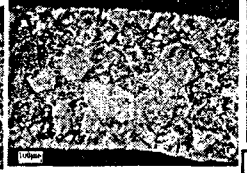
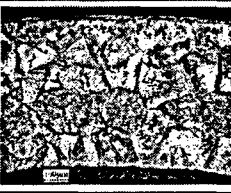
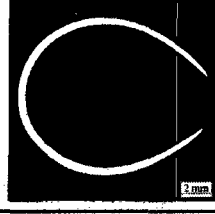
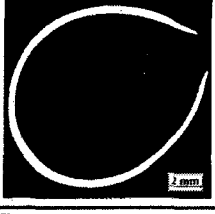
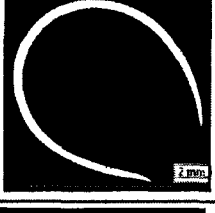
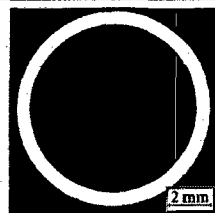
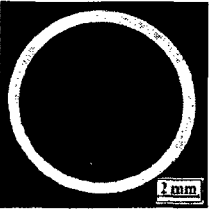
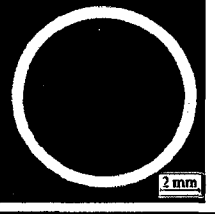
	106 (FRAP-T6)	109 (FRAP-T6)	119 (FRAP-T6)
Fuel enthalpy at failure (cal/g fuel) (calculated)			2296 K (FRAP-T6)
Peak fuel temperature (calculated)	1959 K (FRAP-T6)	2016 K (FRAP-T6)	1727 K (FRAP-T6)
Peak cladding temperature (calculated)	1545 K (FRAP-T6)	1606 K (FRAP-T6)	2.05 MPa (FRAP-T6)
Internal gas pressure at failure (calculated)	2.02 MPa (FRAP-T6)	2.04 MPa (FRAP-T6)	1285 K (FRAP-T6)
Outer cladding temperature at failure (calculated)	1279 K (FRAP-T6)	1266 K (FRAP-T6)	634-700 μm
Cladding thickness <i>out</i> of the rupture zone (measured)	649-677 μm	649 μm	24%
Cladding hoop strain <i>in</i> the rupture zone (measured)	33.4%	42.3%	6.3%
Cladding hoop strain <i>out</i> of the rupture zone (measured)	3.7%	7.3%	$\delta_{\text{ZrO}_2} = 10-15 \mu\text{m}$
ZrO ₂ thickness on the cladding <i>out</i> of rupture zone (measured)	$\delta_{\text{ZrO}_2} = 10 \mu\text{m}$	$\delta_{\text{ZrO}_2} = 10 \mu\text{m}$	
Cladding micro-structure <i>out</i> of rupture zone			
Cross-section of cladding <i>in</i> rupture zone			
Cross-section of fuel rod <i>out</i> of rupture zone			
Peak fuel enthalpy (cal/g)	116	119	146
Number of fuel rod	#B10T	#B9T	#B12T

Fig. 5.7. Parameters of high burnup fuel rods tested in air coolant.

In general, the following characteristic results can be drawn from this data base:

1. Before cladding rupture cladding thickness reduces not only in the main ballooning zone, but also over the entire fuel rod length. However, reduction of thickness may be both uniform and significantly non-uniform in the zones where secondary ballooning is initiated. As a result, cladding hoop strain for these sections of cladding is 3.7–7.3 %.
2. Since maximum temperature of the cladding of these fuel rods reached 1500–1700 K, the claddings were oxidized to ZrO_2 thickness about 10–15 μm . Important feature characterizing the test results of this group of fuel rods is a high cladding hoop strain in rupture zone of up to 42 %.

To compare behavior of high burnup fuel rods and fuel rods with fresh fuel, see test results of fuel rods with fresh fuel in Fig. 5.8.

Behavior of this group of fuel rods is similar to that of the high burnup fuel rods:

- reduction of the fuel rod cladding thickness happens over the entire fuel rod length; this process is more pronounced because minimal cladding thickness is 575–606 μm , and cladding hoop strain outside the rupture zone reached 17.2 %;
- maximum cladding hoop strain in the rupture zone reached approximately 50 %;
- since in three out of four fuel rods tested in this group peak fuel enthalpy reached 120–190 cal/g fuel, cladding oxidation during tests is very pronounced;
- peculiarity of this group of fuel rods is the fact that one of them (#B22T) was tested practically at the failure threshold which was 77 cal/g fuel in agreement with the FRAP-T6 estimate.

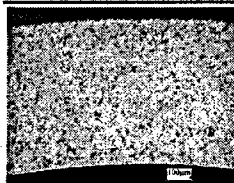
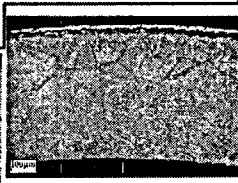
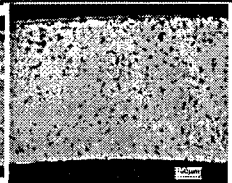
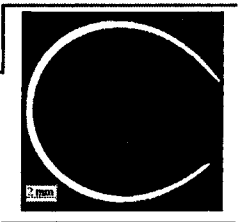
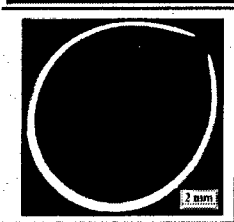
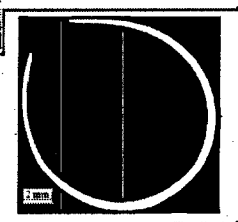
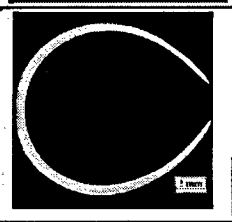
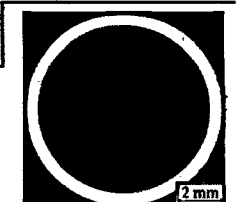
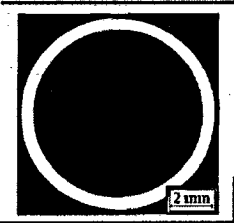
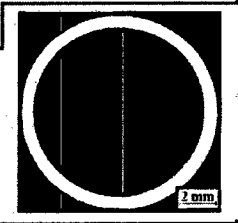
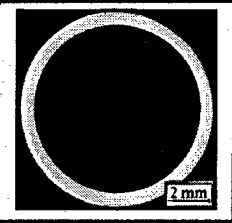
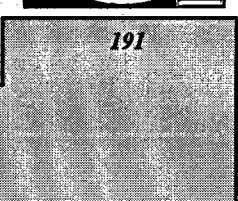
	77 (FRAP-T6)	119 (FRAP-T6)	120 (FRAP-T6)	147 (FRAP-T6)
Fuel enthalpy at failure (cal/g fuel) (calculated)		2112 K (FRAP-T6)	2143 K (FRAP-T6)	2763 K (FRAP-T6)
Peak fuel temperature (calculated)	1523 K (FRAP-T6)	1593 K (FRAP-T6)	1593 K (FRAP-T6)	1929 K (FRAP-T6)
Peak cladding temperature (calculated)	1258 K (FRAP-T6)	2.32 MPa (FRAP-T6)	1.99 MPa (FRAP-T6)	2.01 MPa (FRAP-T6)
Internal gas pressure at failure (calculated)	1.94 MPa (FRAP-T6)	1276 K (FRAP-T6)	1282 K (FRAP-T6)	1286 K (FRAP-T6)
Outer cladding temperature at failure (calculated)	1258 K (FRAP-T6)	575-610 μm	606-691 μm	606-677 μm
Cladding thickness out of the rupture zone (measured)	649-677 μm	48.1%	49.5%	32.8%
Cladding hoop strain in the rupture zone (measured)	46.3%	17.2%	6.7%	8.9%
Cladding hoop strain out of the rupture zone (measured)	10.4%			$\delta_{z_{\text{O}_2}} = 25-40 \mu\text{m}$
ZrO ₂ thickness on the cladding out of rupture zone (measured)	$\delta_{z_{\text{O}_2}} = 5 \mu\text{m}$	$\delta_{z_{\text{O}_2}} = 20 \mu\text{m}$	$\delta_{z_{\text{O}_2}} = 15 \mu\text{m}$	
Cladding microstructure out of rupture zone				
Cross-section of the cladding in rupture zone				
Cross-section of fuel rod out of rupture zone				
Peak fuel enthalpy (cal/g fuel)	79	123	125	191
Number of fuel rod	#B22T	#B20C	#B20T	#B19T

Fig. 5.8. Parameters of fuel rods with fresh fuel and irradiated and unirradiated claddings tested in air coolant.

6. ANALYSIS OF THE IGR TEST RESULTS BY USE OF RESULTS OF OUT-OF-PILE MECHANICAL TESTING

6.1. Formulation of the problem

Despite the fact that comparison of test results of the VVER high burnup fuel is not among priorities of the present report, intention to compare results obtained within the framework of this program with the results of similar research is quite understandable. That is why, at a certain stage of development of the data base presented in the present report, comparative analysis of the test results of the VVER and PWR high burnup fuel rods produced in the IGR, CABRI and NSRR reactors was carried out [13-16].

Results of this analysis are schematically shown in Fig. 5.1, Fig. 5.2.

Type of fuel rod	⇒	PWR	VVER
Pulse width	⇒	4.3–64 ms	630–850 ms
Rod internal pressure	⇒	0.1–5.1 MPa	1.7 MPa
Fuel burnup	⇒	33–64 MWd/kg U	48 MWd/kg U
Initial parameters of irradiated cladding	⇒	1. Oxidation up to 100 μm 2. Hydride concentration up to 800 ppm	1. Oxidation up to 3–5 μm 2. Hydride concentration up to 50 ppm
Type of failure	⇒	Low temperature failure due to PCMI mechanism	High temperature cladding due to ballooning mechanism

Fig. 6.1. Comparative parameters of RIA tests with PWR and VVER high burnup fuel rods.

These results were used as the basis of discussion, which allowed us to make the following conclusions:

1. High burnup fuel rods of VVER type tested in the IGR reactor were free of the PCMI type failure because irradiated Zr-1%Nb cladding has a low level of oxidation and hydriding, and, therefore, retains enough ductility to accommodate the PCMI strains.
2. The IGR reactor has a much wider power pulse (700 ms), than the CABRI and NSRR reactors (4–64 μs). As a result, the PCMI stage can be shifted towards higher cladding temperatures, besides, the strain rate and the cladding stress may be higher for the narrow pulses.

3. The VVER fuel has a central hole, therefore under otherwise equal conditions, the PCMI stress for this type of fuel rods will be lower due to lower thermal expansion and fission gas induced swelling.

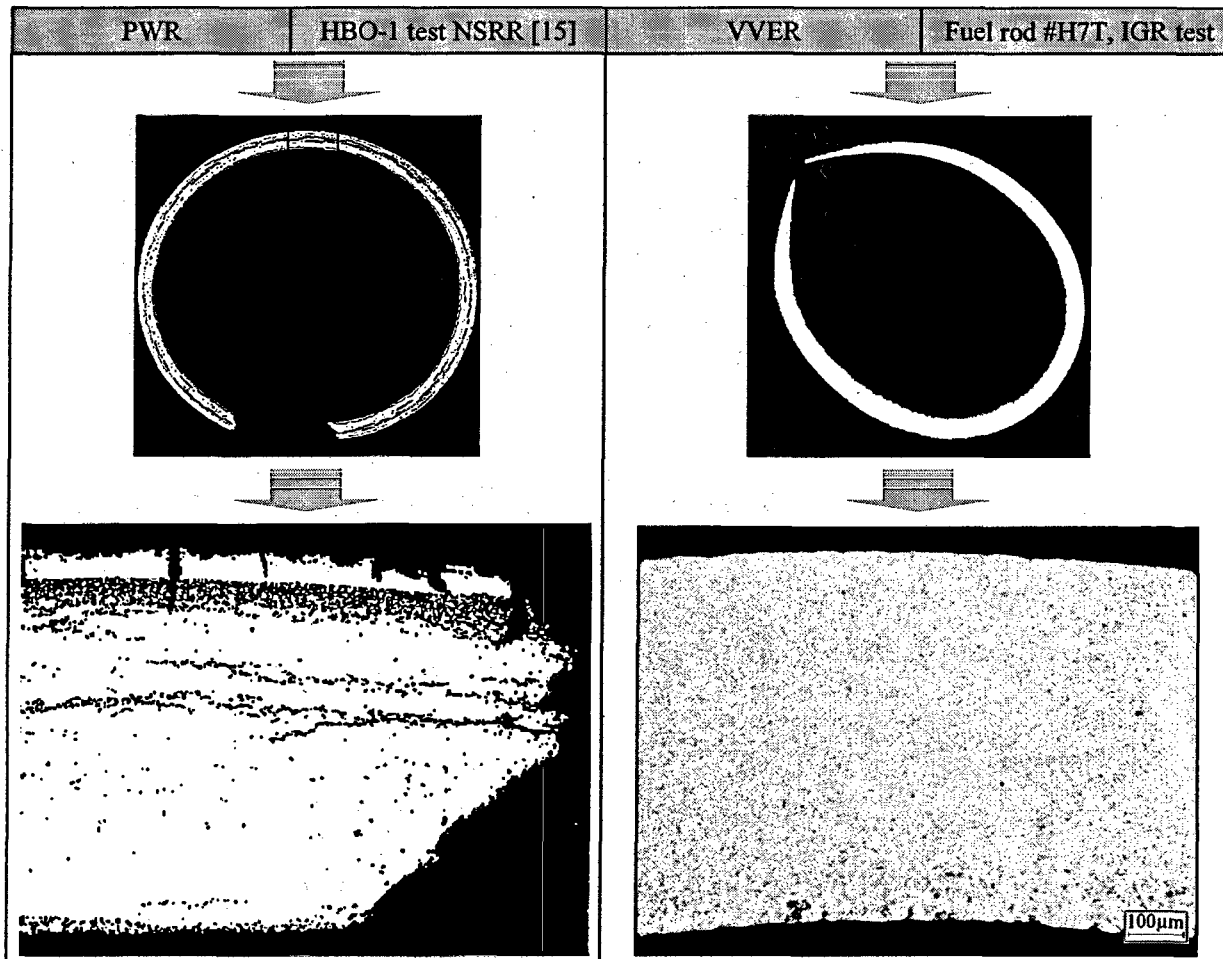


Fig. 6.2. Appearance of cross-sections of the PWR and VVER cladding and corresponding microstructure after RIA tests.

So, detailed discussion of these conclusions for this group of fuel rods made it possible to outline the list of primary problems to be resolved for the sake of final clarification of this issue. First, the data base of mechanical properties of the VVER cladding was to be developed. Second, this data base was to be included in the MATPRO package and the SCANAIR input data to be used in calculation of thermal mechanical behavior of the fuel rods under test. Solution of these two problems provided a possibility for conducting detailed computer analysis of behavior of Zr-1%Nb cladding under various conditions of the PCMI loading.

Besides, one more problem appeared at the stage of preliminary analysis of the IGR tests. The problem was associated with the fact that one needs experimental data to predict Zr-1%Nb cladding rupture under ballooning conditions because this failure mechanism was the main one during the VVER high burnup fuel rod test in the IGR reactor. Obviously, the IGR tests fail to correspond to typical RIA conditions because ballooning process is a key event in the loss of coolant accidents. It should be noted, that modern test data base characterizing behavior of irradiated cladding under LOCA conditions is practically unavailable. Corresponding cycle of work to obtain such data base is currently being scheduled. That is why, the data base for ballooning processes obtained within the framework of the IGR tests may be used in the LOCA analysis. This consideration was another argument in favor of complementing this data base with results of special out-of-pile tests.

Summary of results of these two research areas is presented in the following Section.

6.2. Results of mechanical tests with simple ring samples

As it was already written in Chapter 4, considerable efforts were made to validate and improve the corresponding test procedures. Description of this research and detailed discussion of the test results are given in Chapter 6 of Volume 2 and Appendix J of Volume 3 of the present report.

As a result, the following data base was obtained: for unirradiated and irradiated Zr-1%Nb cladding:

- ultimate strength, yield stress, total elongation, uniform elongation versus temperature;
- mechanical properties versus strain rate.

The strength properties versus temperature are shown in Fig. 6.3.

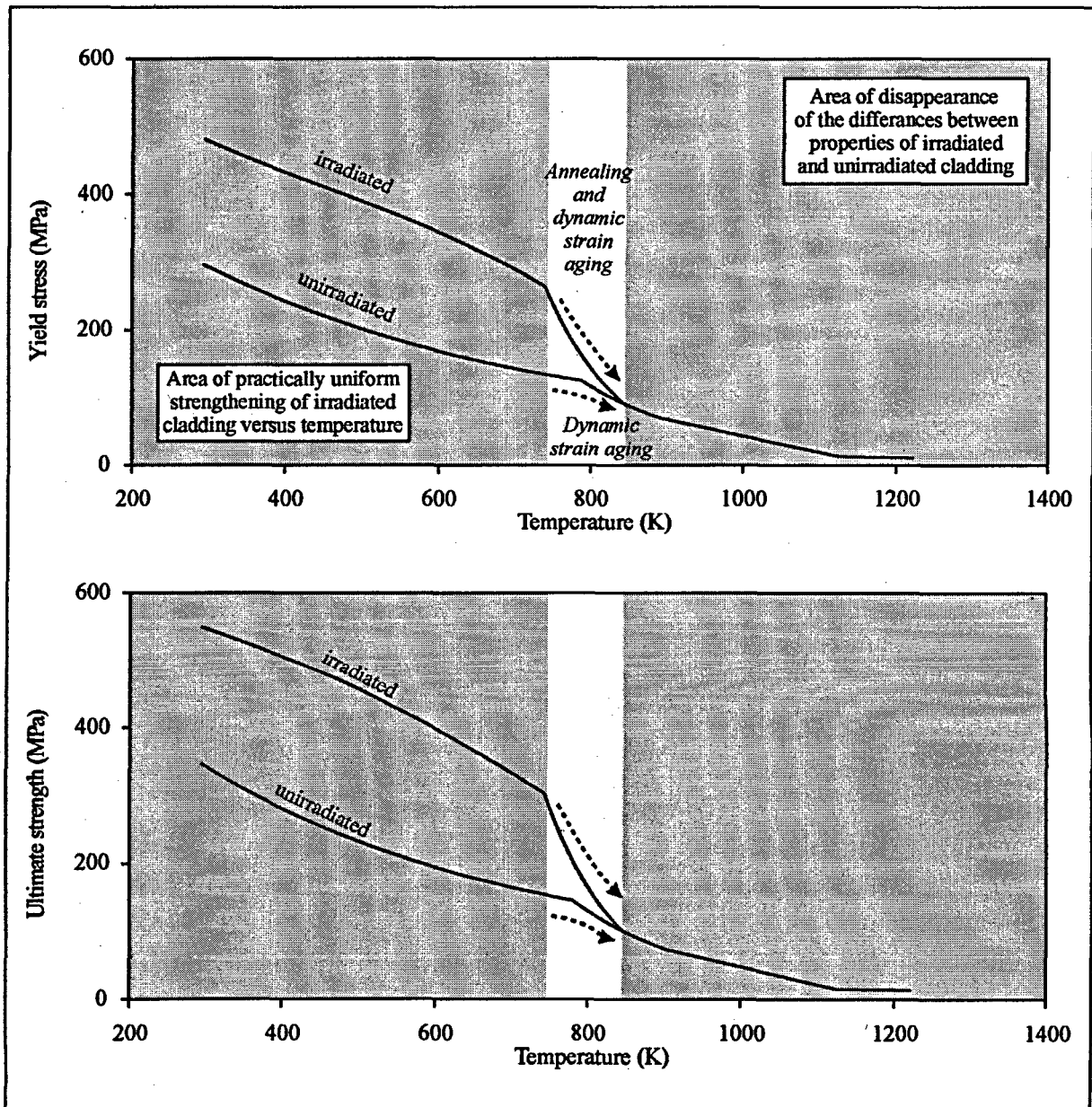


Fig. 6.3. Engineering ultimate strength and yield stress vs. temperature for unirradiated and irradiated cladding at the strain rate $2 \cdot 10^{-3} \text{ s}^{-1}$.

Analysis of this data demonstrates that considerable strengthening of the claddings of high burnup fuel rods occurs in the temperature range 293–750 K due to the base irradiation effects. Also, discrepancy between properties of irradiated and unirradiated cladding practically does not depend on the temperature in the specified range. However, starting from temperature 750 K, the annealing and dynamic strain aging effects are occurring and cause abrupt decrease of irradiated cladding strength. The dynamic strain aging effect is manifested also in unirradiated cladding, however, this effect becomes pronounced at a temperature of approximately 790 K. The whole complex of these physical effects influence strength properties of irradiated and unirradiated cladding so that these properties become the same at a temperature of 860 K, and can be further defined by the same correlations reflecting a rather moderate reduction of the cladding strength versus temperature.

Another important task of this research was to measure parameters of cladding ductility because these characteristics define the value of cladding strain under various loading conditions. Total and uniform elongation measurement results are shown in Fig. 6.4. Also, this Figure shows photos of several tested ring samples which demonstrably illustrate peculiarities of total elongation versus temperature.

So, the total elongation data base is characterized by the following features:

1. At a temperature of 293 K total elongation of irradiated cladding is approximately two times lower than the total elongation of unirradiated cladding.
2. This relationship is valid till the temperature of approximately 650 K with total elongation of both types of cladding practically independent of the temperature in this range due to the dynamic strain aging effect.
3. Like in the case of strength properties, annealing of irradiation damages clearly manifests itself beginning from temperature 750 K, therefore, total elongation of irradiated cladding noticeably increases, and by the beginning of the α - β phase transformation (883 K), total elongation of both types of cladding is practically the same.
4. The most interesting part of the data base characterizing total elongation is associated with the temperature range of 883–1153 K, because, in this range, Zr-1%Nb alloy contains both α and β phases. As it is obvious from Fig. 6.4, at a definite percent relation of these phases maximum values of total elongation for this alloy were registered in the range 1000 ± 50 K. Nevertheless, super plasticity effects at total elongation of 150–200 % were not observed although many authors claimed them, including the authors of present report. However, detailed analysis of the data shown in [17], indicated there was a procedural error which was initially incorrectly interpreted.
5. Obtained data demonstrate that when the β phase becomes considerable, total elongation of Zr-1%Nb claddings reduces, and reaches a minimal value at a temperature 1223 K within the tested temperature range. Photos of ring samples tested in β phase demonstrate a very specific nature of sample damage when no neck is practically formed, and the sample appearance after test reminds of brittle failure.

Uniform elongation is another important result of mechanical property measurement. Analysis of data shown in Fig. 6.4, indicates that irradiated Zr-1%Nb cladding preserves high plastic properties even at low temperatures. Like in the previous cases, annealing of radiation defects causes a situation when at a temperature of 860 K uniform elongation of irradiated and unirradiated claddings is the same. Further measurements showed that monotonous reduction of uniform elongation is observed in the temperature range of 860–1220 K.

Appearance of irradiated ring samples after mechanical tests

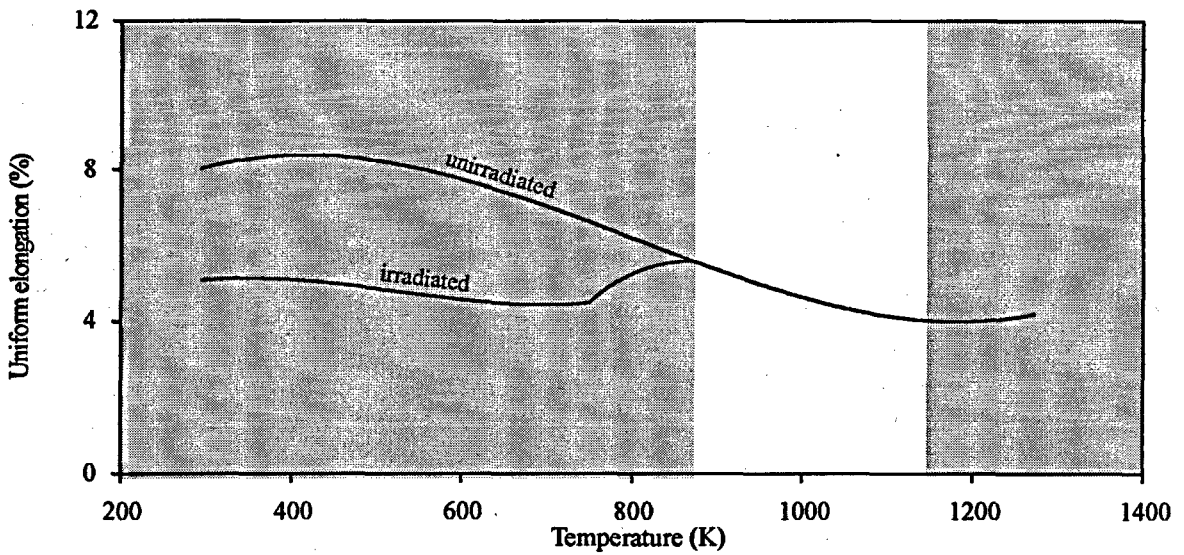
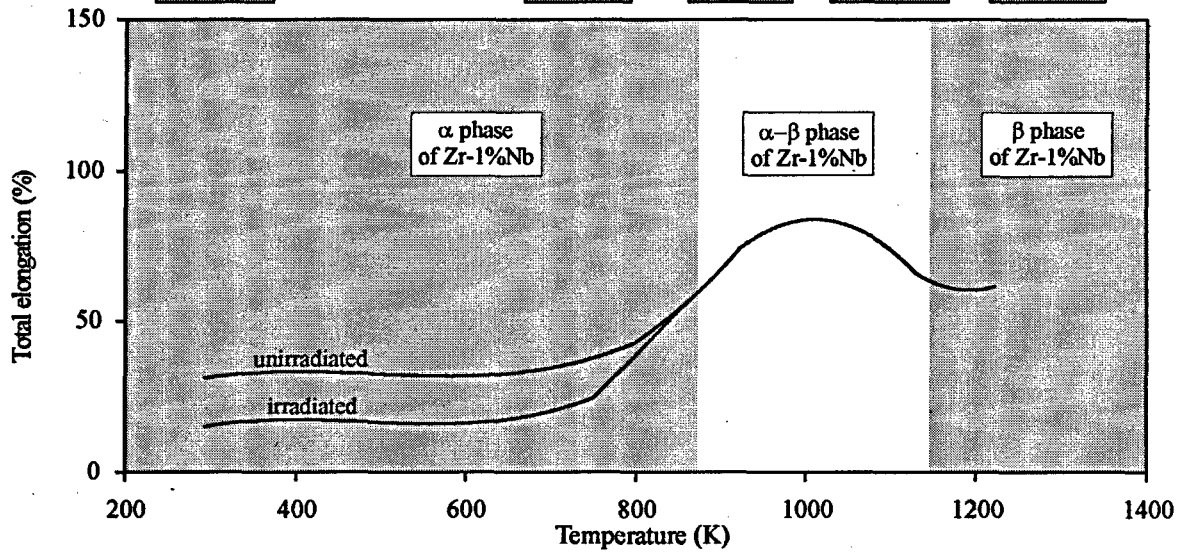
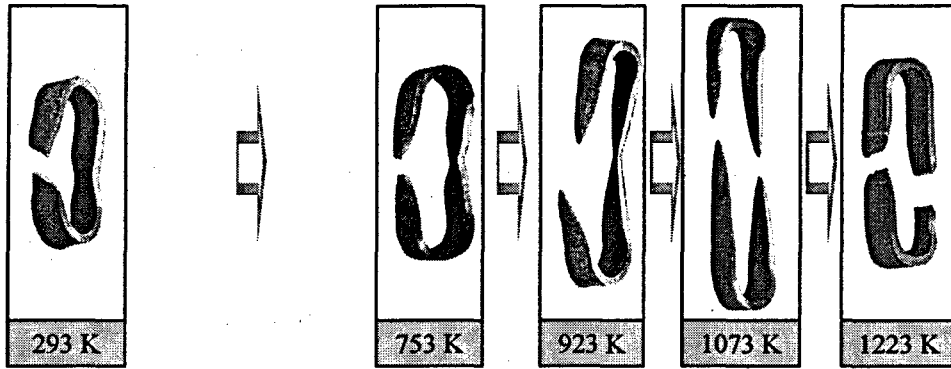


Fig. 6.4. Total elongation and uniform elongation vs. temperature for unirradiated and irradiated Zr-1%Nb cladding at the strain rate $2 \cdot 10^{-3} \text{ s}^{-1}$.

6.3. Results of burst tests

The main results characterizing behavior of pressurized Zr-1%Nb claddings under the burst conditions obtained during the tests are the following relationships:

1. Burst pressure versus temperature and strain rate;
2. Circumferential strain at burst versus temperature.

Generalized results as per Item 1 are presented in Fig. 6.5.

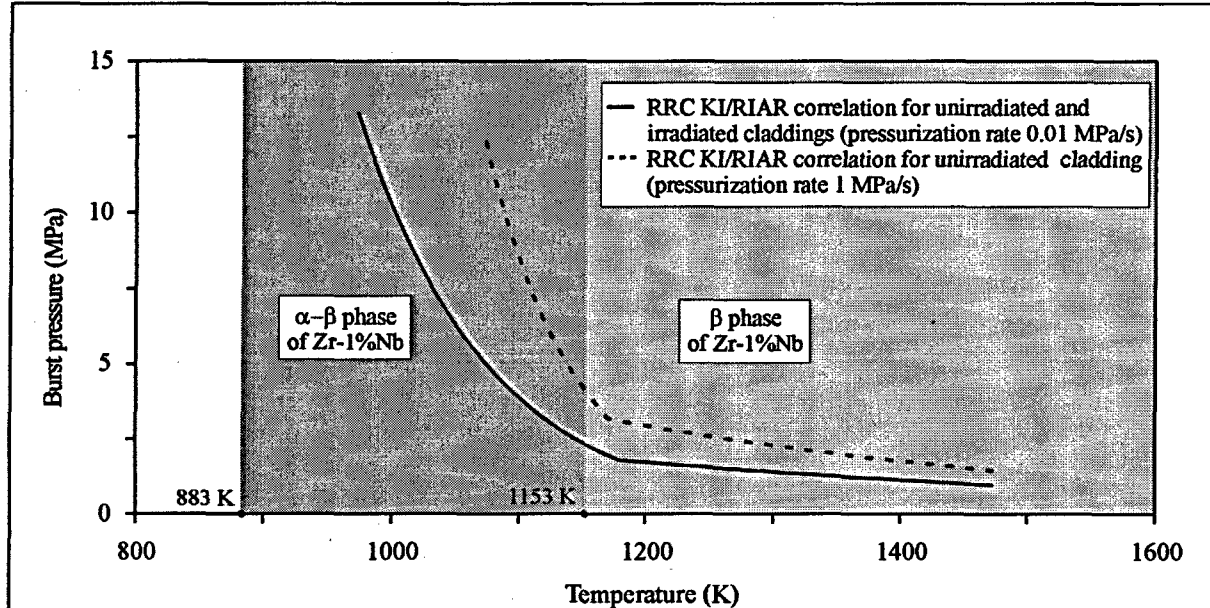


Fig. 6.5. Burst pressure vs. temperature and strain rate for unirradiated and irradiated Zr-1%Nb claddings.

We have to admit that the term “strain rate” in this case is not quite correct, because, actually, we are talking here of the pressure increase rate. However, these two notions are interrelated, and in the present Section, the term “strain rate” is used for agreement of perception of presented information. Therefore, data presented in Fig. 6.5 makes it possible to draw the following conclusions:

- burst pressure sensitivity to temperature is very high in the region of α - β phase of Zr-1%Nb alloy;
- in the region of β phase of Zr-1%Nb, burst pressure weakly responds to temperature variation, and, therefore, this case is in practice poorly predictable, i.e. it will be practically impossible to ensure the precise prediction of cladding burst moment in the temperature range 1200–1500 K, using the computer codes;
- it can be expected that the strain rate increase will raise the burst pressure at the same temperature, however, the effect of the strain rate on this process is governed by the laws similar to those governing the burst pressure versus temperature:
 - ⇒ in the α - β phase of Zr-1%Nb, strain rate considerably affects the values of burst pressure;
 - ⇒ in the β phase of Zr-1%Nb, the strain rate effect reduces with the temperature increase.

The next key item studied during the research was circumferential strain at the burst versus temperature. Importance of this parameter is determined first of all by the fact that it determines the flow area reduction in the fuel assembly under accident conditions, and, therefore, defines conditions for fuel rod cooling. Measurement results of this parameter and photos showing the change of cladding shape are presented in Fig. 6.6.

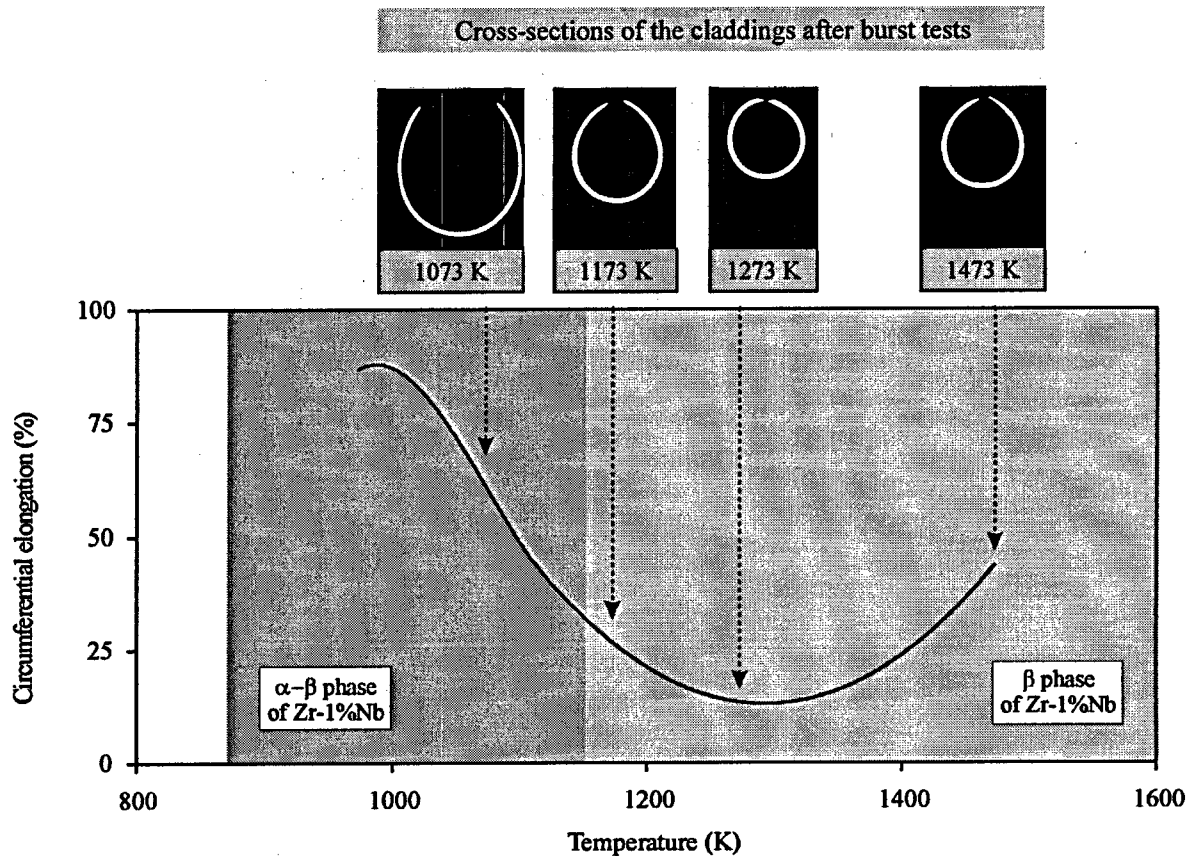


Fig. 6.6. Circumferential elongation at the rupture zone vs. temperature for the unirradiated and irradiated Zr-1%Nb claddings at pressure increase rate 0.01 MPa/s.

The obtained correlation supports the conclusions made previously on the basis of the ring tensile tests, i.e.:

- maximum hoop strain occurs in samples tested in the middle of the region of the α - β phase Zr-1%Nb;
- as the share of the β phase increases the hoop strain reduces strongly, reaching its minimum at 1300 K inside the β - region.

Some difference between these results and the results of the ring tensile tests is in the fact that minimum cladding hoop strain was registered in the burst tests at a temperature of about 1300 K. Further test temperature increase leads to growth of the cladding hoop strain. However, these results will naturally require a more thorough experimental proof and special attention should be given to the potential effect of the kinetics of phase transition.

7. ANALYSIS AND GENERALIZATION OF RESEARCH RESULTS

7.1. Decomposition of the IGR/RIA test scenario and selection of the key phenomena for analysis

To structure the analysis of the results, the sequence of events of the typical IGR test scenario has been established and presented in Fig. 7.1. Specifics of each of the identified process stages are schematically described in Table 7.1.

In agreement with this approach the following key phenomena were analyzed in present Chapter:

- PCMI and departure from nucleate boiling (DNB) → Stage 2;
- Ballooning and rupture conditions → Stages 4, 5;
- Criteria, thresholds and mechanisms of the VVER fuel rods failure under IGR test conditions.

Bearing in mind that analysis of results of special mechanical tests (ring tensile and burst) and analysis of the quality of developed VVER/IGR versions of FRAP-T6 and SCANAIR codes are presented in Volume 2 of the report, it was decided that these items would be reviewed only to the extent necessary for the analysis of the key phenomena.

7.2. Analysis of PCMI stage and estimation of conditions for the departure from nucleate boiling

Analysis of maximum strain level in cladding clearly indicates that mechanical interaction between fuel and cladding in high burnup fuel rods is a significant effect. As it was mentioned in Section 6.1, this type of failure was observed in several tests of the PWR high burnup fuel rods on the NSRR and CABRI. That is why, analysis of this stage for the VVER high burnup loading under the IGR test conditions is of vital importance despite the fact that presented data base does not contain any fuel rod with this type of damage.

The first problem that was discussed was associated with evaluation of validity of the PCMI parameters obtained with the use of the FRAP-T6 and SCANAIR codes. Therefore, the fuel total hoop strain, which determines the clad stress-strain conditions is mainly a sum total of two components:

- thermal expansion;
- fission gas induced swelling.

Within the framework of this analysis, the problem of thermal expansion modeling was not discussed, because we believe, that, obviously, calculation of this component does not cause great problems in the final results. Main attention was concentrated on evaluating the validity of predictions of fuel hoop strain due to swelling, rather than considering the absolute values of results, obtained by the two codes, too seriously different, as it is mentioned in Section 5.10 of Volume 2 of the report.

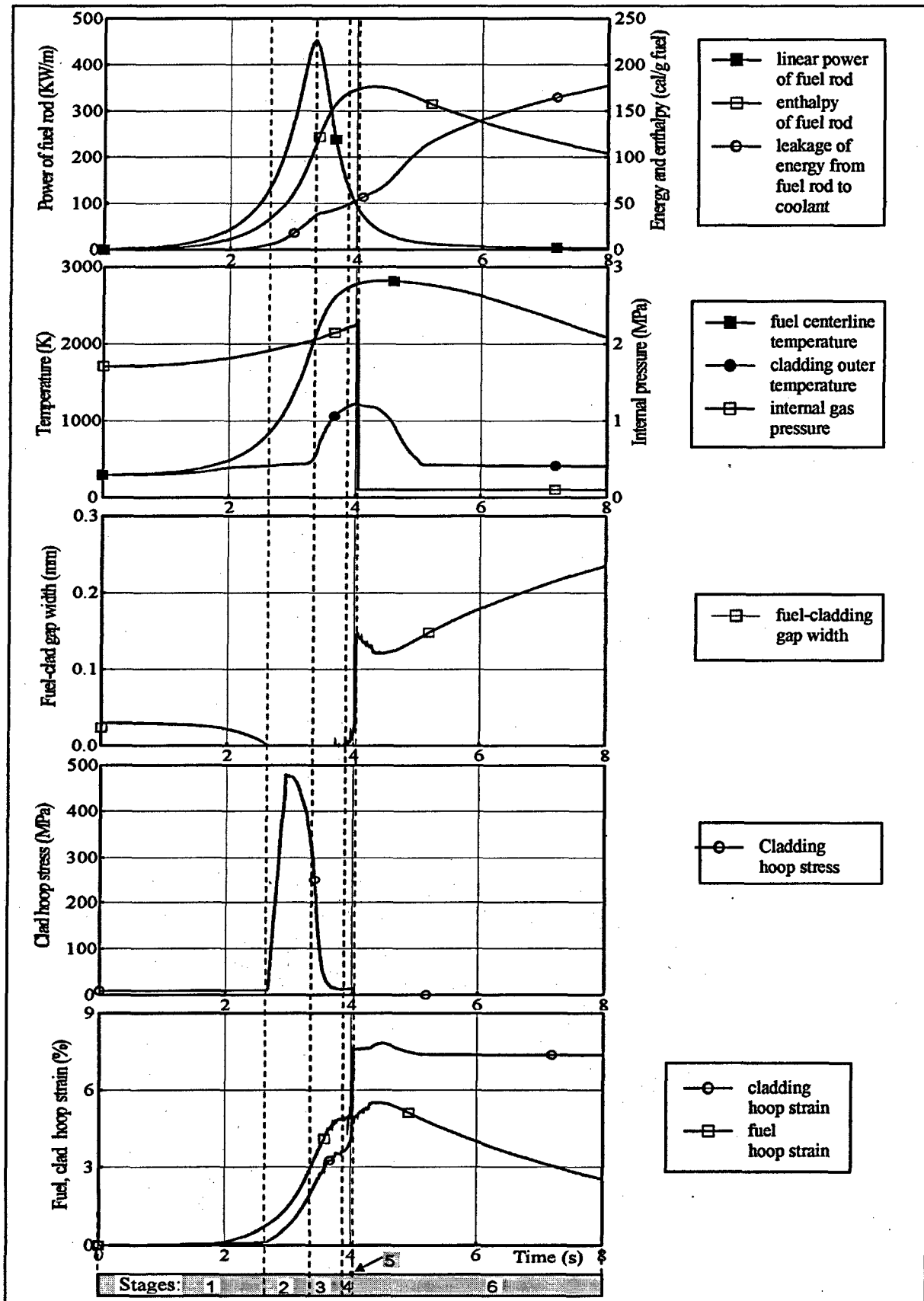


Fig. 7.1. FRAP-T6 predictions of VVER high burnup fuel rod behavior (#H5T) under IGR test.

Table 7.1. Description of the main stages of the thermal-mechanical behavior of high burnup fuel rod following the data presented in Fig. 7.1.

Number and name of stage	Description of the physical phenomenon
1. <u>Stage 1</u> "Closing of the gap"	Fuel rod power increases, fuel temperature increases, fuel expands due to thermal expansion and swelling till complete closure of the fuel-cladding gap.
2. <u>Stage 2</u> "PCMI"	Fuel rod power continues to increase, and fuel enthalpy and its temperature continue to increase; as a result, fuel hoop strain including components of thermal expansion and swelling continue to grow, but the cladding temperature still remains low. Sharp increase of the hoop stress occurs in the cladding due to the effect of expanding fuel.
3. <u>Stage 3</u> "Departure from nucleate boiling (DNB)"	Boiling crisis appears first on the cladding surface, and produces a sharp increase of the cladding surface temperature. Consequently the plastic deformation of cladding also increases sharply. At the same time the cladding hoop stress decreases despite the fact that fuel expansion strain continues.
4. <u>Stage 4</u> "Reopening of the gap"	Cladding temperature and internal gas pressure continue to grow, as a result, strength of cladding is so low, that sharp increase of cladding hoop strain happens exclusively due to internal gas pressure, and fuel-cladding gap reopens despite the fact that fuel total hoop strain continues to grow.
5. <u>Stage 5</u> "Ballooning and rupture of the cladding"	<p>All time dependent processes at this stage develop so quickly that in Fig. 7.1 they are presented by vertical line coinciding with termination of Stage 4 and reflecting time interval of 4.02–4.04 s. From the point of view of physics, this stage means that there is a criterion value of cladding hoop strain at which local ballooning of cladding is formed in this axial sector in a very short time, and, if cladding stress reaches a criterion value in the maximum deformation region, rupture of the cladding occurs. Obviously, the following issues at this stage are the most crucial ones:</p> <ul style="list-style-type: none"> • criterion of ballooning start; • criterion of cladding rupture; • cladding hoop strain in rupture zone.
6. <u>Stage 6</u> "Behavior of fuel rod after the cladding rupture"	So, the fuel rod is already ruptured, however, in this case, fuel enthalpy continues to grow, which maintains high temperature of the fuel rod, and, therefore, creates conditions for its oxidation, hydriding and embrittlement. Therefore, the process of fuel swelling and fission gas release actively continues. Nevertheless, eventually, fuel enthalpy starts to reduce, rewetting conditions appear on cladding surface, and its temperature sharply drops.

Note, that at high heat-up rate characteristics of the pulse tests fuel matrix expands due to increased gas pressure both on the grain boundaries and due to intragranular bubbles expansion. Increased pressure in intergranular pores may cause microcracking of the fuel, especially, in the rim zone, as indicated by experimental data. That is why, in the swelling analysis we can actually check only the total effect of swelling and cracking. This inspection was made during the posttest examinations of fuel rods on the basis of diameters of fuel pellets measured at four azimuth positions with the use of corresponding cross-sections. These results were rated for the initial pellet size prior to the test and calculated in swelling deformation. Results of comparison of calculated values of swelling and its measured values, which actually characterize residual hoop deformation of the fuel, are shown in Fig. 7.2.

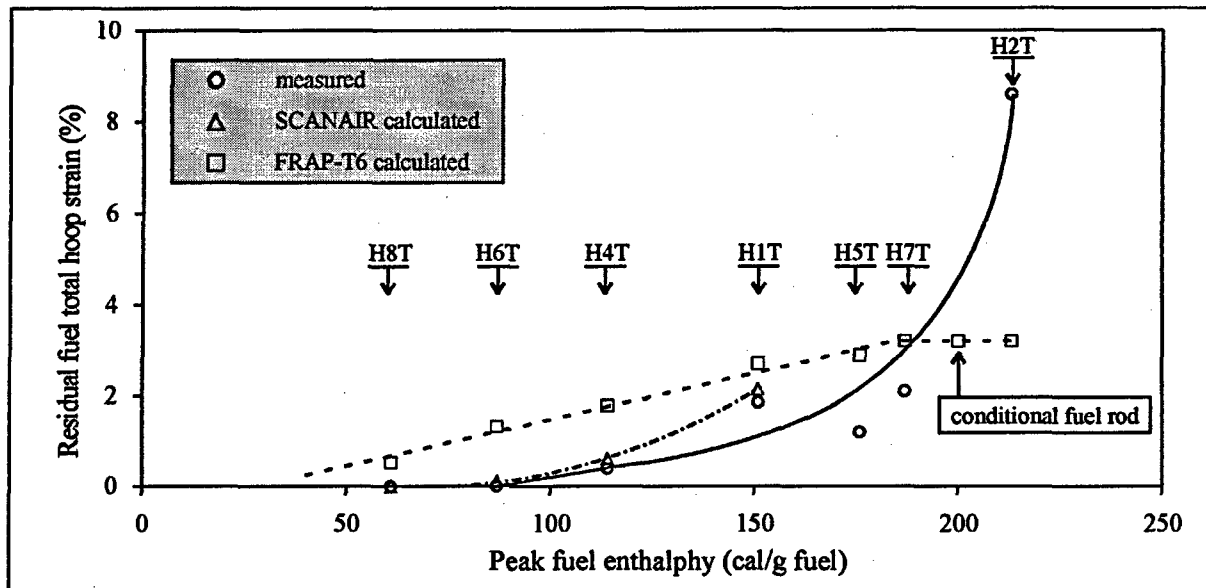


Fig. 7.2. Comparison of calculated and measured residual fuel hoop strain.

Obtained data indicate that the SCANAIR code correctly predict total residual fuel hoop strain for low values of the peak fuel enthalpy. The FRAP-T6 code considerably overestimates this parameter at low enthalpy. At higher peak fuel enthalpy discrepancy between the codes reduces. Above the 150 cal/g fuel the comparison was made only for FRAP-T6 results and measured data. As can be observed the FRAP-T6 code significantly underestimates total fuel hoop strain at fuel enthalpy above 200 cal/g fuel. But from the point of view of the objectives of this analysis we can state that calculated fuel total hoop strain values lead to re-estimation of the cladding hoop stress for enthalpy range 50–175 cal/g fuel for the FRAP-T6 code and 115–150 cal/g fuel for the SCANAIR code, which introduces reasonable conservatism element into the calculation results. However, resultant cladding hoop stress in the PCMI stage are determined not only by the fuel deformation, but also by mechanical properties of cladding. The value of cladding hoop strain was calculated by both codes on the basis of original mechanical properties of Zr-1%Nb cladding obtained as a result of the ring tensile tests.

Analysis of validity of predictions of the cladding hoop strain calculated with the use of the FRAP-T6 and SCANAIR codes was performed in Section 5.7 of Volume 2 of the report. Results of this analysis showed that both codes adequately predict cladding hoop strain at this stage, and the SCANAIR code copes with this task practically perfectly up to ~ 150 cal/g fuel.

To summarize the above, we can make the following conclusions:

- maximum cladding hoop stress calculated with the FRAP-T6 and SCANAIR codes for the PCMI stage in the VVER fuel rods tested in RIA conditions may be somewhat overestimated;
- taking into account the fact that the results are conservative, the obtained data base can be used for analysis of the VVER cladding failure under PCMI conditions.

Analysis of the PCMI stage is made with due regard for analysis of validity of calculated cladding parameters, but, the main issue of the analysis remained undisclosed, that is: what was safety margin of the tested VVER fuel rod before failure at the PCMI stage. Approach to finding the answer to this question will be discussed in Section 7.4. The present Section of the report ends in analysis of results characterizing the DNB phenomenon because the PCMI stage of fuel rod loading ends when the process of departure from nucleate boiling begins. Summing-up of calculation results for five high burnup fuel rods, which were tested above the critical heat flux, showed that the DNB threshold for this group of fuel rods is within the fuel enthalpy range of 93–102 cal/g fuel. For fuel rods with fresh fuel and high initial fuel cladding gap (#H15T) this value grew up to 115 cal/g fuel. However, we should note, that the DNB initiation parameters are basically stipulated by correlations, which were used to calculate critical heat flux. In this case Kutateladze correlation was used for this purposes (see Section 5.4 of Volume 2).

7.3. Ballooning and rupture conditions

Analysis of these effects should begin from the moment when the gas gap reopens due to clad thermal expansion and intensive plastic deformation of cladding resulted in internal gas pressure. Two versions of development of these events were observed in the IGR tests:

1. Plastic hoop strain of cladding grows up to the moment when cladding temperature begins to reduce due to fuel rod cooling. However, no cladding rupture happens, and the fuel rod remains intact. A characteristic example of this case is fuel rod #H1T (see Fig. 7.3). Nevertheless, data presented in Fig. 7.3 (c) to characterize cladding hoop strain versus fuel rod length, may be interpreted in the context of beginning of initial stages of two ballooning (60 and 140 mm), although from a theoretical point of view, cladding hoop strain profile should follow fuel enthalpy profile (or, rather, cladding temperature axial profile).
2. The second version of scenario is characterized by the fact that plastic hoop strain grows under the effect of internal gas pressure up to a criterion value, after which the process of local deformation of the fuel rod cladding, known as ballooning, begins in this section of cladding. This happens very quickly (within several milliseconds), and, normally, ends in the cladding rupture. However, experience with fresh fuel rod tests indicates that this sometimes fails to happen.

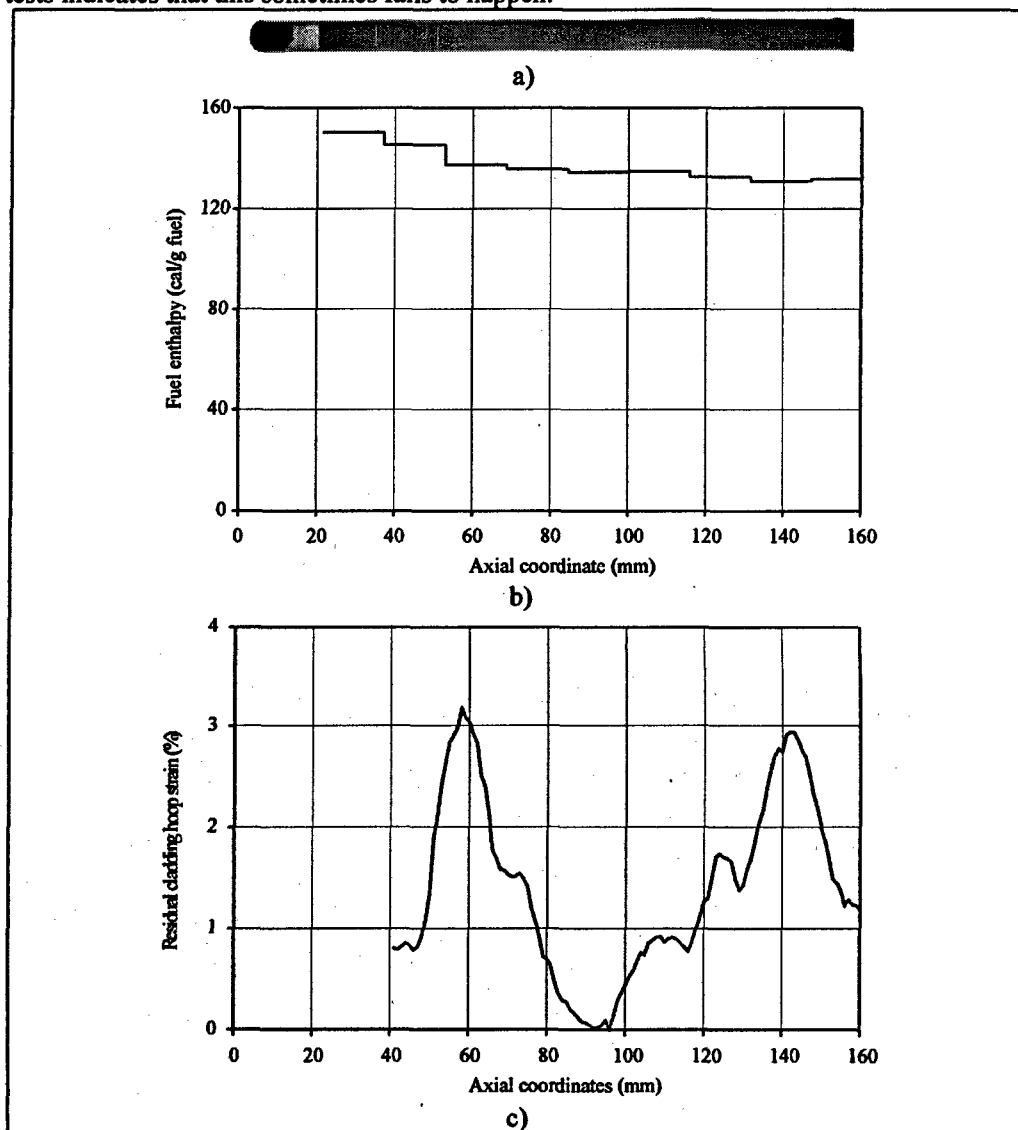


Fig. 7.3. X-ray photograph of the fuel rod #H1T after test (a), axial distributions of the fuel enthalpy (b) and measured axial distribution of the cladding hoop strain for the fuel rod #H1T after test (c).

As it was indicated in Table 7.1, to correctly interpret the processes under consideration and have boundary conditions for analysis of their consequences we must know the following three key parameters:

1. Criterion of ballooning start.
2. Criterion of cladding rupture.
3. Maximum cladding hoop strain in the rupture zone.

Besides, fundamental problem ensuring possibility for calculating the cladding strain and cladding rupture, is availability of the data base on the cladding mechanical properties. Table 7.2 contains characteristics of these parameters as they were used for prediction of behavior of each unfailed and failed fuel rod with the use of FRAP-T6 code.

Table 7.2. Approach, used to determine ballooning key parameters.

Key parameters	Method
1. Criterion of ballooning start	Calculated cladding effective strain equals cladding uniform elongation measured at ring tensile tests.
2. Criterion of cladding rupture	Calculated cladding stress in the hot node equals cladding burst stress, measured during burst tests.
3. Maximum cladding hoop strain in the rupture zone	Maximum cladding hoop strain is calculated using mechanical properties obtained with the help of the ring tensile tests.

Analysis of results obtained by this approach allows us to make some conclusions regarding each of the key parameters.

7.3.1. Criterion of ballooning start

Objective experimental data to check the quality of this criterion still has to be obtained, but analysis of the test curve characterizing uniform elongation versus temperature shows that in the temperature range of 900–1300 K, uniform elongation is within the range of 4–5 %. In other words, for the whole group of the VVER fuel rods for which ballooning was predicted, the start of this process happened when cladding deformation reached the value of about 5 %. To evaluate this data at least indirectly, all available data base of the VVER fuel rods tested in IGR reactor was analyzed, and representative value of the maximum cladding hoop strains for fuel rods without ballooning effect was determined. This value was approximately 3.5–4.0 %. Thus, we can assume that the employed criterion of the start of ballooning is adequately plausible.

7.3.2. Criterion of cladding rupture

To define the cladding rupture criterion, special burst tests were performed on unirradiated and irradiated Zr-1%Nb cladding. These tests clearly proved the conclusions made on the basis of the ring tensile tests about similarity of mechanical properties of unirradiated and irradiated Zr-1%Nb cladding at temperatures above 900 K. This made it possible to compare results of these tests with the results obtained previously on unirradiated Zr-1%Nb cladding [11, 12], and produce generalized data base shown in Fig. 7.4.

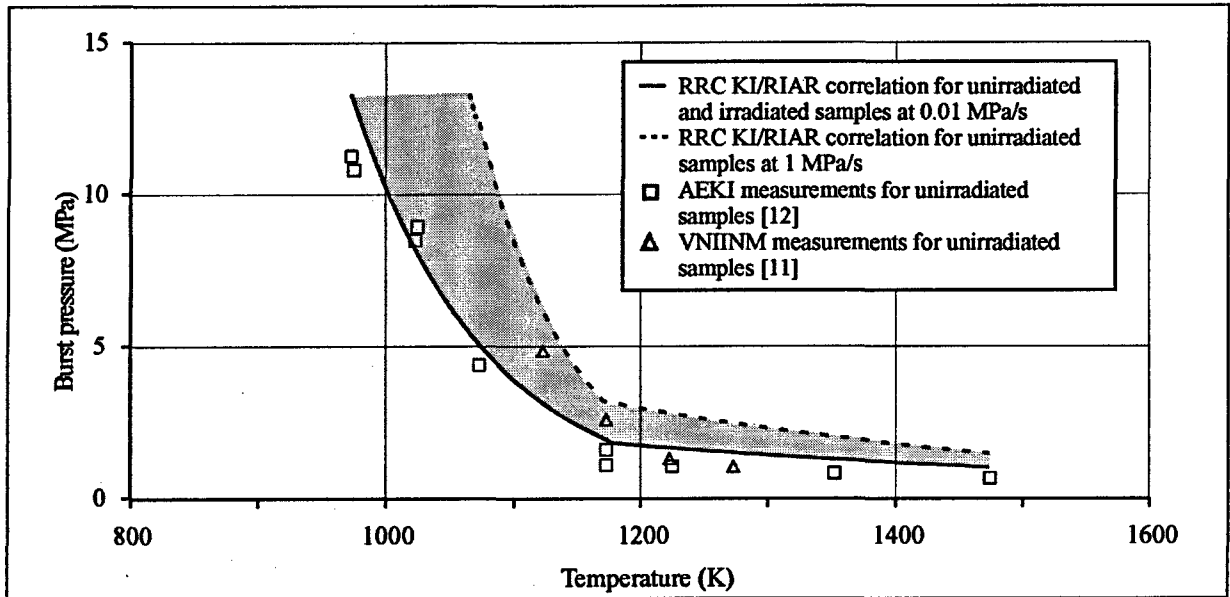


Fig. 7.4. Summary of burst test results with Zr-1%Nb claddings.

Analysis of this data base shows that a good agreement of results occurs in all three data groups if we assume that cladding strain rates in all the tests were equal, and that they corresponded to the strain rate implemented in the RRC KI/RIAR burst tests at a pressure increase rate of 0.01 MPa/s.

Comparison of the MATPRO data base on Zircaloy and the data base obtained as a result of the RRC KI/RIAR tests was the next step in the analysis (see Fig. 7.5).

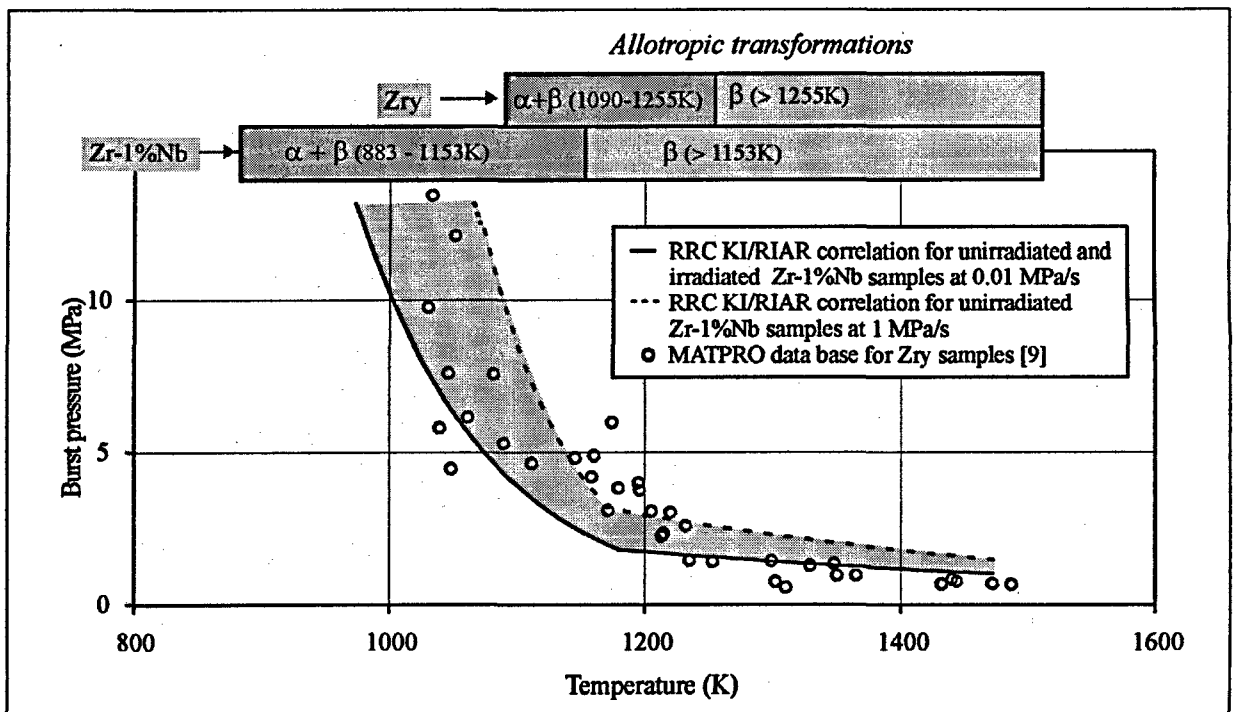


Fig. 7.5. Comparative burst data base for Zr-1%Nb and Zry claddings.

This comparison showed that despite differences in the test conditions, alloys Zry and Zr-1%Nb demonstrated good compliance of strength characteristics. Nevertheless, noncoincidence of temperatures of the $\alpha \rightarrow \beta$ transformation, obviously affected the nature of the burst pressure temperature dependence. After the obtained data on burst pressure versus temperature was proved to be representative, and specific behavior of Zr-1%Nb cladding was observed, analysis of validity of criterion of cladding rupture was performed. To this end, use was made of results of the tests of VVER fuel rods in air coolant. In agreement with the procedure used for processing the burst test results, burst stress versus temperature was found for fuel rods ##B9T, B10T, B12T, B19T, B22T. Comparison of obtained results with the burst tests results is shown in Fig. 7.6.

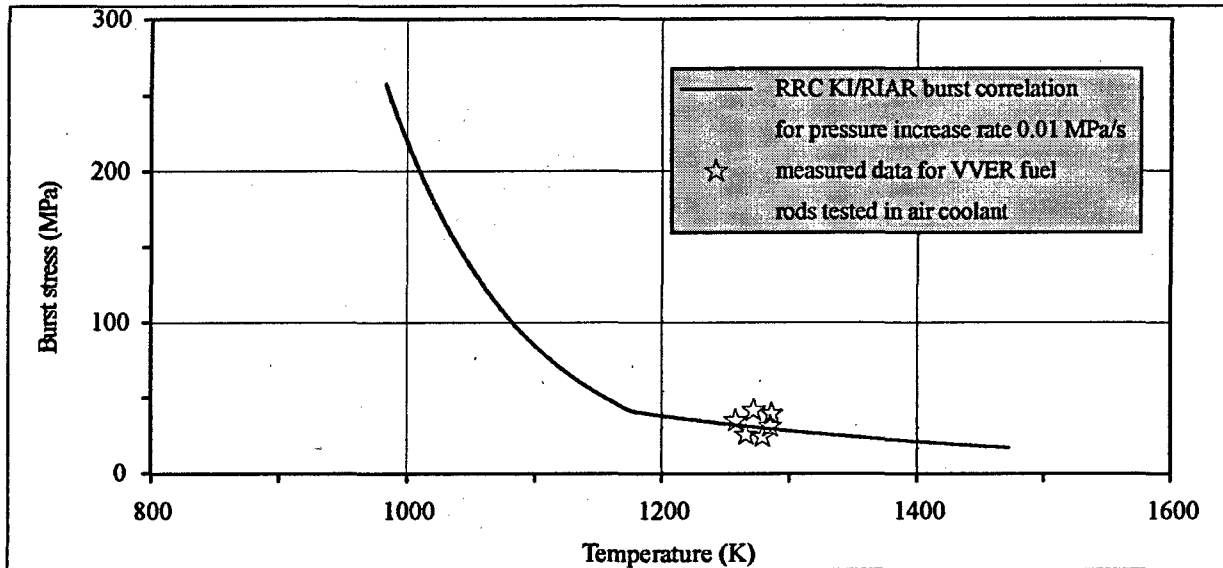


Fig. 7.6. Comparison burst stresses vs. temperature obtained using burst test and VVER fuel rod with irradiated cladding tested in air coolant in IGR reactor.

We can see good agreement between two data groups, and this fact proves that burst stress may be used as a criterion of cladding rupture, although, it was absolutely useful to add the results characterizing burst stress in VVER high burnup fuel rods tested in the IGR reactor in water coolant to the data base.

7.3.3. Maximum cladding hoop strain in the rupture zone.

Analysis has shown that so far this particular issue has not been fully resolved.

To demonstrate the actual scale of the problem, the following criterion was introduced for assessing the predicted cladding hoop strains in the rupture zone, using the FRAP-T6 code:

$$\delta_{\epsilon_2} = \frac{\epsilon_{rm} - \epsilon_{rc}}{\epsilon_{rm}} 100\%,$$

where δ_{ϵ_2} = the relative error in cladding hoop strain prediction (%);

ϵ_{rm} = the cladding hoop strain in the rupture zone as measured (%);

ϵ_{rc} = the cladding hoop strain in the rupture zone as calculated (%).

To improve the representativeness of the results obtained with the help of this criterion, the following groups of fuel rods were dropped out from consideration:

- Fuel rods for which an evident disagreement between calculated results and data of measurements is observed for the entire range of the parameters lending themselves to comparison, incorrectness of the value of energy deposition being the most likely cause of the disagreement (#B21T);

- Fuel rods with fuel stacks severely damaged in the course of manufacture, due to which the ballooning of the cladding was located far above the upper end of the fuel stack (#B12T, see Volume 3 of the report);
- Fuel rods in which two cases of ballooning with ruptures (#H7T, #H2T, #H3T) were detected; such a situation is not covered by the numerical scheme developed;
- Fuel rods with fuel and cladding melting (#H3T).

The remaining group of tested fuel rods was subjected to an analysis using the criterion δ_{ϵ} , and the results of the analysis are displayed in Fig. 7.7.

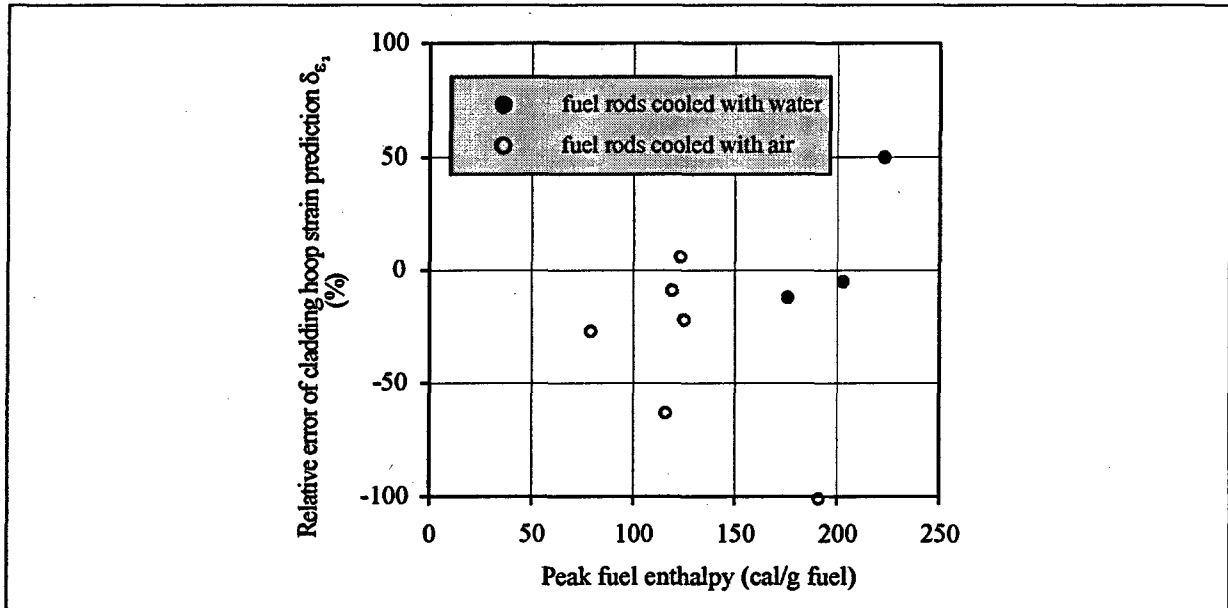


Fig. 7.7. Results characterising the quality of prediction of maximum cladding hoop strain in the rupture zone.

Thus, despite the small sampling size, it is evident that:

- Generally, cladding hoop strains are overestimated, the worst results having been obtained for air cooled fuel rods;
- Significant underestimation of the cladding hoop strain was observed for one of water cooled fuel rods.

In this connection, it should be noted that at the stage of FRAP-T6 verification a number of steps had been taken to improve the results of cladding hoop strain calculation. Therefore, the variant presented in Fig. 7.7 features certain improvement in the calculation results.

Inasmuch as the problem of predicting the maximum cladding hoop strain in the rupture zone (especially in the case of gas coolant) is far beyond the limits of RIA investigations and is of extreme importance for LOCA analysis, it is meaningful to make an attempt of unravelling more carefully possible reasons for disagreement among predicted cladding hoop strains. The list of the possible reasons and brief comments for each of them are given in Table 7.3.

Thus, five possible sources of systematic errors in prediction of the cladding hoop strain in rupture zone are presented in Table 7.3. The stage of thorough analysis of consequences for each error type has not been completed yet and will be addressed in detail in the Final version of this Volume of the present report. However, some preliminary results of the research, related to one of the basic items of the table (item 5) are given in the paragraph below.

Table 7.3. Possible sources of errors in predicting the maximum cladding hoop strain in rupture zone.

Source of errors	Comments	Assessment of the necessity of additional analysis
1. Energy deposition in fuel rods	Can be treated only as a random error, i.e., it cannot give rise to a systematic error in cladding hoop strain estimates	No
2. Initial internal pressure in fuel rods	There exists an uncertainty in the input data characterizing this parameter in the range of ± 0.2 MPa, i.e., the error is of random nature and its consequences as well must be of random rather than systematic nature.	No
3. Cladding temperature and internal gas pressure, calculated with the FRAP-T6 code	If the uncertainty described in item 2 is eliminated from consideration, the parameters in question were the subject of a special verification described in Volume 2 of the present report. Nonetheless, it is impossible to guarantee the absolute accuracy when calculating these parameters, the more so with the systematic error available.	Yes
4. Assessment of azimuthal temperature non-uniformity around the circumference of the cladding at the beginning of ballooning	There are no recommendations on assessing this parameter; in this research, such assessment was empirical, and we have to acknowledge that the depth of studying the problem was inadequate. Therefore, the availability of a systematic error in the obtained data base may be assumed.	Yes
5. Inadequate representativeness of ring tensile test results as a data base on mechanical properties of claddings, or imperfect interpretation of the obtained data base under the MATPRO approach	Within the FRAP-T6/BALON2 approach, the calculation of the cladding hoop strain under ballooning conditions is made using the results of uniaxial tests (here, ring tensile tests) as mechanical properties of the cladding. However, the cladding loading is biaxial. Additionally, the power law is applied to approximate the measured mechanical properties and employ them for calculation of mechanical behavior of the cladding. When doing so, the results are extrapolated to the region where the measurements were not carried out. All these factors may give rise to a systematic error.	Yes
6. Error in the definition of the cladding rupture criterion	Obviously, if the criterion of cladding rupture has a systematic error, this leads automatically to a systematic error in cladding hoop strain estimates.	Yes
7. The mathematical model used for ballooning prediction	FRAP-T6/BALON2 codes calculate the ballooning, using the so-called "thin-walled membrane model". When doing so, a number of assumptions without adequate validation are employed. Inadequate representation of the actual process in the mathematical model may result in a systematic error.	Yes

7.3.4. Analysis of possible sources of errors in predictions of cladding hoop strain due to imperfection of the data base on mechanical properties of claddings and imperfect interpretation of the data base

The list of the issues to be analyzed may be presented as follows:

1. Comparison of parameters characterizing the hoop strain of claddings versus the temperature for uniaxial tests (ring tests), biaxial tests (burst tests), real fuel rods tested under the conditions with a relatively uniform axial and circumferential temperature distribution (IGR tests with air cooled fuel rods).
2. Hoop strain versus strain rate phenomena.
3. Extrapolation of mechanical properties with the power law beyond the test area.

This list was considered item after item. The primary data base for comparing the results of various test types is presented in Fig. 7.8.

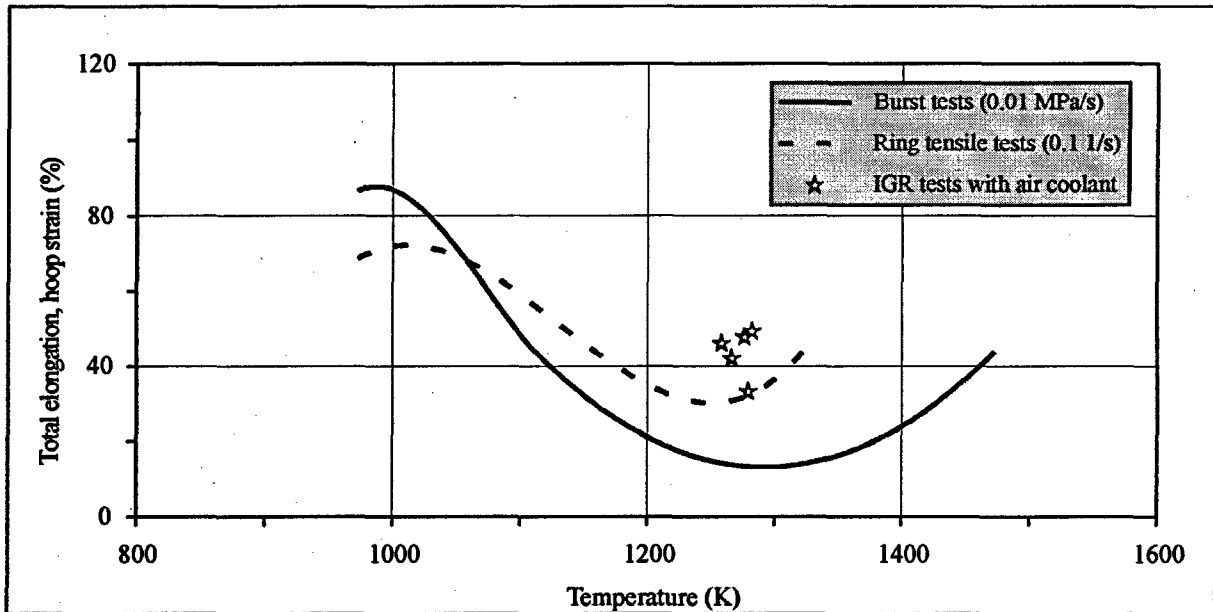


Fig. 7.8. Comparison of the cladding hoop strains from three type of tests.

An additional problem arose as a result of the efforts to obtain the comparison data base. This problem consisted in that all the three types of data must be obtained at the same strain rate of cladding. We cannot consider this problem fully solved, but some estimates show that the results of burst tests obtained at a pressure increase rate of about 0.01 MPa/s are in approximate correspondence to a strain rate of 0.1 s^{-1} in ring tests. Therefore, the two correlation expressions characterizing the hoop strain (total elongation) of cladding versus the temperature inferred from the ring tests (ring samples of the cladding) and burst tests (pressurization cladding tubes) are deduced at approximately equal strain rate values.

Additionally, the results for IGR tests with air coolant (real VVER fuel rods) are given in the figure as measured (i.e., without any correction for the strain rate). An analysis of this data base allows the following conclusions:

- in general, ring tests and burst tests reflect in a similar way the trend in hoop strain versus temperature variation;
- nevertheless, the difference in predictions of absolute cladding hoop strain values is rather significant in some temperature regions;
- the measured hoop strains in real fuel rods are in a considerable excess over the corresponding values obtained in the ring and burst tests.

An additional analysis performed for the first two conclusions above has suggested the necessity in further studies in order to substantiate in a more rigorous fashion the equality of strain rate values in both test types and, besides, to refine the expression for each correlation on the basis of more representative statistics. Nonetheless, it cannot be ruled out that the discrepancy between the two test types will not vanish entirely even after such additional studies are completed.

As for the disagreement between the hoop strains in real fuel rods and those measured in out-of-pile tests, the strain rate was calculated for each fuel rod tested. The results of these calculations evidence that pressure increase rates under rupture conditions ranged within 0.08–0.11 MPa/s. Therefore, these results were compared against the results of the burst tests at a pressure increase rate of 0.1 MPa/s (see Fig. 7.9). The comparison data base obtained exhibits a relatively good agreement for the two test types, though, in general, burst test results lead to a slight underestimation of actual cladding hoop strains.

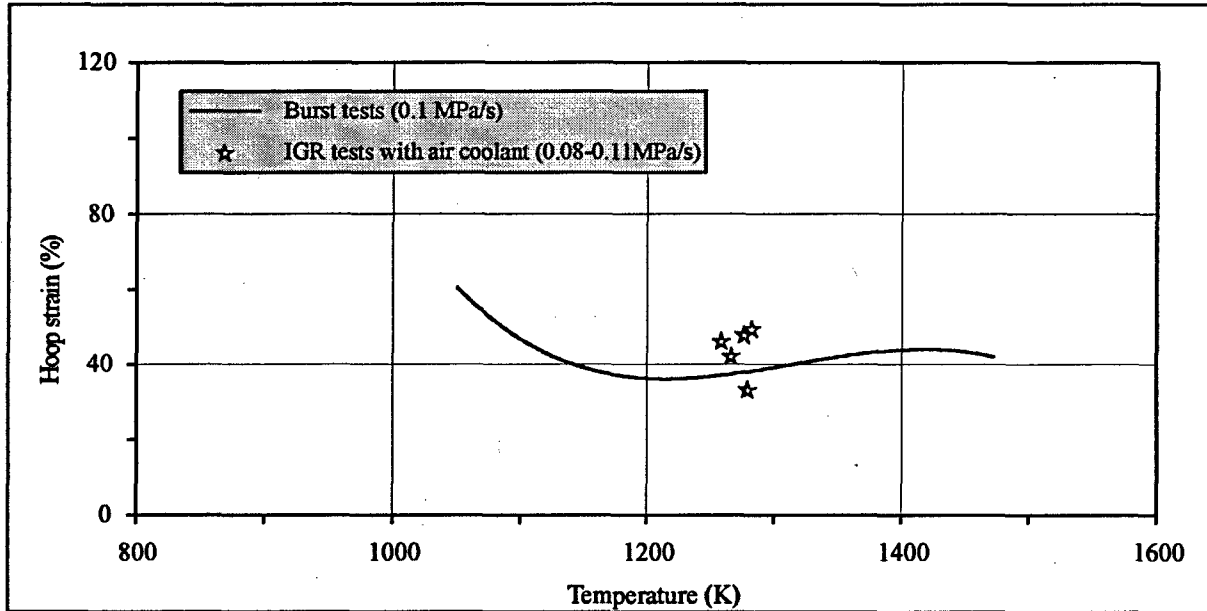


Fig. 7.9. Comparison results of burst tests and reactor tests on cladding hoop strain.

A comparative analysis of the hoop strain vs. strain rate dependence for the two test types (ring and burst tests) was the next stage of the research under consideration. Unfortunately, this analysis has revealed the following:

- according to the results of ring tests, the hoop strain decreases as the strain rate rises, throughout the temperature range studied (293–1123 K);
- according to the results of burst tests, the hoop strain decreases as the strain rate rises in a temperature range of 973–1100 K; for a temperature range of 1150–1473 K (β -phase of Zr-1%Nb), some abnormal results have been obtained, namely, an increase in the hoop strain as the pressure increase rate rises. An explanation to this phenomenon is given in Chapter 6, Volume 2 of the present report.

Thus, the major conclusions that can be inferred from the results of this analysis are as follows:

- calculation of the hoop strain under ballooning conditions should be performed, using the data base obtained within the ring tests if the extrapolation of the hoop strain vs. strain rate dependence to the temperature range of 1.150–1.473 K is incorrect; since this dependence changes its sign in the given range, the hoop strain predictions based on the FRAP-T6 code would lead to underestimation as compared to the measured values;
- the size of the sampling used for deriving the hoop strain versus strain rate dependence is insufficient to deduce reliable correlation expressions for both ring and burst tests;

- some efforts should be made to enlarge the statistical sampling size and extend the temperature range to determine the hoop strain versus strain rate dependence in ring tensile tests.

The last item of this analysis deals with assessing possible errors in predicting the hoop strain of claddings when using results of power law extrapolation beyond the test area. Graphically, this problem for fuel rods with water and air coolant is schematically illustrated in Fig. 7.10.

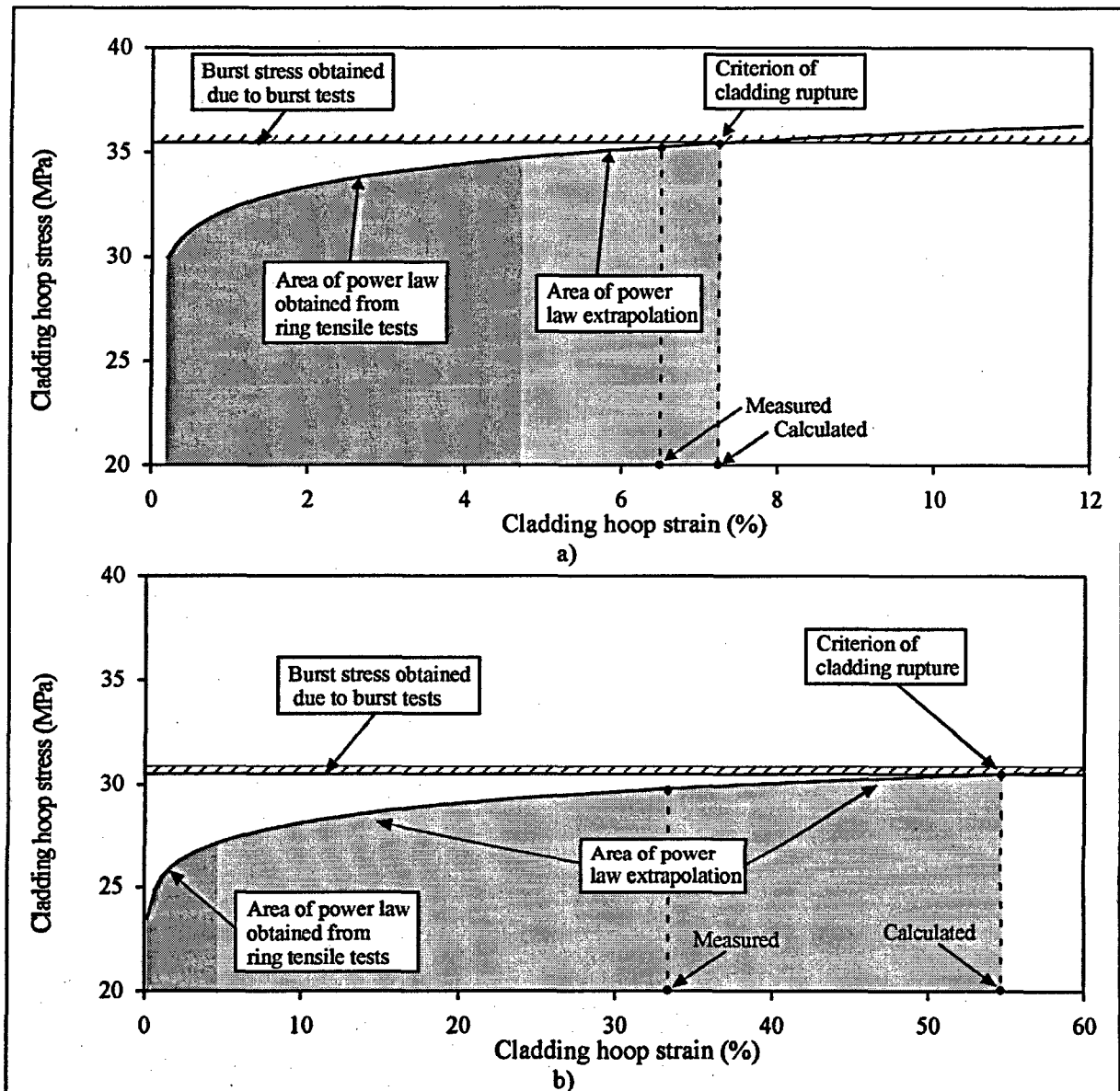


Fig. 7.10. Extrapolation of the power law beyond the test area for water-cooled fuel rod #H5T (a) and air coolant fuel rod #B10T (b).

The following conclusions can be made on the basis of an analysis of the data in this plot:

1. In both cases under consideration (water coolant; gas coolant), the IGR test area (hoop stress and hoop strain of a VVER cladding) is beyond the test area within which the mechanical properties of the VVER cladding had been measured, and the parameters of the power law, employed for calculation of the cladding hoop strain vs. cladding stress dependence had been determined.

2. As can be readily seen from the data in Fig. 7.10, the extrapolation of the available power law beyond the test area is rather convincing for water coolant. Evidently, some correction of the law will not result in a significant change in hoop strain unless the burst stress line is changed. However, the extrapolation of the power law for air coolant should be considered unconvincing and misgiving until additional experimental evidence is obtained, sufficient for its validation.
3. It is quite clear that in both cases particular attention should be paid to the burst stress line since even an insignificant refinement of the line will result in essentially different values of the hoop strain calculated with the help of the FRAP-T6 code.

Thus, the analysis performed has enabled to identify possible sources of errors in cladding hoop strain predictions and outline a number of steps that might be helpful from the viewpoint of positive elucidation of the issue within the efforts on improving the data base on mechanical properties of claddings.

7.4. Criteria, thresholds and mechanisms of VVER fuel rod failure under IGR test conditions

Thus, the results presented in Chapter 5 show clearly that the failure mechanism for all fuel rod types tested in the IGR reactor was ballooning leading to cladding rupture. If we drop the issue of cladding hoop strain, since it is considered at length in Section 7.3, only one specific difference in the behavior of high burnup fuel rods with water coolant is left as compared to all the other types of tested fuel rods, viz., two local ballooning cases with ruptures have been observed for three out of four high burnup failed fuel rods (see Fig. 7.11).

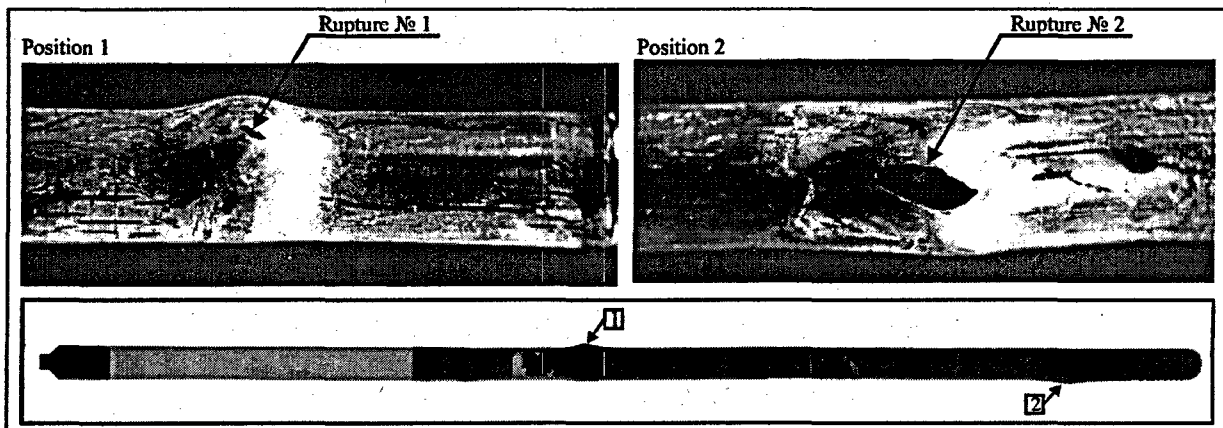


Fig. 7.11. Appearance of high burnup fuel rod #H7T with two ballooning and two cladding ruptures.

A detailed calculation of possible causes of this effect has not been performed yet. However, general physical considerations make possible to postulate that in the case under consideration the process of reopening of fuel-cladding gap does not cover the entire height of the fuel stack simultaneously. Therefore, the gas volume inside this fuel rod was divided into at least two isolated volumes in which the processes of ballooning and rupture of cladding were independent of each other.

The next item of the analysis was focused to consider of the quantitative parameters characterizing the failure of tested fuel rods. The peak fuel enthalpy is employed as a criterion generally accepted for assessing the threshold of fuel rods failure under RIA conditions. The corresponding results were obtained in Chapter 5 for the two types of high burnup fuel rods:

- the failure threshold of high burnup fuel rods with water coolant is about 160 cal/g fuel;
- the failure threshold of high burnup fuel rods with air coolant is about 75 cal/g fuel.

The failure threshold for a fuel rod with an irradiated cladding and fresh fuel was not determined in these tests, but it is quite evident that it equals the failure threshold for non-irradiated fuel rods since the mechanical properties of irradiated and non-irradiated claddings are the same under these conditions.

However, the IGR tests have demonstrated quite clearly that one should be very careful when using enthalpy criteria to assess the failure threshold for fuel rods featuring a failure mechanism different from PCMI mechanisms as in the case of the PCMI failure mechanism the respective threshold is generally characterized by two practically interchangeable and mutually adequate criteria:

- peak fuel enthalpy (for the case when the time of failure is close to the time of peak fuel enthalpy);
- fuel enthalpy at failure (for the case when the failure occurs before the fuel enthalpy reaches its peak value).

The IGR tests have demonstrated clearly that, for a high-temperature cladding failure with reopening of the gap, these two parameters yield different failure threshold estimates (see Fig. 7.12).

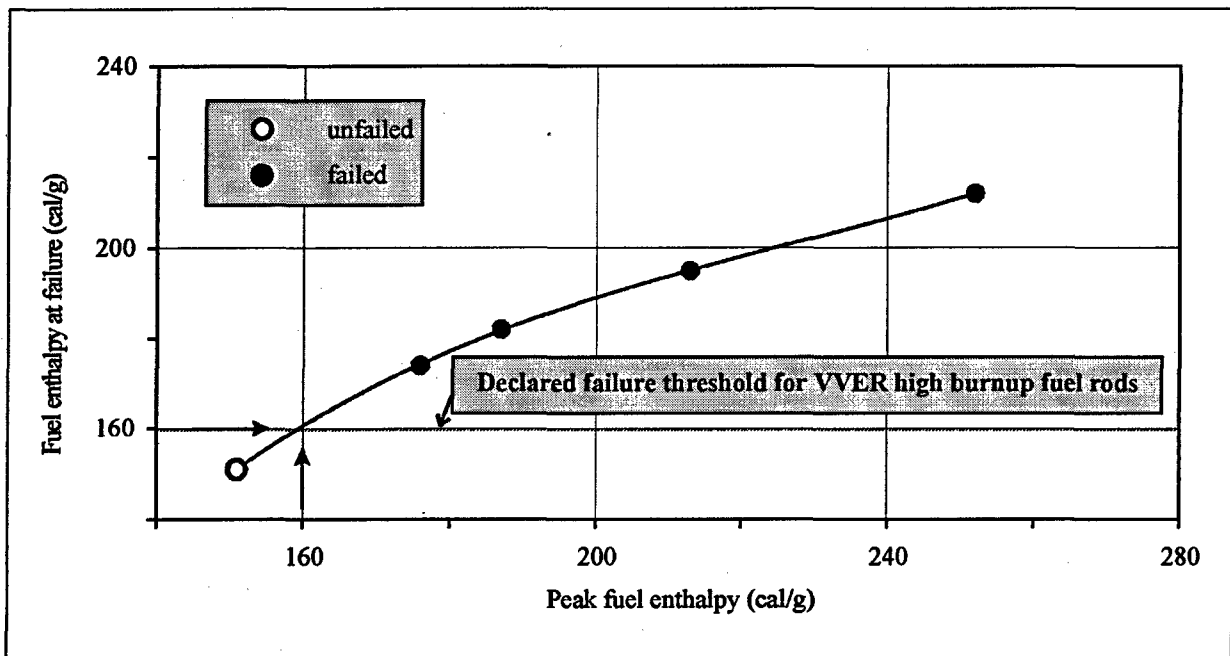


Fig. 7.12. Fuel enthalpy at failure vs. peak fuel enthalpy for VVER high burnup fuel rods tested in water coolant.

So, the results presented prove that the higher the peak fuel enthalpy in fuel rods, the higher the fuel enthalpy at which fuel rod failure occurs. To be able to understand the nature of this phenomenon, one has to bear in mind that cladding ballooning is the mechanism responsible for cladding failure, and hence two basic parameters that determine the cladding failure under these conditions are:

- gas pressure inside the fuel rod at failure;
- cladding temperature.

If we take into account that the gas pressure varied very insignificantly for all the fuel rods tested and assume that the influence of the strain rate of the cladding upon the temperature of cladding rupture was not essential either, we may suppose that the effect under consideration can be studied with the help of a data base characterizing the temperature of cladding rupture of different types of tested fuel rods versus peak fuel enthalpy (see Fig. 7.13).

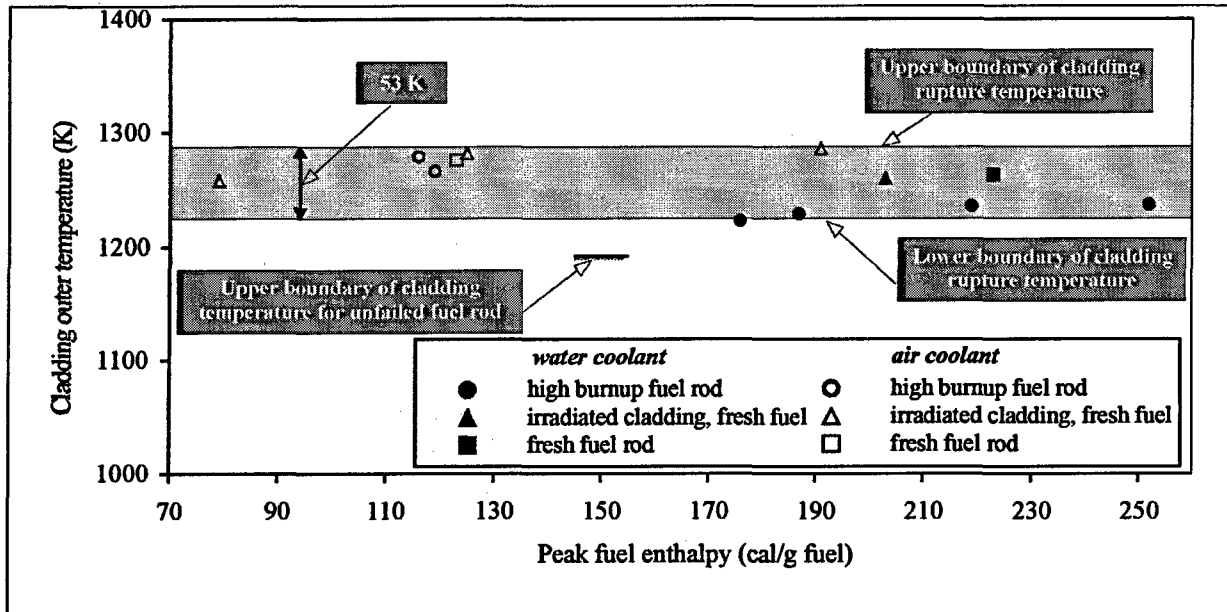


Fig. 7.13. Data base characterizing the outer temperature of the cladding at failure calculated with FRAP-T6 code.

An analysis of the results obtained under this approach shows that the temperature of cladding rupture for all types of fuel rods and test conditions is practically constant and could be used as a criterion. And so, the failure threshold of the fuel rods tested in the IGR reactor can be characterized, first and foremost, by the parameters of the state of the thin-walled cladding under an internal-pressure load rather than the fuel enthalpy, which can be confirmed by analysis of the equation describing the energy balance in a fuel rod:

$$H_{fuel} = E_{\Sigma} - (H_{cl} + E_{leakage} + H_{gas}),$$

where H_{fuel} = the fuel enthalpy at failure (cal/g fuel);

E_{Σ} = the energy deposition in the given axial zone at failure (cal/g fuel);

H_{cl} = the cladding enthalpy corresponding to the cladding temperature at failure (cal/g fuel);

$E_{leakage}$ = the energy of leakage from the fuel rod up to cladding failure (cal/g fuel);

H_{gas} = the enthalpy of internal gas (cal/g fuel).

A quantitative estimation of all the terms of this equation for failed high burnup fuel rods with water coolant is given in Table 7.4.

Table 7.4. Parameters of energy balance vs. fuel enthalpy at failure.

Fuel rod number	H	E_{Σ}	H_{cl}	$E_{leakage}$	H_{gas}	$H_c + E_{leakage} + H_{gas}$
#H5T	169	244	21	54	~0	75
#H7T	171	235	20	44	~0	64
#H2T	195	264	20	49	~0	69
#H3T	212	276	21	43	~0	64

The data presented bear witness to the fact that the following states are nearly true for IGR failure conditions:

- cladding enthalpy is the constant;
- gas enthalpy equal zero;
- leakage of energy comes to 16–22 % from energy deposition;
- the sum of these three components are varied merely in the range of 68_{-4}^{+7} cal/g fuel.

This is a reason that the tendency of increase of the fuel enthalpy at failure versus the energy deposition takes place for IGR test conditions. That is why to compare the failure thresholds of VVER fuel rods obtained in IGR tests with results of other tests only one criterion should be used, namely radial averaged peak fuel enthalpy strictly corresponding to failure time. Formally, the analysis of failure thresholds and failure mechanisms observed in the IGR tests could be considered completed but for one problem of appreciable practical significance. This problem is addressed in a special paragraph below.

7.4.1. Analysis of conditions of PCMI failure for VVER fuel rods

Despite the fact that no PCMI failures were observed during the tests of the VVER high burnup fuel rods in the IGR reactor this issue is of key importance merely by the virtue of the fact that failures of this type were experimentally obtained for the PWR high burnup fuel rods. Nevertheless, as was indicated in Chapter 6, these PWR fuel rods on the one hand had high oxidation and hydriding of cladding, and on the other hand, were tested in very narrow pulses. The VVER irradiated cladding has a low level of oxidation and hydriding, the fuel pellet has a central hole and the tests were performed with wide pulses. Therefore, it is important, at least to evaluate the behavior of these claddings at narrow pulses. Special calculation analysis with the use of the FRAP-T6 code was performed for this purpose. The FRAP-T6 code is selected because this version of the code allows us to obtain a most conservative evaluation of the studied process. A certain difficulty was encountered in setting this task because the FRAP-T6 code does not contain models to describe low temperature failure of cladding under PCMI conditions.

Preliminary substantiation for selection and entering of corresponding criteria in the code was performed on the basis of analysis of mechanical properties of irradiated Zr-1%Nb cladding obtained during ring tensile tests. These tests proved high ductility of irradiated Zr-1%Nb cladding at low temperatures and strain rate of up to $5 \cdot 10^{-1} \text{ s}^{-1}$. Total elongation was not below 10 % at a temperature of 293 K throughout the entire range of studied strain rates.

Analysis of rupture type for the tested ring samples showed that this is ductile shear, which occurs at an angle of 45° to the expansion axis (see Fig. 7.14). That is why, uniform elongation could be recommended as cladding failure criterion for the PCMI stage.

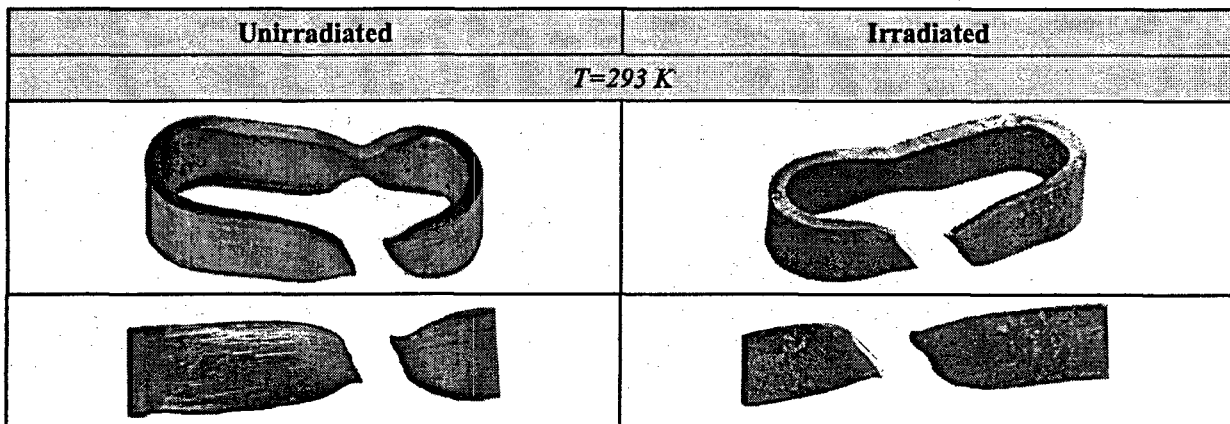


Fig. 7.14. Appearance of ring samples after tests.

However, it is important to mention, that this criterion is very conservative, because it characterizes only the beginning of the localization of deformation in a limited volume. To obtain cladding rupture additional energy supply is required.

Unfortunately, the data base on uniform elongation, which has been obtained within the framework of this program, has an upper strain rate limit equal to $5 \cdot 10^{-1} \text{ s}^{-1}$. However, as shown below, the strain rate range, for which the behavior of the claddings under PCMI conditions in narrow pulses was analyzed, reached 6.0 s^{-1} . According to the data presented in Chapter 6 of the Volume 2, the uniform elongation is only weakly sensitive to the strain rate within the range studied. Taking into consideration that the difference between 0.5 s^{-1} and 6 s^{-1} is greater than an order of magnitude, it is believed that extrapolation of the correlations, accounting for the strain-rate sensitivity, to the required range will not be fully correct. Therefore, the ultimate strength was put forth as the second criterion in order to assess cladding rupture by comparing this criterion with peak stresses. From the viewpoint of accounting for the effect of strain rate, a problem arises, similar to that described for the case of uniform elongation. However, one can assume with a fair degree of confidence that simultaneous use of these two criteria will allow the results, credible enough to be able to assess the cladding integrity under PCMI conditions.

Thus, the next objective of the analysis under consideration was to assess the mechanical behavior of a VVER high burnup fuel rod versus pulse width under PCMI conditions. To reveal the effect of the pulse width as clearly as possible, the following procedure was employed:

- the input data to calculate the thermal behavior of VVER high burnup fuel rod #H1T with the FRAP-T6 and SCANAIR codes were prepared;
- the first variant of the calculations corresponded to real IGR conditions for this fuel rod:
 - ⇒ the pulse width was 750 ms;
 - ⇒ the energy deposition in the fuel rod was 253 cal/g fuel;
- as a result of the first variant of the calculations, the thermal mechanical parameters of fuel rods, including uniform elongation and ultimate strength versus time dependencies, were determined; the calculated peak fuel enthalpy was about of 151 cal/g fuel;
- three more variants of the calculations were performed for this fuel rod under the condition that:
 - ⇒ the peak fuel enthalpy was approximately 150 cal/g fuel;
 - ⇒ the pulse width was 100, 10, and 5 ms, respectively;
 - ⇒ in all the variants, the power shape was in agreement with the initial IGR power shape.

The results of the calculations performed are presented in Fig. 7.15, Fig. 7.16.

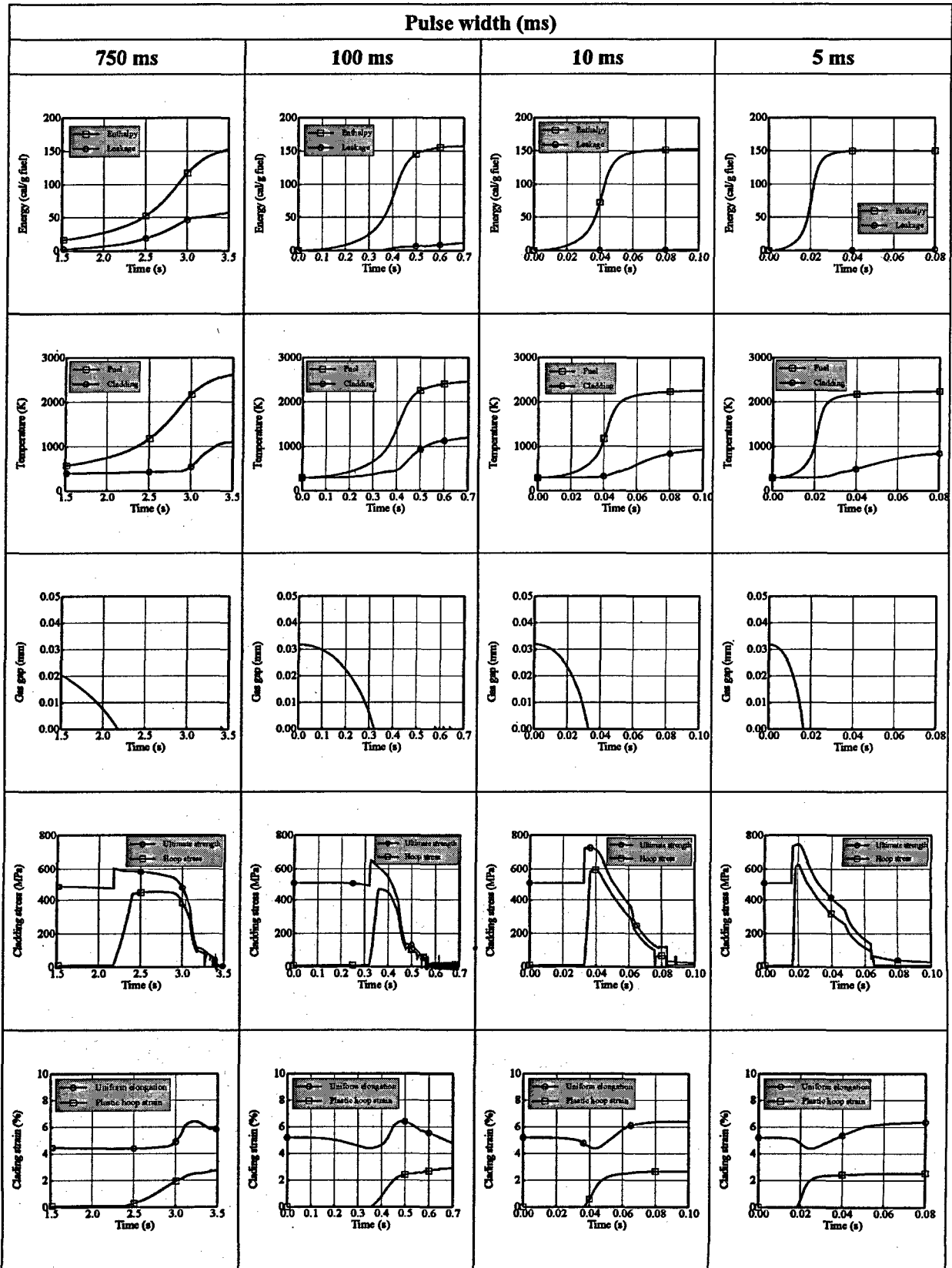


Fig. 7.15. Thermal mechanical parameters of the VVER high burnup fuel rod #H1T vs. pulse width, calculated using the FRAP-T6 code.

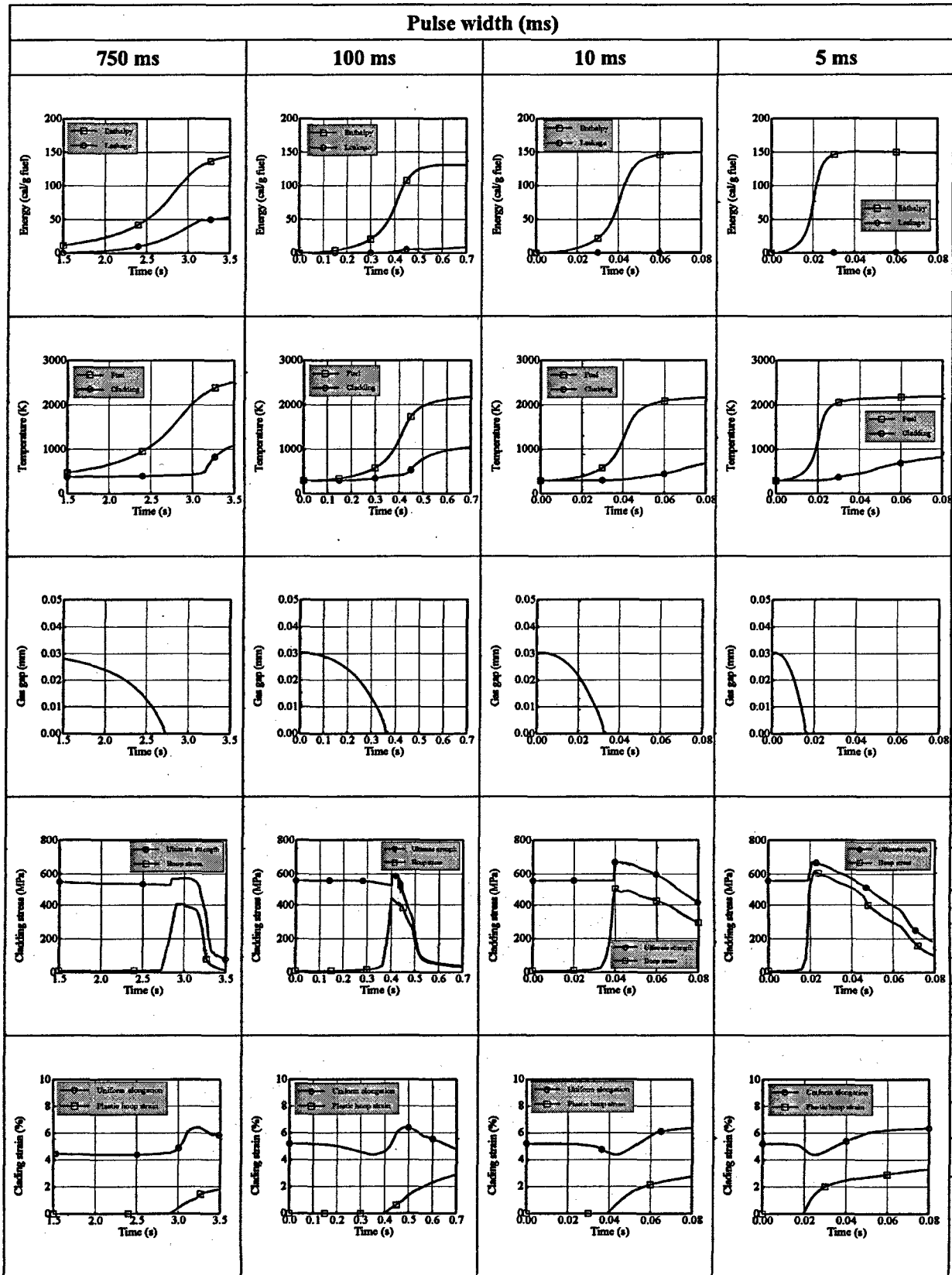


Fig. 7.16. Thermal mechanical parameters of the VVER high burnup fuel rod #H1T vs. pulse width, calculated using the SCANAIR code.

To make these results more vivid, the following additional parameters are depicted in Fig. 7.17.

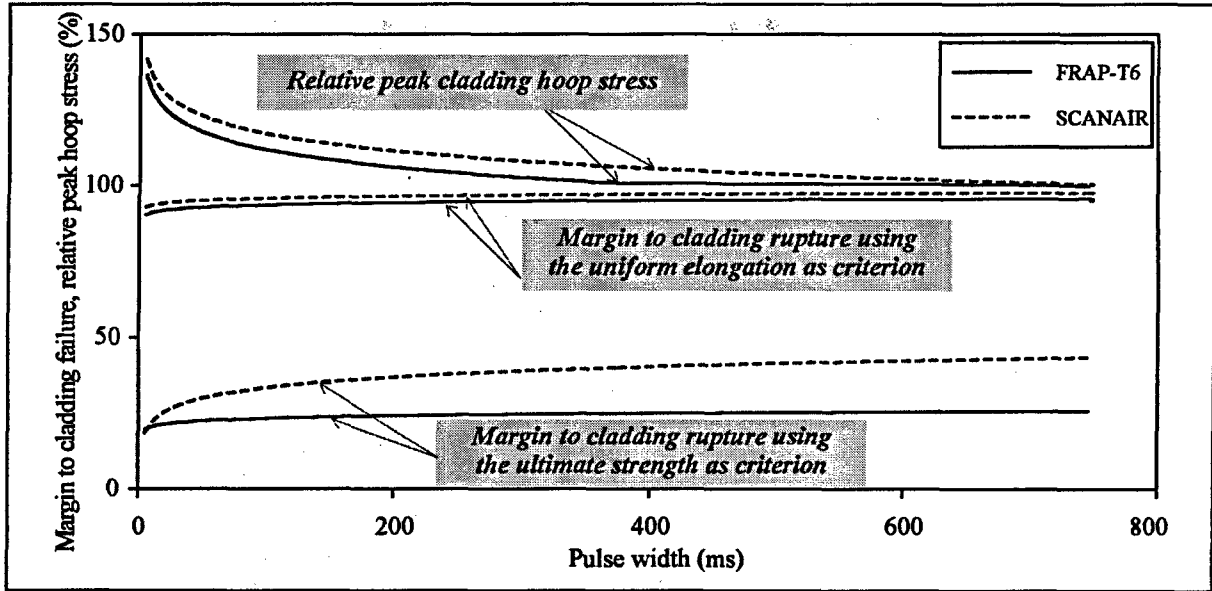


Fig. 7.17. Margins to PCMI failure for a VVER irradiated cladding.

1. The relative margin to cladding rupture, determined through the uniform elongation as a failure criterion, using the following formula:

$$\Delta_{un} = \frac{\delta_{un} - \varepsilon_{max}}{\varepsilon_{max}} 100\%,$$

where Δ_{un} = the margin to cladding rupture, with the uniform elongation taken as the criterion (%);

δ_{un} = the uniform elongation determined at the peak hoop stress (%);

ε_{max} = the cladding plastic hoop strain due to PCMI (%).

2. The relative margin to cladding rupture, determined by the ultimate-strength criterion:

$$\Delta_{ult} = \frac{\sigma_{us} - \sigma_{max}}{\sigma_{max}} 100\%,$$

where Δ_{ult} = the margin to cladding rupture, with the ultimate strength as the criterion (%);

σ_{us} = the ultimate strength at the peak hoop stress (MPa);

σ_{max} = the peak hoop stress (MPa).

3. The relative peak hoop stress in the cladding during the PCMI stage:

$$\delta_{stress} = \frac{P_i}{P_{750}} 100\%,$$

where δ_{stress} = the relative peak hoop stress (%);

P_i = the peak hoop stress for each of the four variants of the pulse width (MPa);

P_{750} = the peak hoop stress for the conventional IGR pulse width, 750 ms (MPa).

Thus, the data presented in Fig. 7.17 allow the following important conclusions:

- irradiated Zr-1%Nb cladding with the given mechanical properties cannot be failed during the PCMI stage;
- the peak cladding hoop stress and margins to cladding rupture are nearly independent on the pulse width in the range 750 ms down to approximately 70 ms; therefore, the results of IGR tests may be considered representative for the whole pulse width range above;
- at very narrow pulses (5–10 ms), the peak cladding hoop stress rises noticeably; however, the margin to fuel rod failure is retained for both criteria of cladding rupture.

Nonetheless, it should be noted in the conclusion of the present Section that in the PCMI analysis, specific effects of fission gas behavior, arising under conditions of fast pulse heat up, were not addressed separately. These effects may not be treated simply as swelling processes. At a very fast heat up, an abrupt rise in the pressure in intergranular bubbles of fuel takes place, especially in the rim zone [14]. This effect may result in fuel microcracking at grain boundaries in the rim layer and in additional loading upon the cladding. The available experimental evidence on this effect is rather contradictory and demands further analysis and systematization. Therefore, it seems of sense to carry out additional reactor tests with VVER high burnup fuel under the conditions of a narrow pulse width in order to validate in a conclusive fashion the behavior of this type of fuel rods.

8. CONCLUSIONS AND RECOMMENDATIONS

The data base containing the results of experimental and numerical studies aimed primarily at investigation of high burnup VVER fuel rods under RIA conditions is presented in three Volumes of present report.

The data base includes:

- a wide spectrum of results obtained in pre- and post-test examinations of fuel rods tested in the IGR pulse reactor;
- the results of ring tensile tests and burst tests performed to procure the data on original mechanical properties of irradiated and non-irradiated Zr-1%Nb claddings and to include them in the input data base of thermal mechanical computer codes;
- the results of numerical modeling of the behavior of each of the tested VVER fuel rods, using the FRAP-T6 and SCANAIR codes modified specially for this purpose.

The whole complex of special test and numerical procedures employed for obtaining the data base is described and substantiated in the report. This volume of the report contains a brief characteristic of the research program, basic results of the studies in each of top-priority directions, and includes an analysis of the results.

As a whole, the complex of activities performed under this program allows statement of the following major findings:

- the failure mechanism of VVER high burnup fuel rods does not differ from the failure mechanism of VVER fresh fuel rods and is, in essence, cladding rupture due to high temperature ballooning;
- the failure threshold of VVER high burnup fuel rods is about 160 cal/g fuel;
- special versions of FRAP-T6 and SCANAIR computer codes had been developed and verified to carry out an analysis of the thermal mechanical behavior of fuel rod tested under RIA conditions;
- a separate complex of experimental efforts aimed at the determination of mechanical properties of VVER claddings has made it possible to recognize that:
 - ⇒ an irradiated Zr-1%Nb cladding keeps a considerable ductility up to a fuel burnup at least 50 MWd/kg U;
 - ⇒ mechanical properties of irradiated Zr-1%Nb claddings become identical to those of non-irradiated ones at a temperature of 860 K and higher;
 - ⇒ burst parameters of Zr-1%Nb claddings have been obtained in an amount sufficient for calculation of specific effects of the ballooning and cladding rupture with accounting for the strain rate;
- a numerical analysis has been made to assess the possibility of PCMI failure for VVER high burnup fuel rods under narrow pulse width conditions; the analysis has shown that a margin to cladding failure is available even at a pulse width of about 5 ms;
- the data base accumulated as a result of these studies can be used extensively when analyzing high burnup fuel rod failure under LOCA conditions.

Nonetheless, further research would be needed in order to amplify and refine the data base on mechanical properties of Zr-1%Nb claddings, with an emphasis on the following aspects:

- development of a ballooning start criterion and additional validation of the burst criterion;
- substantiation of the adequacy of the data base obtained for ring and burst tests;
- refinement of the dependence of the cladding hoop strain versus temperature and strain rate for β -phase of Zr-1%Nb alloy;
- validation of conditions for extrapolation of the power law used to specify the cladding stress-strain relation beyond the test area.

In addition, a more careful review of mathematical models implemented in computer codes could be performed on the basis of a comparison with the available test data base on behavior of high burnup fuel rods.

And finally, reactor tests with narrow pulse would have to be carried out on fuel with a burnup of 50–60 MWd/kg U to validate the failure mechanism and the failure enthalpy threshold under these conservative conditions.

9. REFERENCES

- [1] J.M.Frizonnet, J.P.Breton, H.Rigat, J.Papin, "The Main Outcomes from the Interpretation of the CABRI REP-Na Experiment for RIA Study", *Proceeding of International Topical Meeting on Light Water Reactor Fuel Performance*, Portland, Oregon, 1997.
- [2] T.Fuketa, Yu.Mori, H.Sasajima, T.Nakamura, Yo.Tsuchiuchi, K.Ishijima "NSRR/RIA Experiments with High burnup PWR Fuels", *Proceeding of International Topical Meeting on Light Water Reactor Fuel Performance*, Portland, Oregon, 1997.
- [3] R.O.Meyer, R.K.McCardell, H.H.Scott "A Regulatory Assessment of Test Data for Reactivity Accidents" *Proceeding of International Topical Meeting on Light Water Reactor Fuel Performance, Portland, Oregon, 1997.*
- [4] V.Asmolov, L.Yegorova "Investigation of the Behavior of VVER Fuel under RIA Conditions", *Proceeding of International Topical Meeting on Light Water Reactor Fuel Performance*, Portland, Oregon, 1997.
- [5] General Regulations to Ensure the Safety of the Nuclear Power Plants under Design, Construction and Operation (OPB-82). *Atomnaya Energia*, v.54(2), 1983 (rus).
- [6] P.E.MacDonald, S.L.Seiffert, Z.R.Martinson, R.K.McCardell, D.E.Owen and S.K.Fukuda "Assessment of Light-Water-Reactor Fuel Damage During a Reactivity-Initiated Accident", *Nuclear Safety*, Vol.21, No.5, 1980.
- [7] M.Ishikawa, S.Shiozawa "A Study of Fuel Behavior under Reactivity Initiated Accident Conditions - Review", *Journal of Nuclear Materials* 95, 1980.
- [8] V.Asmolov, L.Yegorova "The Russian RIA Research Program: Motivation, Definition, Execution, and Results", *Nuclear Safety*, Vol.37, No.4, 1996.
- [9] D.L.Hagman, G.A.Reymann and R.E.Mason, "MATPRO-V.11: A Hand Book of Materials Properties for Use in the Analysis of Light Water Reactor Fuel Rod Behavior". NUREG/CR-0497 TREE-1280, Rev2, 1981.
- [10] E.H.Karb, M.Prußman, L.Sepold, P.Hofmann, G.Shanz "LWR Fuel Rod Behavior in the FR2 In-pile Tests Simulating the Heatup Phase of a LOCA", KfK 3346 (1982).
- [11] V.Solyany, Yu.Bibilashvily, V.Tonkov, "High temperature oxidation and deformation of Zr-1%Nb alloy claddings of VVER fuels", IWGFRT-16 IAEA Specialist Meeting on Water Reactor Fuel Safety and Fission Product Release in off-Normal and Accident Conditions, Denmark, 1983.
- [12] Cs.Gyori, Z.Hozer, L.Maroty, L.Matus "VVER Ballooning Experiments" *Enlarged Halden Programme Group Meeting*, 15-20 March 1998, Lillehammer.
- [13] R.O.Meyer, R.K.McCardell, H.M.Chung, D.J.Diamond, and H.H.Scott "A Regulatory Assessment of Test Data for Reactivity-Initiated Accidents", *Nuclear Safety*, Vol.37, No.4, 1996.
- [14] J.Papin, M.Balourdet, F.Lemoine, F.Lamare, J.M.Frizonnet, and F.Schmitz "French Studies on High-Burnup Fuel Transient Behavior Under RIA Conditions", *Nuclear Safety*, Vol.37, No.4, 1996.
- [15] T.Fuketa, F.Nagase, K.Ishijima, and T.Fujishiro "NSRR/RIA Experiments with High-Burnup PWR Fuels", *Nuclear Safety*, Vol.37, No.4, 1996.
- [16] R.O.Montgomery, Y.R.Rashid, O.Ozer, and R.L.Yang "Assessment of RIA-Simulation Experiments on Intermediate- and High-Burnup Test Rods", *Nuclear Safety*, Vol.37, No.4, 1996.
- [17] V.Asmolov, L.Yegorova, E.Kaplar, K.Lioutov, V.Smirnov, V.Prokhorov, A.Goryachev "Development of Data Base with Mechanical Properties of Un- and Preirradiated VVER Cladding". *Proc. of Twenty-Fifth Water Reactor Safety Information Meeting*, 1997. NUREG/CP-0162 Vol.2.

BIBLIOGRAPHIC DATA SHEET

(See instructions on the reverse)

1. REPORT NUMBER
(Assigned by NRC, Add Vol., Supp., Rev.,
and Addendum Numbers, if any.)

NUREG/IA-0156
Volume 1

2. TITLE AND SUBTITLE

Data Base on the Behavior of High Burnup Fuel Rods with Zr-1%Nb Cladding and UO₂ Fuel (VVER Type) under Reactivity Accident Conditions

Volume 1 Review of Research Program and Analysis of Results

3. DATE REPORT PUBLISHED

MONTH	YEAR
July	1999

4. FIN OR GRANT NUMBER

W6500

5. AUTHOR(S)

L. Yegorova

6. TYPE OF REPORT

NSI RRC KI-2179

7. PERIOD COVERED (Inclusive Dates)

manuscript completed Dec 1998

8. PERFORMING ORGANIZATION - NAME AND ADDRESS (If NRC, provide Division, Office or Region, U.S. Nuclear Regulatory Commission, and mailing address; if contractor, provide name and mailing address.)

Nuclear Safety Institute of Russian Research Center - Kurchatov Institute
Moscow 123182
Russia

9. SPONSORING ORGANIZATION - NAME AND ADDRESS (If NRC, type "Same as above"; if contractor, provide NRC Division, Office or Region, U.S. Nuclear Regulatory Commission, and mailing address.)

Division of Systems Analysis and Regulatory Effectiveness
Office of Nuclear Regulatory Research
U.S. Nuclear Regulatory Commission
Washington, DC 20555-0001

10. SUPPLEMENTARY NOTES

11. ABSTRACT (200 words or less)

The present report contains a data base used for analyzing the behavior of three types of VVER fuel rods (fresh fuel rods; fuel rods with fresh fuel and irradiated cladding; high burnup fuel rods) which have been tested in the IGR under reactivity accident conditions. The basic test parameters are as follows: capsule tests with stagnant water or air coolant under ambient conditions; pressurized fuel rods; fuel burnup: 0 and 48 MWd/kg U; pulse width - about 700 ms. The presented data base includes the results of reactor tests of 25 fuel rods as well as results of pre- and post-test examinations of fuel rods, computer simulations of fuel rod behavior under test conditions; in addition, the report presents the results of special out-of-pile tests carried out to measure mechanical properties of Zr-1%Nb cladding. The report consists of three volumes, each volume contains the following information:
Volume 1: Brief description of the test program, testing and analytical techniques and summary of results;
Volume 2: Description and validation of procedures used to obtain the data base. Summarization of test results as supported by mechanical properties of Zr-1%Nb cladding;
Volume 3: Data base consisting of: parameters of VVER fuel rods before and after irradiation at the NovoVoronezh Nuclear Power Plant; parameters of fresh and refabricated fuel rods before and after IGR tests; results of out-of-pile mechanical tests of non-irradiated and irradiated Zr-1%Nb cladding.

12. KEY WORDS/DESCRIPTORS (List words or phrases that will assist researchers in locating the report.)

reactivity initiated accident
impulse graphite reactor (Kazakhstan Atomic Energy Agency)
Zirconium-1% Niobium alloy
FRAP-T6 & SCANAIR computer codes
material properties
cladding strain and ballooning
refabrication of VVER fuel rods
post-test examinations

13. AVAILABILITY STATEMENT

unlimited

14. SECURITY CLASSIFICATION

(This Page)

unclassified

(This Report)

unclassified

15. NUMBER OF PAGES

16. PRICE



Federal Recycling Program